

## Modern Microwave Methods in Solid-State Inorganic Materials Chemistry: From Fundamentals to Manufacturing

Helen J. Kitchen,<sup>†</sup> Simon R. Vallance,<sup>†,‡</sup> Jennifer L. Kennedy,<sup>†,§</sup> Nuria Tapia-Ruiz,<sup>†</sup> Lucia Carassiti,<sup>†</sup> Andrew Harrison,<sup>||</sup> A. Gavin Whittaker,<sup>⊥</sup> Timothy D. Drysdale,<sup>§</sup> Samuel W. Kingman,<sup>‡</sup> and Duncan H. Gregory\*,<sup>†</sup>

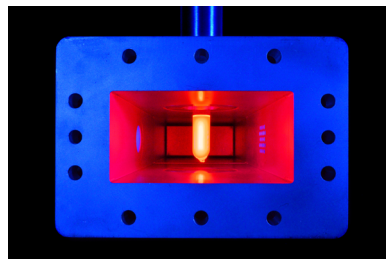
<sup>†</sup>WestCHEM, School of Chemistry, University of Glasgow, Joseph Black Building, Glasgow G12 8QQ, United Kingdom

<sup>‡</sup>Department of Chemical and Environmental Engineering, University of Nottingham, University Park, Nottingham NG7 2RD, United Kingdom

<sup>§</sup>School of Engineering, University of Glasgow, James Watt South Building, Glasgow G12 8QQ, United Kingdom

<sup>||</sup>Institut Laue-Langevin, 6 rue Jules Horowitz, BP 156, F 38042, Grenoble, Cedex 9, France

<sup>⊥</sup>Tan Delta Microwaves Limited, 7 Nettlingflat, Heriot EH38 5YF, United Kingdom



### CONTENTS

1. Introduction	1170
2. History of Microwave Heating	1171
3. Properties of Microwave Heating	1172
3.1. Direct Heating	1172
3.2. Volumetric Heating	1172
3.3. Instantaneous Heating	1172
3.4. Selective Heating	1172
4. Microwave Heating Mechanisms	1172
5. Apparatus for Microwave Heating	1173
6. Microwave Synthesis of Solids	1174
6.1. Oxides	1175
6.2. Chalcogenides	1177
6.3. Borides	1180
6.4. Carbides	1180
6.5. Silicides	1183
6.6. Nitrides and Pnictides	1184
6.7. Carbonitrides and Oxynitrides	1186
7. In-Situ Approaches to the Study of Microwave Reactions	1187
7.1. Necessity of in-Situ Techniques	1187
7.2. In-Situ Studies Using X-rays	1187
7.3. In-Situ Studies Using Neutrons	1190
7.4. In-Situ Studies Using Other Techniques	1193
7.5. Summary of in-Situ Techniques	1194
8. Chemistry–Engineering Interface	1194
9. Concluding Remarks	1200
Author Information	1200
Corresponding Author	1200
Notes	1200
Biographies	1201
Acknowledgments	1202

### References

1203

### 1. INTRODUCTION

In the materials manufacturing sector, energy efficiency, sustainability, and economic viability have become increasingly important to industry and society in recent years. Microwave (MW) methods can help to achieve these criteria by providing rapid processing, increased energy efficiency, and reduced equipment costs. MW methods not only offer potential solutions to industry but also provide the added attraction to materials chemists of the opportunity to access new and potentially metastable materials and understand the interaction of solids with electromagnetic fields.

For many years, MW heating techniques have been known to offer faster, simpler, and more cost-effective processes, often affording high-yield, high-purity products.<sup>1</sup> MW synthesis is now commonplace in synthetic organic and solution-phase chemistry, as reflected in numerous reviews,<sup>2–5</sup> but comparatively little work has been carried out in the solid state. In 1999, Rao et al. summarized the state of the art in materials chemistry and captured the excitement and potential of the discipline with specific case studies in the area of inorganic solids.<sup>6</sup> In the past decade, rapid growth in this field of research has embraced many new materials systems and seen significant technical and experimental advances, such that, just as in synthetic organic chemistry, the MW reactor has the potential to become a standard feature in many solid-state synthetic laboratories.

This review will analyze the significant advances in the area of solid-state MW synthesis with an emphasis on the opening period of the 21st century. A brief introduction to the merits of MW heating will be presented, along with a discussion of the current level of understanding of MW heating and interaction mechanisms. The major focus of the review will be on the use of MW heating to make novel materials or materials whose properties are changed or improved when conventional synthetic methods are replaced with MW heating. We will also discuss developments in MW techniques and instrumentation and their

**Received:** April 30, 2013

**Published:** November 21, 2013

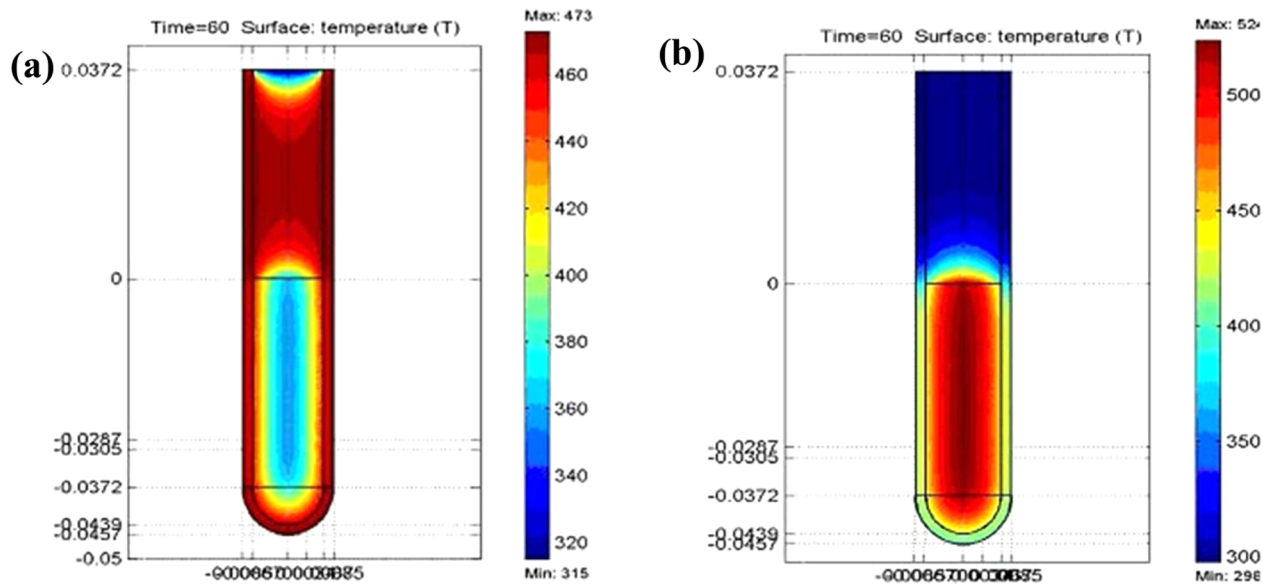


**Figure 1.** Difference in the temperature profile of (a) conventional and (b) microwave heating. The image shows a slice through a tube showing temperature gradients after 60 s of heating in (a) a water bath and (b) an CEM Discover MW system.<sup>24</sup> Copyright 2003. Reprinted from ref<sup>24</sup> with kind permission from Springer Science and Business Media.

potential to foster interest among the materials chemistry research and industrial communities and widen access to MW methods. We will examine recent progress in rationalization of the mechanisms and outcomes of MW synthesis, with particular focus on development of in-situ techniques that allow time-resolved study of MW reactions. Final emphasis will be that of MW materials chemistry at the interfaces, not just those of the materials themselves but also at the boundaries of the discipline, especially with chemical, electrical, and electronic engineering. At these interfaces, we see the best chance of furthering our understanding of the mechanisms and outcomes of MW synthesis and developing appropriate instrumentation to allow MW synthesis to be accessible to a wider range of research activities and ultimately for large-scale industrial processes.

## 2. HISTORY OF MICROWAVE HEATING

MWs are broadly regarded as those electromagnetic waves which are situated between infrared and radio wavelengths in the electromagnetic spectrum, with wavelengths between 0.01 and 1 m, corresponding to frequencies between 0.3 and 300 GHz. Use of radiation within the MW region is regulated at national and international levels to avoid interference with telecommunications. Numerous frequencies have been allocated for industrial, scientific, and medical uses, but the most widespread are ~900 MHz (896 MHz in the United Kingdom and 915 MHz in the United States) and 2.45 GHz. The latter value is the most common, as all domestic MW ovens and laboratory-scale synthesis systems operate at this frequency.

In 1971, use of MW heating in chemical research was reported for the first time.<sup>7</sup> This precipitated several more publications on this novel technique, but it was not until 1986 that the first successful chemical reactions in conventional domestic MW ovens (DMOs) were performed,<sup>8</sup> bringing easily accessible MW chemistry to the attention of the wider chemical research community. Since these early experiments, MW heating has become an important method of chemical synthesis and processing,<sup>1,4,9–12</sup> especially in the case of organic and solution-phase reactions. Particular interest in MW methods

was catalyzed by several notable synthetic studies describing high yields, with up to 1000-fold increases in the reaction rates.<sup>8,13</sup> In the laboratory, the availability of cheap, high-power, MW sources led to an explosion of papers describing MW-induced chemical processing, and MW techniques are now well established in many areas of industrialized life. More recently, MW applicators designed specifically for laboratory use have made MW heating more convenient to nonspecialists and made use of MWs far less unconventional.

Over the same period, MW-induced solid-state chemistry has developed steadily but without the exponential growth and widespread acceptance that has accompanied solution-phase applications. Several reasons for this slower growth may be identified. First, there are no commercial laboratory MW applicators aimed at solid-phase reaction chemistry, as there are for solution-phase work. Second, the complexity of MW–solid interactions appears to be much greater than that in solution, and our understanding of the processes involved is far less comprehensive. Third, the complexity of the heating process means that there are significant difficulties associated with monitoring temperature conditions inside the sample. Finally, the absence of (or maybe simply the practical difficulty of producing) clear, critically assessed information on sample temperatures allowed many authors of early papers to claim that some MW heating enhancements are due to nonthermal effects of the MW electric or magnetic field, effects that are not easily quantifiable or verifiable.<sup>14,15</sup>

Stemming from this final point, practical difficulties and lack of understanding in early MW studies resulted in claims for effects that were often contentious (and occasionally outrageous), and it has taken some time for the field to overcome a degree of scepticism. With subsequent insight into how MWs couple directly to charge carriers and mediate solid-state reactions, many of the results from the earlier years of MW chemistry have been reasoned and discussed in a number of reviews.<sup>6,16–21</sup> Since Rao's review in 1999, research on MW synthesis of inorganic solids has continued apace. In parallel, application of MW heating to chemistry and materials processing has progressed from the laboratory to pilot-scale or full-scale applications in

chemical processing, such as wood, paper, and material drying, sintering of ceramics, and vitrification of waste materials. It is to some degree ironic that the area with probably the greatest potential for energy savings from MW processing is also among the least explored. The overwhelming majority of solid-state processing or synthesis at high temperatures involves at least one of three stages, namely, combination of the reactants, homogenization (annealing) of the product, and densification. MW heating has demonstrated advantages over conventional methods in all three of these areas,<sup>22,23</sup> due to the unique properties of MWs and their interaction with solids, which will be discussed in the following sections.

### 3. PROPERTIES OF MICROWAVE HEATING

MW heating is characterized by a number of properties, discussed below, that make the technique fundamentally different from conventional heating methods, both in theory and in practice. It is these factors that can make MW synthesis much more rapid and energy efficient than the corresponding conventional heating techniques. They also result in the potential for different reaction pathways to exist and can lead to structural and/or chemical differences in the reaction product.

#### 3.1. Direct Heating

MW radiation interacts directly with the reaction components, so the sample alone is heated with minimal need for energy to be expended in heating furnaces, containment materials, and the sample environment.<sup>16</sup> In theory, this requires at least one of the reactants to be capable of converting MW energy into heat, but the efficiency of modern MW applicator designs effectively allows almost all materials to be heated in this way. As a consequence of the direct heating of samples, the temperature profile of a microwave-heated material is the inverse of that seen in conventionally heated examples (Figure 1), resulting in the surface being cooler than the interior.<sup>19</sup>

#### 3.2. Volumetric Heating

As a consequence of the MW heating process taking place directly in the sample, heating also occurs volumetrically.<sup>25</sup> In a homogeneous material, this means that heating is uniform throughout the sample. In most real samples, the thermal homogeneity is reduced by MW field and sample inhomogeneities and the temperature dependence of the interaction of the sample with a MW field. In contrast with conventional heating, volumetric heating results in a reduced requirement for heat transfer via thermal conduction within the sample, and this allows relatively large samples to be heated much more efficiently and with a much more uniform thermal history throughout the sample.

#### 3.3. Instantaneous Heating

The direct and volumetric nature of MW heating results in a very fast transfer of MW energy into heat, which can lead to extremely rapid temperature rises, far beyond that which can be achieved in a conventional furnace, which results in very rapid reaction times.<sup>16</sup> Similarly, when the application of MW power is terminated at the end of a reaction, heating stops immediately,<sup>19</sup> which often results in the reaction essentially being quenched and can lead to metastable reaction products that are inaccessible using conventional methods.

#### 3.4. Selective Heating

The direct heating process allows specific reactants that interact more strongly with the MW field to be heated selectively. As a result, MW heating is uniquely capable of generating extremely

high temperatures in specific regions of the sample while maintaining lower temperatures in others.<sup>9,16</sup> This principle is widely used in the specific heating of active sites in supported metal catalysts.<sup>26</sup> It also enables successful synthesis of, for example, metal chalcogenide systems, which can be difficult to synthesize conventionally due to the volatility of the chalcogen starting materials. Using MWs, the metal components of the reaction mixture are heated preferentially and react very quickly with the chalcogen before it has chance to volatilize.<sup>27</sup>

### 4. MICROWAVE HEATING MECHANISMS

The overwhelming majority of MW-induced chemical reactions rely directly on the heating effects that MWs induce in many materials. These heating effects primarily result from the interaction of the electric component of the MW field with charged particles in a material (or more rarely, the magnetic component may interact with magnetic dipoles). The precise nature of the interaction depends upon the mobility of charged particles and may give rise to one or both of the two major MW-heating processes. In substances where the charges are bound as dipoles, the electric field induces motion until it is balanced by electrostatic interactions; this is known as dipolar polarization ( $P_d$ ) and is most significant in the liquid phase. For materials in which the charge carriers are mobile, as with electron and fast ion conductors, the alternating MW field gives rise to a current traveling in phase with the field and causing resistive heating in the sample. Generally, this mechanism is the dominant effect in solid materials and is referred to as conduction heating. Despite these generalizations, solids with bound solvent molecules, for example, may display dipolar polarization effects, and ionic solutions may equally well display the effects of conduction heating.

It is important to note that MW heating in condensed phases is quite distinct from the quantized energy absorption observed in MW spectroscopy. While absorption of MWs in solid and liquid samples is frequency dependent, it is, in effect, nonquantized. Instead, the material behaves as though reacting to a high-frequency electric field, and so may be subjected to classical analysis. Details of this analysis are beyond the scope of this work, although some of its chemically significant aspects will be introduced and discussed below.

The principles behind MW heating and the interactions of MWs with solids have been discussed extensively previously. For such information the reader is referred to the existing literature, such as the seminal text by Metaxas and Meredith.<sup>25</sup> Several terms are important for reference nevertheless, and we discuss these briefly below.

Dipolar polarization,  $P_d$ , occurs on a time scale of the order of those associated with microwaves. Hence, when a dielectric is subjected to an external electric field of strength  $E$ , the polarization is related to the intrinsic properties of the material through the relation in eq 1<sup>25,28</sup>

$$P_d = \epsilon_0(\epsilon_r - 1)E \quad (1)$$

where  $\epsilon_0$  is the permittivity of free space and  $\epsilon_r$  is the relative permittivity of the material. Given that in reality the permittivity is a complex quantity,  $\epsilon^*$  (equal to the product  $\epsilon_0\epsilon_r$  and expressed as  $\epsilon^* = \epsilon' + i\epsilon''$ ),<sup>25,29</sup> then the loss tangent,  $\delta$ , is commonly used to describe the interaction of a dielectric with microwaves (eq 2)

$$\tan \delta = \frac{\epsilon''}{\epsilon'} \quad (2)$$

where  $\epsilon'$  represents the time-independent polarizability of a material in the presence of an external electric field and  $\epsilon''$ , the time-dependent component of the permittivity, quantifies the efficiency with which electromagnetic energy is converted to heat.<sup>25,28</sup> The angle  $\delta$  represents the phase lag between the polarization of the material and the applied electric field. This is therefore an extremely useful quantity in determining how efficiently microwave heating will take place.

Even though the frequency is usually fixed, the loss tangent is important as the temperature of a reaction has been shown to vastly affect the dielectric properties of a material.<sup>30,31</sup> This observation is important, particularly in the case of solids that do not absorb microwave energy at room temperature; often such materials will begin to absorb when the temperature is increased. In these cases, a susceptor material is often used to raise the reaction temperature to a point where the dielectric properties are more favorable for the reactant.<sup>32</sup> An example of this is in the MW heating of alumina which becomes 3000% more efficient when the temperature is raised from 200 to 1200 °C.<sup>16</sup> However, this increase in heating efficiency can cause problems such as thermal runaway (where an increase in temperature results in a change in reaction rate which leads to further increase in temperature), and without careful monitoring the temperature can become uncontrollable.<sup>20</sup>

By contrast, the interaction of charge carriers with the applied electric field in solids leads to ohmic heating. In such cases the complex permittivity is modified to take account of losses by including a separate conduction term (eq 3)<sup>28</sup>

$$\epsilon^* = \epsilon' - i\epsilon'' - \left( \frac{i\sigma_i}{\omega\epsilon_0} \right) \quad (3)$$

where  $\sigma_i$  is the conductivity of the material and  $\omega$  is the frequency of the microwave field. The losses in this case arise not from a phase lag, as the relaxation time for this process is of the order of that of a microwave phase period, but from the intrinsic resistance of the material to an electric current. This term is extremely significant in metallic conductors or semiconductors such as carbon.

The dielectric properties of a material can also be used to determine the amount of power absorbed,  $P$ , by a sample as shown in eq 4<sup>28</sup>

$$P = \sigma |E|^2 = 2\pi f\epsilon_0 \epsilon'' |E|^2 = 2\pi f\epsilon_0 \epsilon' \tan \delta |E|^2 \quad (4)$$

where  $\sigma$  is the total effective conductivity,  $E$  is the magnitude of the internal electric field,  $\epsilon_0$  is the permittivity of free space, and  $f$  is the microwave frequency.

Finally, a key aspect in practical design of microwave solid-state syntheses and processes is consideration of how the efficiency of MW heating is mediated by sample volume. As the size of the sample being irradiated is increased, an absorbance loss factor becomes progressively more significant. The penetration depth,  $D_p$ , is the distance into the sample at which the electric field is attenuated to 1/e of its surface value (eq 5)<sup>25</sup>

$$D_p = \frac{\lambda_0 \sqrt{\epsilon'}}{2\pi\epsilon''} \quad (5)$$

where  $\lambda_0$  is the wavelength of the microwave radiation. For materials at microwave heating frequencies,  $D_p$  ranges between several micrometers for metals and several tens of meters for some low-loss polymers. For many materials at microwave frequencies, the penetration depth is of the same order of magnitude as the dimensions of the sample, a fact that often has

important implications for heating uniformity. From the above it is apparent, for example, that high dielectric loss materials, such as carbon, are more suited for small batch processes or a continuous feed system. If the volume of the sample is too large then insufficient microwave energy reaches the center of the sample, resulting in nonuniform heating and inhomogeneous, impure products.

## 5. APPARATUS FOR MICROWAVE HEATING

Design of MW apparatus depends strongly upon its purpose. Key concerns are achieving maximum efficiency in the transfer of power from the generator to the material that is to be heated, both for economy and longevity of the equipment and for obtaining repeatable and reliable results. In an industrial setting each system is typically required to treat only one particular material and can be optimized without unnecessary compromise.<sup>25</sup> Conversely, at home, the DMO is designed to treat a wide range of food types and portion sizes. The unavoidable trade off is a reduction in the efficiency and repeatability that can be achieved in any given heating task. Despite this, the ease of use and ready availability of the DMO is at least partly responsible for the burgeoning interest in MW chemistry, although superior systems are available and will be described later in this section.

The relationship between the wavelength and the size of the applicator's cavity determines the nature of the applicator. In a DMO the applicator is typically a rectangular cavity with dimensions several times larger than the wavelength of the MW radiation. Thus, the cavity can support many different possible configurations of the MW field (modes), and the precise configuration present at any given moment is a function of the material that is placed in the cavity, its position within the cavity, and the evolution of the material's dielectric properties during heating. The applicator in a DMO is hence also known as a multimode cavity (MMC). The repeatability of DMO experiments remains low due to the essentially random electric field pattern which is created each time the experiment is run, and it is difficult or impossible to calculate with certainty the power delivered into the reaction.

To remedy the inherent shortcomings of the DMO, commercial suppliers have created an automated benchtop single-mode cavity (SMC) apparatus that is suitable for sealed vessel experiments with volumes from 0.2 to 80 mL or more depending on the particular product. In single-mode cavities, the field is well defined in space and the material to be heated can be placed at a point of known and relatively even intensity (assuming that it is small as a function of wavelength). Examples of such machines include CEM Discover S and SP series (Figure 2),<sup>33</sup> Biotage Initiator,<sup>34</sup> and Milestone Ethos One.<sup>35</sup> Typically, key reaction parameters such as pressure, power, temperature, and time can be automatically controlled, including ramp up, hold, and ramp down. Infrared temperature<sup>36</sup> and Raman spectroscopy<sup>37</sup> accessories among others are available for tracking reaction progress. Accessories for agitation, stirring, and pumping are available.<sup>38</sup> For liquid-phase scale up by the batch method, reaction volumes of up to 1–12 L can be accommodated in multimode cavity systems that are akin to the DMO but better instrumented, for example, CEM MARS (Figure 3),<sup>38</sup> Milestone MultiPrep,<sup>39</sup> and Accelbeam.<sup>40</sup> Notably, the Milestone Multisynth can operate as either single or multimode. Continuous-flow systems are also available, e.g., the Milestone Flowsynth, shown in Figure 4.<sup>41,42</sup> All these systems are very attractive to users of liquid-based protocols; however, the maximum reaction temperature is typically 300 °C



**Figure 2.** CEM Discover single-mode MW reactor.<sup>38</sup> Reprinted from ref 38 with kind permission from Springer Science and Business Media.



**Figure 3.** CEM MARS multimode MW reactor. Copyright 2003. Reprinted from ref 38 with kind permission from Springer Science and Business Media.

and the maximum pressure 300 psi. Thus, their utility for solid-state chemistry is severely hampered. Alternative systems that are designed to cope with high temperatures are required.

Given the difficulties of controlling the electric field distribution in a cavity that is large with respect to the wavelength, for small reaction volumes chemists often turn to single-mode systems that use a length of waveguide as the applicator. In this way, the number of degrees of freedom in the field distribution is drastically reduced to the point where it is possible to ensure optimum conditions throughout the reaction so long as provision is made for suitable impedance matching structures.<sup>43</sup>

## 6. MICROWAVE SYNTHESIS OF SOLIDS

In an ideal situation, some or all of the reagents in the synthesis of a material will exhibit a high coupling efficiency at MW frequencies and therefore be good MW absorbers. This will facilitate rapid heating of the reagents in a MW field and lead to



**Figure 4.** Milestone Flowsynth continuous-flow MW reactor.<sup>42</sup> Reprinted with permission from ref 42. Copyright 2008 American Chemical Society.

successful synthesis of the target material in a short period of time. In some cases, the reagents that are used conventionally will be poor MW absorbers, but it is often possible to select alternative precursors for synthesis with more favorable dielectric properties.

In the event that there are no good MW-absorbing reagents available for synthesis of a material, it is usually possible to find another material that can act as a heat source. Such a material is commonly referred to as a susceptor, which is defined simply as a substance that has the ability to absorb electromagnetic energy and convert it to heat. This essentially means that a susceptor is a material that has a high dielectric loss tangent. Commonly used susceptors include carbon (in the form of either graphite or amorphous carbon), silicon carbide, and copper(II) oxide. A susceptor can be either in direct contact with the sample (either mixed in with other reagents or used to surround a pellet) or kept separate, generally by surrounding the reaction vessel in a container of the susceptor material. It is important to note that use of a susceptor can cause problems. Reactions that require the susceptor to be intimately mixed or in contact with the other reagents can naturally result in contamination of the products, adding an additional separation step to the synthesis or even resulting in unwanted side reactions. Clearly, when scale-up is considered, use of susceptors is also highly undesirable.

In the most difficult cases, the reaction components are transparent to MWs and MW susceptors cannot be used. In these circumstances, use of single-mode cavities can sometimes provide an effective way of maximizing power transfer to a sample.<sup>44</sup> An alternative solution for reactions in which the precursors do not couple with MWs is the use of MW-induced plasma (MIP),<sup>45</sup> as shown in Figure 5. The MIP is effectively used as a replacement for a susceptor in these reactions; the plasma transfers energy between the MW radiation and the reactants, allowing any solid to be heated. Use of the MIP also avoids contamination of the product by the susceptor and issues of unwanted side reactions. A further useful characteristic of MIP reactions is that the plasma may also serve as a source of reactive species (e.g., N<sub>2</sub> or NH<sub>3</sub> plasmas for nitriding solids).

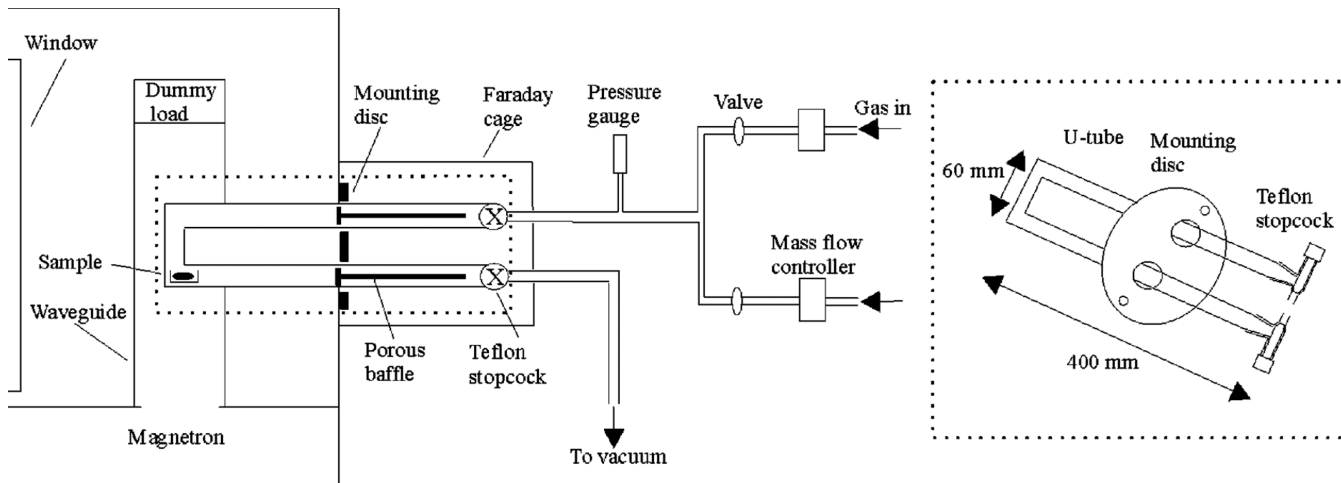


**Figure 5.** Schematic of an MIP reactor. The portion of the apparatus shown in the dotted box can be isolated to allow manipulation of air-sensitive products and precursors.<sup>46</sup> Reprinted with permission from ref 46. Copyright 2004 AIP Publishing LLC.

### 6.1. Oxides

Oxides have always been a major focus of research in conventional solid-state chemistry, as they generally require reasonably simple experimental conditions for their synthesis and exhibit a huge variety of interesting properties or industrially important applications, so it is perhaps not surprising that oxides represent the largest single class of MW-synthesized solid-state materials. Many hundreds of oxide compounds synthesized using MW methods have been documented in the past decade. In the majority of these cases, it has been reported that reaction times are considerably shorter and reaction temperatures significantly lower when using MW irradiation compared to conventional synthetic techniques, for instance, in the synthesis of  $\text{LaCrO}_3$ ,<sup>47</sup>  $\text{GaAlO}_3$ ,<sup>48</sup>  $\text{Li}_{0.35}\text{La}_{0.55}\text{TiO}_3$ ,<sup>49</sup>  $\text{La}_{1-x}\text{Sr}_x\text{CoO}_3$ ,<sup>50</sup> oxide bronzes,<sup>51,52</sup> and numerous lithium, copper, cobalt, and nickel ferrites.<sup>53</sup> However, the particularly interesting cases are those in which the use of MW heating is able to improve the properties of the resulting oxide when compared to a conventionally synthesized material. Previously, properties of oxides have been most commonly improved by MW heating at the sintering stage, and a recent example where the photoelectrochemical performance of MW-annealed  $\alpha\text{-Fe}_2\text{O}_3$  thin films can be improved compared to those heated conventionally demonstrates this.<sup>54,55</sup> The low processing temperatures, rapid reaction times, and subsequent retention of the microstructure of the films was key in this respect, and Binner et al. demonstrated that ceramic microstructure is very sensitive to conventional vs MW heating parameters; yttria-stabilized zirconia (YSZ) synthesized in a hybrid microwave/radiant sintering furnace (600 W) exhibits an intergranular fracture mechanism, whereas larger grains of YSZ synthesized conventionally follow a transgranular fracture mechanism.<sup>56</sup>

Many transition metal binary oxides exhibit high dielectric loss tangents at MW frequencies,<sup>57</sup> and furthermore, the products themselves are very often MW susceptors, which facilitate postreaction MW-induced sintering. In many cases, it is possible to select starting materials that couple strongly with MWs. For instance, in the case of lead zirconium titanate synthesis, it has been observed that use of reduced oxide precursors ( $\text{TiO}_{2-x}$  and "partially stabilized" doped zirconia) instead of the conventional reagents  $\text{TiO}_2$  and  $\text{ZrO}_2$  is preferable, due to their better MW-absorbing properties.<sup>58</sup> Similarly, in the MW synthesis of  $\text{NaZr}_2(\text{PO}_4)_3$  (sodium zirconium phosphate, NZP) and related

compounds such as sodium titanium phosphate, use of the same nonstoichiometric precursors was found to be preferable; Figure 6 shows a comparison between the MW heating profile of

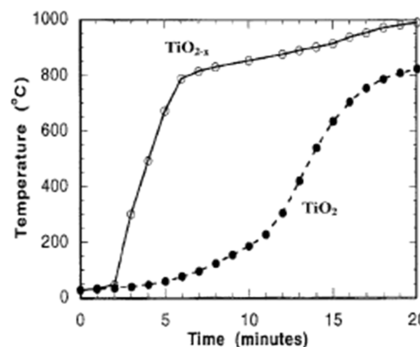


**Figure 6.** MW absorption characteristics of regular  $\text{TiO}_2$  (in air) and reduced  $\text{TiO}_{2-x}$  (in  $\text{N}_2$  atmosphere).<sup>59</sup> Reprinted with permission from ref 59. Copyright 2004 The American Ceramic Society.

stoichiometric  $\text{TiO}_2$  and  $\text{TiO}_{2-x}$ .<sup>59</sup> MW synthesis of some colossal magnetoresistive manganites,  $\text{La}_{1-x}\text{A}_x\text{MnO}_3$  ( $\text{A} = \text{Ca}, \text{Sr}, \text{Ba}, 0 < x < 1$ ), has been achieved using metal nitrate precursors instead of the conventional metal oxides.<sup>60</sup> Primarily, the nitrates couple strongly with MWs, removing the need for a susceptor, but in this case they have the further advantage of providing a source of oxidizing  $\text{NO}_2$ , which induces mixed valency in the samples.

Of course, there are many materials for which there are no suitable MW-absorbing precursors, and in these cases, a susceptor is often used. Examples of MW syntheses of oxides that proceed via the use of a susceptor include  $\text{Li}_{0.35}\text{La}_{0.55}\text{TiO}_3$ ,<sup>49</sup>  $\text{LiV}_3\text{O}_8$ ,<sup>61</sup> and  $\text{LaCrO}_3$ ,<sup>62</sup> and gadolinium aluminum perovskite<sup>48</sup> using carbon susceptors,  $\text{YBa}_2\text{Cu}_3\text{O}_{7-x}$ ,<sup>63</sup>  $\text{NiAl}_2\text{O}_4$ ,<sup>64</sup>  $\text{LaCoO}_3$  and  $\text{LaNiO}_3$ ,<sup>62</sup> and yttrium aluminum garnet,<sup>65</sup> which use  $\text{SiC}$  as a susceptor, and  $\text{LiMn}_2\text{O}_4$ ,<sup>66</sup> and  $\text{Na}_x\text{WO}_3$ ,<sup>52</sup> using  $\text{CuO}$  susceptors.

While multimode cavities in the form of DMOs have been used most extensively in oxide synthesis, there are also some examples of the use of single-mode MW cavities. SMCs can maximize the MW power transferred to the sample, which is particularly useful when the precursors are poor MW absorbers, and it is also considerably easier to gain deeper insight into a MW

reaction performed in a SMC. For instance, synthesis of  $\text{La}_{0.8}\text{Sr}_{0.2}\text{MnO}_3$  (LSMO) by Grossin et al. shows clearly the effect on temperature and reaction rate with change in power.<sup>67</sup> For a fixed time of 10 min the power was varied between 700 and 1000 W for a number of samples, and it can clearly be seen how the temperature rises much faster as the power increases. Directly related to this is the phase purity of the product, which improves with temperature.

Microwave-induced plasma has also been used for synthesis of oxides. These cases demonstrate how heating via interaction with plasma eliminates the requirement for a susceptor. The MIP-promoted process has been used, for example, in the synthesis of ternary titanate and niobate phases using plasmas of argon and oxygen<sup>68</sup> and preparation of the spinel phases ( $\text{MAl}_2\text{O}_4$ ,  $\text{M} = \text{Mg, Zn, Ni}$ ; and  $\text{MFe}_2\text{O}_4$ ,  $\text{M} = \text{Mg, Zn, Mn}$ ) using an oxygen plasma.<sup>69</sup> In all these cases it was observed that heating reactants in a MIP resulted in an improvement of their ability to couple with the microwave field, which can be directly linked to an enhancement of the dielectric properties of the reactants with increasing temperature. Interestingly, in the MIP-promoted preparation of tetragonal  $\text{BaTiO}_3$ , an alternative reaction mechanism to that reported in conventional synthesis was observed, with powder X-ray diffraction (PXD) revealing the presence of hexagonal  $\text{BaTiO}_3$  as an intermediate.<sup>68</sup>

In their work on the MIP synthesis of various ternary oxides, Chou et al. note that the dielectric properties of the intermediate and product phases will be important in determining if a reaction is driven to completion.<sup>70</sup> They also suggest that MIP is a viable route to facilitate MW heating of materials which will not otherwise interact with MWs to heat from room temperature. Binary oxides demonstrating plasma-promoted heating via in-situ temperature measurement were used subsequently in the synthesis of several ternary oxides (Table 1).

**Table 1. Ternary Oxides Synthesized via MIP Methods from the Respective Binary Oxides (with appropriate reaction conditions)<sup>70 a</sup>**

precursors	power (W)	time (min)	product
$\text{TiO}_2$ , $\text{BaCO}_3$	900	3	t- $\text{BaTiO}_3$
$\text{TiO}_2$ , $2\text{BaCO}_3$	900	6	m- $\text{Ba}_2\text{TiO}_4$
$\text{ZrO}_2$ , $\text{BaCO}_3$	500	5	$\text{BaZrO}_3$
$\text{Ga}_2\text{O}_3$ , $\text{BaCO}_3$	700	3	$\gamma\text{-BaGa}_2\text{O}_4$
$\text{NiO}$ , $\text{TiO}_2$	900	10	$\text{NiTiO}_3$
$\text{MgO}$ , $\text{Al}_2\text{O}_3$	900	20	$\text{MgAl}_2\text{O}_4$
$\text{ZnO}$ , $\text{Al}_2\text{O}_3$	900	20	$\text{ZnAl}_2\text{O}_4$
$\text{NiO}$ , $\text{Al}_2\text{O}_3$	900	20	$\text{NiO}, \text{Al}_2\text{O}_3, \text{NiAl}_2\text{O}_4$
$\text{NiO}$ , $\text{Al}_2\text{O}_3$	1800	60	$\text{NiAl}_2\text{O}_4$

<sup>a</sup>Adapted with permission from ref 70. Copyright 2010 The Royal Society of Chemistry.

The very fast heating rates provided by MW methods have advantages beyond the reduction of reaction times. There are numerous reports on the effect of MW synthesis on the size of particles or grains in solids. In some cases, MW heating leads to a reduction in particle size compared to the conventionally synthesized analogue. In the synthesis of tetragonal zirconia nanoparticles using a MW-assisted sol–gel technique, the very fast combustion time leads to extremely small particle sizes in the region of 5–10 nm.<sup>71</sup> Similarly, finer microstructures were observed in  $\text{NaZr}_2(\text{PO}_4)_3$ ,<sup>59</sup>  $\text{CuCrO}_2$ ,<sup>72</sup> and  $\text{LiMn}_2\text{O}_4$ <sup>66</sup> synthesized using MW techniques than samples synthesized conventionally. In the case of the electrode material  $\text{LiMn}_2\text{O}_4$ ,

the small grain size resulted in an increased capacity and enhanced cycle performance.<sup>66</sup>

There are also some examples of MW synthesis resulting in larger particle sizes than conventional synthesis, with consequent influences on the properties of materials. In the production of  $\text{CaCu}_3\text{Ti}_4\text{O}_{12}$  in either a modified DMO<sup>73</sup> or a 1600 W commercial MMC,<sup>74</sup> the products are reported to have a higher permittivity than conventionally synthesized samples, which was attributed to a larger grain size in the MW-synthesized powders. Intriguingly, there is some disagreement in observations of the dielectric loss of these samples; in the report by Yu et al., the dielectric loss of the MW-prepared sample was relatively high, apparently as a result of increased sample porosity.<sup>74</sup> In contrast, Thomas et al. observed that the dielectric loss was lower than that seen in conventional samples, but this can be attributed to the short sintering time used in the synthetic method.<sup>73</sup> In the synthesis of cerium-stabilized yttrium aluminum garnet (YAG:Ce), which is a common component of yellow light-emitting diodes, MW heating leads to YAG:Ce particles that show higher luminescence intensity compared with those prepared by the conventional method.<sup>75</sup> The particle size of the MW-prepared sample was established by analysis of PXD data and found to be larger than conventionally prepared YAG:Ce, despite negligible differences in the measured reaction temperature in each case. The conclusion reached was that the emission intensity of this material has a linear relationship to the crystallite size.

Sample morphology and crystallinity can also be influenced by MW synthesis. In the DMO synthesis of  $\text{LiV}_3\text{O}_8$ , a commonly investigated cathode material for lithium batteries, it was found that morphology, crystallite size, and defect concentration were dependent on irradiation time and power, which in turn directly affected conductivity, discharge capacity, and cycle performance in the product.<sup>61</sup> Samples prepared at a relatively high irradiation power and very high temperatures presented a very stable cycle performance, because as-prepared crystallites had a similar microstructure and small distribution of crystal size.

There have been many studies on the effect of MW heating on the density of samples. Densification and sintering will not be a primary concern of this review, but it should be noted that Wang et al. provided evidence for enhanced densification in the presence of a MW field and the relationship of this phenomenon to MW power. Using a hybrid furnace capable of heating purely conventionally or by a combination of microwave and conventional processes, it was observed that an increase in microwave power results in an increase in relative density, as shown in Figure 7.<sup>76</sup> This conclusion is corroborated by numerous other publications. For instance, sample density is enhanced in MW-synthesized samples of  $\text{YBa}_2\text{Cu}_3\text{O}_{7-x}$ ,<sup>63</sup>  $\text{NaZr}_2(\text{PO}_4)_3$ ,<sup>59</sup>  $\text{LaCrO}_3$ ,  $\text{LaCoO}_3$ , and  $\text{LaNiO}_3$  perovskites,<sup>62</sup>  $\text{La}_{0.8}\text{Sr}_{0.2}\text{MnO}_3$  and  $\text{BaZrO}_3$ ,<sup>77</sup> and yttrium aluminum garnet,<sup>65</sup> among many others.

Prado-Gonjal et al. conducted an extensive study into the use of MWs for synthesis of a range of  $\text{LaMO}_3$  ( $\text{M} = \text{Al, Cr, Mn, Fe, Co}$ ) perovskite materials and observed that only certain precursors yield the respective ternary oxide in a single MW step (Figure 8).<sup>78</sup> Substituted samples could be similarly prepared by MW heating a sol–gel precursor for 30 min prior to a calcination step (500 °C, 2 h, air) in a conventional furnace. As metallic conductors  $\text{LaMnO}_3$  and  $\text{LaCoO}_3$  act as susceptors to drive the MW reaction to completion.<sup>78</sup> The magnetic and electrical properties of the MW-synthesized and MW-assisted

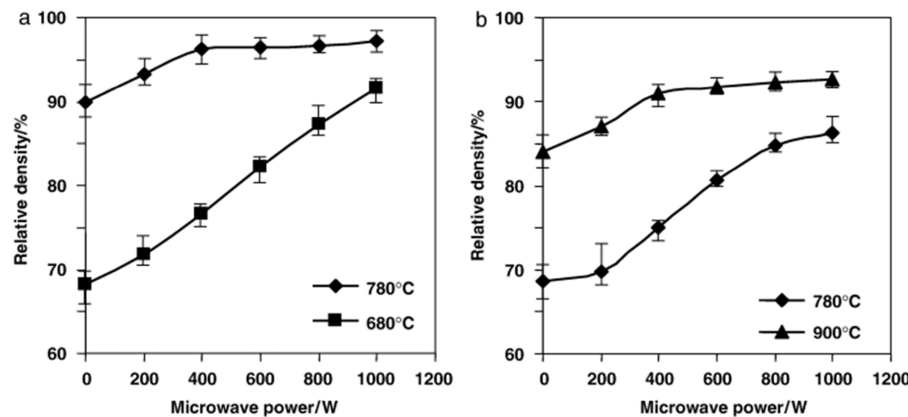


**Figure 7.** Final density curves of (a) “submicrometer” zinc oxide sintered using hybrid MW heating at 680 and 780 °C and (b) “micrometer” zinc oxide hybrid sintered at 780 and 900 °C.<sup>76</sup> Reprinted with permission from ref 76. Copyright 2006 The American Ceramic Society.

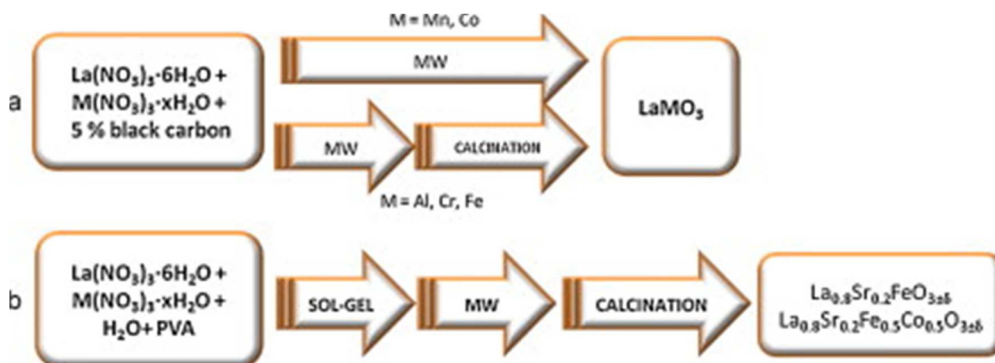


**Figure 8.** Schematic of MW and MW-assisted synthetic routes to lanthanum perovskites.<sup>78</sup> Reprinted with permission from ref 78. Copyright 2011 Elsevier.

synthesized materials compared very favorably to previous literature reports for these phases.

Similarly, LaMO<sub>3</sub> (M = Mn, Co, Fe) perovskites could be synthesized directly using MWs from the respective nitrate hydrates.<sup>79</sup> The resulting samples, however, contained varying amounts of the component binary oxides. It is not clear whether this was a consequence of insufficient mixing of the starting materials or from inefficiencies in the MW heating process. The authors acknowledged that use of an external susceptor may improve the process.

Nonetheless, when phase purity is achieved, MW synthesis can promote catalytic activity in oxide materials such as perovskites. Synthesis of La<sub>1-x</sub>A<sub>x</sub>MnO<sub>3.15</sub> (A = Sr, Ag; x = 0 or 0.2) was achieved using a MW-assisted sol–gel method, and it was observed that the activity of the product in the catalysis of methane combustion was considerably enhanced compared to the corresponding perovskite synthesized using a conventional process.<sup>80</sup> This improvement in activity was attributed to an increase in the surface area of the MW-synthesized material, and it was suggested that lanthanum manganese oxide-based catalysts could compete, in terms of activity and cost, with currently used supported platinum catalysts. Similarly, MWs have been investigated in the production of synthetic todorokite, which is a complex manganese oxide-based mineral used as an oxidation catalyst.<sup>81</sup> The MW reaction is predictably much faster than the conventional synthetic route, and this high reaction rate serves to prevent formation of reduced phases such as Mn<sub>3</sub>O<sub>4</sub> and Mn<sub>2</sub>O<sub>3</sub>. Furthermore, the MW heating profile inhibits growth of magnesium hydroxide deposits on the todorokite surface, leading

to an improvement in catalytic properties; the yield of styrene was improved considerably from the oxidative dehydrogenation of ethylbenzene.

## 6.2. Chalcogenides

Chalcogenide materials are of considerable technological and industrial interest due to their applications in areas including thermoelectrics, semiconducting devices, high-temperature lubrication, catalysis, and optical devices. Conventional solid-state synthesis of chalcogenides can involve multiple steps and therefore be complex and time consuming. There are many examples of the use of MWs to simplify synthesis and reduce reaction times. The majority of examples in the literature have involved solution-based processes, particularly in the case of nanomaterial synthesis. For instance, ZnS nanoballs,<sup>82</sup> CuS nanorods,<sup>83</sup> and Cu<sub>2-x</sub>Te and HgTe nanoparticles<sup>84</sup> have been prepared using solutions refluxed under MW heating. The polyol method is also common in the synthesis of chalcogenides, such as nanosized Cu<sub>2</sub>SnSe<sub>4</sub>,<sup>85</sup> Bi<sub>2</sub>Se<sub>3</sub>,<sup>86</sup> Bi<sub>2</sub>Te<sub>3</sub>,<sup>87</sup> and Cd<sub>1-x</sub>Zn<sub>x</sub>Se<sup>88</sup> alloys. Similarly, fast synthesis of lead, tin, copper, cadmium, silver, iron, and nickel sulfides, selenides, and tellurides has been achieved using simple reactions in alkaline aqueous solutions,<sup>89</sup> while nanocrystalline metal (Cu, Hg, Bi, Zn, Pb) sulfides have been prepared in formaldehyde solution.<sup>90</sup>

In some solution-phase reactions, there have been advantages beyond the decrease in reaction time. For instance, synthesis of ZnS nanoribbons with a hexagonal wurtzite structure was observed for the first time using a MW solvothermal procedure, and these nanoribbons were the smallest to have been obtained at the time.<sup>91</sup> Sample morphology was found to be related to

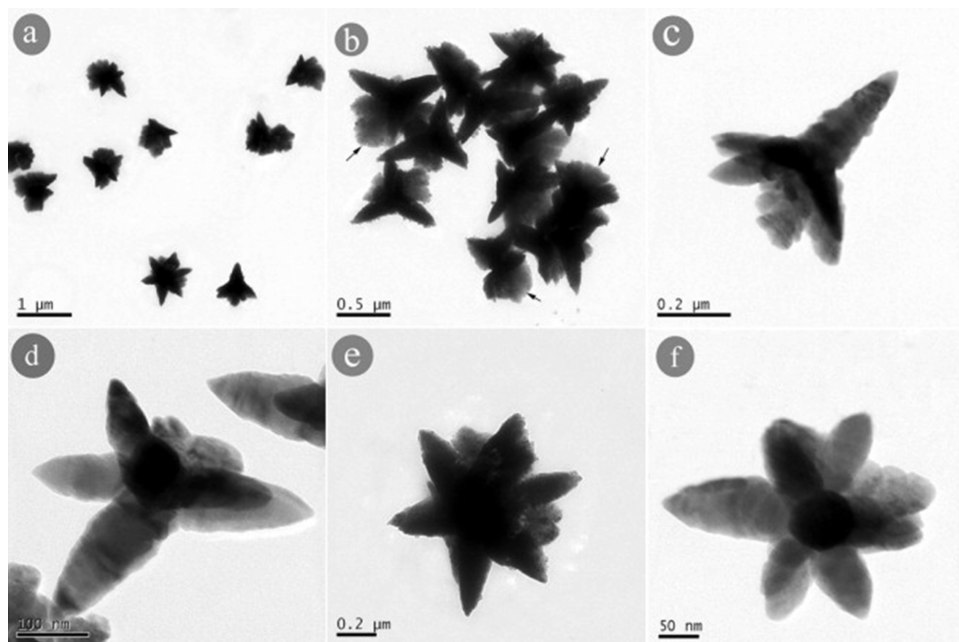


**Figure 9.** Representative TEM images of CdSe multipods synthesized in the presence of polyvinylpyrrolidone (PVP).<sup>93</sup> Reprinted with permission from ref 93. Copyright 2009 Elsevier.

MW irradiation time in the solution-based DMO synthesis of MoS<sub>2</sub>; shorter reaction times resulted in fullerene-like structures containing randomly oriented, highly folded MoS<sub>2</sub> layers with short-range ordering, while longer irradiation periods generated a nanotube morphology alongside the fullerene-like material.<sup>92</sup> These unusual structures featured numerous defects and edges, resulting in the MoS<sub>2</sub> samples being suitable as potential catalysts for hydrodesulfurization reactions. In some cases, the precursors used in MW synthesis are preferred from safety and environmental perspectives than the reagents used conventionally, as is the case in the MW synthesis of CdSe multipods from Cd(NO<sub>3</sub>)<sub>2</sub> and Se.<sup>93</sup> Conventional synthesis of these materials uses hazardous phosphine-based precursors, so use of nitrate starting materials in this MW synthesis offers an attractive alternative. In addition, the morphology of these CdSe nanocrystals was found to be controlled by addition of capping agents of different polarity to give tetrapods, hexapods, octapods, or more complex structures; Figure 9 shows the most complex multipods, which are formed when a nonionic capping agent is used.

In general, solid-state MW synthesis of chalcogenide materials takes place by direct reaction of the appropriate elemental powders, usually in an evacuated silica ampule. In the solid state, it is often possible to take advantage of the dielectric properties of the sulfur, selenium, or tellurium component to improve upon conventional reaction processes, which often suffer from volatilization of the chalcogen, particularly in the case of sulfur and selenium. Chalcogens are generally relatively poor MW absorbers, so application of MW radiation to a mixture of chalcogen and metal powders generally serves to selectively heat the metallic element very rapidly, resulting in extremely fast reaction with the chalcogen before it is able to volatilize.<sup>27</sup>

An example of a direct reaction between elemental powders is the preparation of the ternary sulfide CuInS<sub>2</sub> in a DMO.<sup>94</sup> This reaction requires a total heating time of just 5 min, and reaction to form CuInS<sub>2</sub> is observed to be faster than sublimation of S. Sintering of the resulting CuInS<sub>2</sub> powder is achieved by embedding the reaction tube in a container of CuO, which acts

as a susceptor and reaches a temperature above the melting point of CuInS<sub>2</sub> after MW heating is applied for 7–9 min. This promotes crystallization of the powder into bulk polycrystals in a melt–solidification process, and the resulting material possesses luminescence properties that compare well with those of single crystals grown using a conventional heating method.<sup>95</sup> Similarly, the zintl phases Na<sub>4</sub>SnSe<sub>4</sub>, K<sub>4</sub>Sn<sub>2</sub>Se<sub>6</sub>, and K<sub>4</sub>Sn<sub>3</sub>Se<sub>8</sub> have been synthesized by reaction of the elemental powders under vacuum in a modified DMO.<sup>96</sup> In this case, the MW heating characteristics of the starting materials were also studied individually, revealing that Se was a poor MW susceptor and that the reactions were initiated by the strong interaction of Na, K, and Sn with MWs. The quality of the products was found to be superior to the conventionally synthesized analogues, in which there are often problems with reaction of the metals with the silica ampule. The lack of Si-containing impurities in the MW-synthesized materials was attributed to the short reaction times and direct, volumetric heating of the samples.

A number of other zintl phases have been synthesized using a similar method. Na<sub>3</sub>SbTe<sub>3</sub>, NaSbTe<sub>2</sub>, and K<sub>3</sub>SbTe<sub>3</sub> were produced in a DMO, and it was found that the necessary reaction time and MW power was dependent on the phase being formed.<sup>97</sup> Higher MW power and a short irradiation time were necessary in the synthesis of Na<sub>3</sub>SbTe<sub>3</sub>, which contrasted with the low power and longer reaction time required to produce NaSbTe<sub>2</sub>, while intermediate conditions favored synthesis of K<sub>3</sub>SbTe<sub>3</sub>. In the case of Na<sub>3</sub>SbTe<sub>3</sub>, MW synthesis enabled a phase-pure sample to be produced for the first time. Magneto-resistive Ag<sub>2-δ</sub>Se samples have also been prepared using elemental precursors.<sup>98</sup> Once again, selective heating of the silver powder resulted in rapid product formation without loss of selenium, and in this case, the product was sintered simultaneously, leading to high sample density. Synthesis of bulk powders of MoS<sub>2</sub> and WS<sub>2</sub> was attempted from powdered elemental precursors but found to be unsuccessful,<sup>99</sup> in contrast to the solution-based synthesis discussed above.<sup>92</sup> However, the same publication reported successful use of elemental precursors

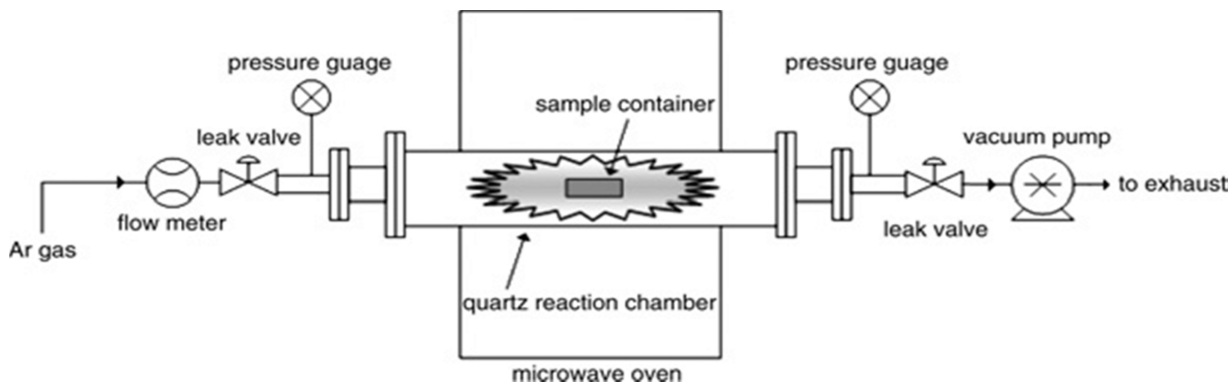


**Figure 10.** Schematic diagram of the apparatus used for synthesis of  $\text{Sb}_2\text{Te}_3$ .<sup>102</sup> Reprinted with permission from ref 102. Copyright 2011 The Institution of Engineering and Technology.

to produce thin films of  $\text{MoS}_2$  and  $\text{WS}_2$ . It is proposed that the success of the *thin film* reactions is related to the higher partial pressure of sulfur in the reaction tube, as the ratio of sulfur:metal is much higher in the thin film case than with the mixture of powders.

Carbothermal reduction is an alternative to direct heating of elemental reagents in the synthesis of strontium sulfide.<sup>100</sup> Conversion of the mineral celestine,  $\text{SrSO}_4$ , to  $\text{SrS}$  is an important step in the commercial processing of strontium ores. In this case,  $\text{SrSO}_4$  was converted to  $\text{SrS}$  in a commercial MW oven in the presence of charcoal, which acted as both a MW susceptor and a reducing agent. A detailed study of the effects of MW irradiation time and percentage of excess charcoal was performed, and it was observed that the rate of temperature increase and the maximum reaction temperature were both higher when the charcoal content was increased, but ultimately 97% conversion to  $\text{SrS}$  occurred after 10 min heating in all cases.

MIP synthesis has also been used in the synthesis of chalcogenides, allowing poor MW absorbers to be heated without use of a susceptor.  $\text{ZnTe}$  nanocrystals have been synthesized by heating elemental Zn and Te powders in an evacuated silica tube using a 900 W MW plasma.<sup>101</sup> Synthesis times were found to be prolonged due to evaporation of Zn and Te during the reactions; the effect of this problem was reduced and reaction times correspondingly decreased when an excess of Zn was used. Similarly,  $\text{Sb}_2\text{Te}_3$  was produced using a near-identical plasma synthesis method, for which the experimental setup is shown in Figure 10, and resulted in the observation that crystallite size increased with increasing irradiation time, although no explanation for the mechanism of crystal growth was provided.<sup>102</sup>

In order for MW methods to become more widely appealing, initially to the solid-state chemistry community and ultimately on an industrial scale, it is necessary to improve our understanding of the way in which these reactions occur. This will allow improvement of predictability and reproducibility and ultimately allow reactions to be designed to give specific products. Some efforts to address this issue have been made in studies of the synthesis of chalcogenides.  $\text{AgInSe}_2$ , for example, has been used as a model system to investigate the effect of sample volume, irradiation time, and grinding of reagents on product phase purity.<sup>103</sup> All three variables were found to have significant effects on the phase purity of  $\text{AgInSe}_2$  in this case. It was observed that product purity varied with sample size, as shown in Figure 11, due to a combination of factors. MW power absorbed by the sample is proportional to the sample volume, which results in

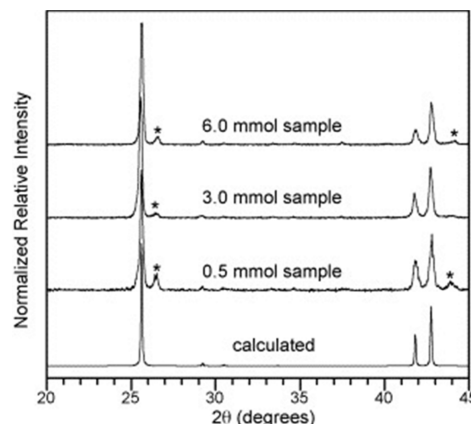


**Figure 11.** PXD patterns obtained for select MW reactions to prepare  $\text{AgInSe}_2$  using different sample volumes as compared to the calculated pattern. All three samples were ground for 20 min followed by irradiation for three 1 min intervals. Asterisks mark diffraction peaks due to the presence of  $\text{AgIn}_3\text{Se}_8$ .<sup>103</sup> Reprinted with permission from ref 103. Copyright 2007 Elsevier.

very small samples not reacting fully. However, it is also necessary to consider penetration depth (eq 5), which means that particularly large samples are also not conducive to high-purity products. Thus, there is an optimum sample size for accessing a pure phase. An optimum irradiation time and procedure was also found, but it was acknowledged that an explanation for this would involve complex analysis of the kinetics and thermodynamics of the reaction. In simple terms, increased grinding time was found to result in improved phase purity. This in itself is not a surprising finding and presumably due to more intimate mixing of reagents, but this is well established and not exclusive to MW reactions.

In the solid-state synthesis of  $\text{Sb}_2\text{Se}_3$ ,  $\text{Sb}_2\text{Te}_3$ ,  $\text{Bi}_2\text{Se}_3$ , and  $\text{Bi}_2\text{Te}_3$  by MW irradiation of elemental powders, the effects of a number of variables on the outcomes of reactions were explored.<sup>104</sup> The effect of sample quantity on phase purity was dependent on which chalcogenide was being synthesized. In the case of  $\text{Sb}_2\text{Te}_3$ , it was observed that there was an optimum sample size at which greatest phase purity was achieved, whereas in  $\text{Sb}_2\text{Se}_3$  reactions, there was a minimum sample size required for reaction to occur. Possible explanations given for the effect of sample quantity on phase purity again invoke MW penetration depth and acknowledge that larger samples are more likely to exceed this depth. Further, it was also recognized that heat dissipation is slower in larger samples due to their smaller surface

area:volume ratio. In fact, the relationships between reaction variables were complex; in some cases, increasing time resulted in increasing purity as might be expected, but in others this was not the case. Sample geometry was reported to have a profound effect on the outcome of reactions; in this case the geometry refers to the powder being either concentrated at the end of the tube in a vertical position or spread along the length of the tube when it was positioned horizontally. Once again, this was rationalized in terms of penetration depth, heat dissipation, or field nonuniformity in the MW apparatus. The findings in this report did not significantly improve understanding of MW reactions, but it was realized that reporting such observations is important to assist in future investigations. Two approaches may ultimately be required to address the lack of understanding of the mechanisms and products of MW reactions. First, use of in-situ techniques is necessary to help rationalize the outcomes of the multitude of reactions that have previously been reported (see section 7). Second, development of reliable models for the MW field distribution and interaction of MWs with solids is essential to help predict the outcome of future reactions (see section 8).

### 6.3. Borides

Significant interest in magnesium diboride arose with the discovery of a superconducting transition of 39 K in the material, and it has since been studied extensively.<sup>105</sup> This interest in MgB<sub>2</sub> inevitably resulted in investigations into alternative synthesis methods, and this led to its successful synthesis in 30 min using a DMO operating at 900 W.<sup>106</sup> Temperatures in this reaction were probed with an optical pyrometer, which showed a surface temperature never exceeding 900 °C, which is noticeably lower than conventional methods ( $\geq 950$  °C). MWs also offer a route to smaller and more uniform MgB<sub>2</sub> grain sizes, which reportedly enhances mechanical properties.<sup>17</sup> Use of carbon as a susceptor in the reaction proves important (as discussed in more detail in a previous publication by the same group).<sup>107</sup> The importance of avoiding C contamination is thus clear, and use of SiC as a susceptor has been reported in successful MW synthesis of MgB<sub>2</sub>.<sup>108</sup> In this way, a complete synthesis in 11 min at only 560 W in a DMO was achieved. A temperature of approximately 800 °C was reported, but the relatively crude nature of the temperature measurement in this study, using a thermocouple postreaction, was acknowledged.

A more recent example of a direct MW synthesis of MgB<sub>2</sub> was performed at various input powers of 0–1 kW.<sup>109</sup> Applying 400–700 W for ca. 10–20 min achieved a temperature of 750 °C. This temperature was then maintained for 30 min using a MW power between 100 and 200 W before cooling to room temperature. PXD indicated that MgB<sub>2</sub> was the major phase and that all impurity peaks were from MgO, which is a common impurity in MgB<sub>2</sub> samples prepared by conventional methods.<sup>110–112</sup> SEM images showed that grain size was homogeneous with a magnitude of several hundred nanometers. The superconducting onset temperature of the sample was measured as 37.6 K, which is in good agreement with MgB<sub>2</sub> prepared by other routes.<sup>113–115</sup>

Another boride which possesses interesting and useful properties is ZrB<sub>2</sub>.<sup>116</sup> ZrB<sub>2</sub> has a number of the advantageous properties associated with refractory materials, e.g., a high melting point (3250 °C) and hardness (36.0 GPa).<sup>117</sup> The material also displays a high resistance to oxidation, high thermal and electrical conductivities, and chemical inertness against molten metals.<sup>118</sup> Importantly, the thermochemical stability of this material meets the requirements applicable to the aerospace industry and more specifically for thermal protection systems for

space re-entry vehicles.<sup>119</sup> MW synthesis of this material has been explored due to the expense and time involved in its production conventionally.<sup>116</sup> Synthesis utilizes ZrO<sub>2</sub> plus either B<sub>2</sub>O<sub>3</sub> or B<sub>4</sub>C as the source of boron. The authors do not provide a specification of the MW cavity, but they reported that the reaction was completed at 1.2 kW in <4 h. The highest reaction temperature reported was 1100 °C, measured by an infrared temperature sensor.

MW arc heating has also been utilized in formation of ZrB<sub>2</sub> nanofibers from the bulk boride.<sup>120</sup> Commercially available ZrB<sub>2</sub> was heated in air inside a 2100 W MMC with a mode stirrer (used to increase the homogeneity of the heating) for 10–45 s per treatment with a variable number of treatments (<5). Use of a 100 mL alumina crucible resulted in arcing in the reactant powder. ZrB<sub>2</sub> heated rapidly during this time and emitted strong flashes of light from the localized arcing. Compared to the starting materials, SEM analysis showed the samples displayed a completely different morphology after MW treatment. The surface appeared much smoother and more homogeneous than the raw powder. Both nanorods and nanofibers were observed, with the larger nanorods being of a mixed composition (mixtures of zirconium, boron, nitrogen, aluminum, and oxygen), while nanofibers were identified as ZrB<sub>2</sub>. It is proposed by the authors that initial MW arcing induces rapid heating, meaning a susceptor is not required. This is possible because the dielectric loss factor increases with temperature, and thus, as the material heats up the absorption efficiency will increase. This treatment of ZrB<sub>2</sub> offers significant potential, and more generally, addition of nanofibers to structural materials to form composites can significantly impact characteristics such as strength, surface energy, conductivity, and reactivity.<sup>121</sup> MW processing might therefore present a route to prepare such (nano)materials that is otherwise not attainable.

### 6.4. Carbides

The refractory carbides are extremely important materials in modern industry. They have a number of advantageous properties<sup>122</sup> and find applications in a variety of fields, e.g., catalysis,<sup>123</sup> high-temperature electronics in nuclear power instrumentation,<sup>124</sup> and optoelectronic devices.<sup>125</sup> However, their synthesis is long and energy intensive.<sup>126</sup> For this reason, as for many other materials, MW heating has been recognized as a viable alternative to conventional heating. A key advantage in the MW synthesis of carbides is the strong coupling of C with MWs. Thus, carbon acts as a combined reactant and susceptor. Synthesis has generally concentrated on the more industrially relevant materials such as tungsten, silicon, and titanium carbide, but many other compounds have also been investigated (Table 2).

In all cases the carbide is synthesized faster and often at a lower temperature by MWs than by conventional heating processes. Many articles also note improved mechanical properties and finer grain size. For example, processing of WC–Co reported by Cheng et al. has a sintering time of less than 30 min in comparison to the hours required conventionally.<sup>154</sup> The reaction setup is illustrated in Figure 12. The reaction temperature was only 1250 °C, which is 250 °C lower than that necessary in the commercial process. In addition, enhanced densification of the product and a fine grain size (~1 μm) was reported. Cheng also reports development of a continuous-flow process in this article; the apparatus is shown in Figure 13. Utilizing a single-mode cavity it is shown how one can successfully sinter up to 1 m long ceramics. This is an important

**Table 2. Examples of Some Carbides Successfully Synthesized by MW Methods Since 1999**

element	carbide
Mg	MgNi <sub>3</sub> C, <sup>127,128</sup> MgCo <sub>3</sub> C <sub>x</sub> <sup>127</sup>
Ca	CaC, <sup>127</sup> Ca <sub>4</sub> Ni <sub>3</sub> C <sub>x</sub> <sup>127</sup>
Si	SiC, <sup>129–131</sup> MoSi <sub>2</sub> –SiC, <sup>132</sup> ZrC–SiC, <sup>133</sup> SiC/C, <sup>134</sup> SiC/SiO <sub>2</sub> , <sup>134</sup> Al <sub>2</sub> O <sub>3</sub> /SiC <sup>135</sup>
Ti	TiC, <sup>134,136–138</sup> Al <sub>2</sub> O <sub>3</sub> –TiC <sup>139</sup>
Fe	Fe–Cu–C and Fe–Ni–C <sup>140</sup>
Co	MgCo <sub>3</sub> C <sub>x</sub> <sup>127</sup>
Ni	MgNi <sub>3</sub> C, <sup>127,128</sup> Ca <sub>4</sub> Ni <sub>3</sub> C <sub>x</sub> <sup>127</sup> Fe–Ni–C <sup>140</sup>
Cu	Fe–Cu–C <sup>140</sup>
Nb	NbC <sup>141</sup> and Nb–Ta–C <sup>141</sup>
Mo	Mo <sub>2</sub> C, <sup>142</sup> Mo <sub>2</sub> C–CNT <sup>143</sup>
Ta	TaC <sup>136,141</sup>
W	WC, <sup>144–151</sup> WC–Co, <sup>18,144,152–154</sup> WC–C <sup>155,156</sup>

step toward development of an industrially viable MW heating apparatus, which will be discussed later (section 8).

Complementing this work, Rodiger et al. published an examination of the penetration depth in various materials, including metals, while investigating WC–Co processing (see Table 3).<sup>144</sup> The article stresses the importance of considering this parameter when designing experiments. The scale-up of batch processes is limited by the penetration depth of the materials to be heated, and this is one reason why considering continuous rather than batch processing is an important step.

In 2005 Breval et al. published work providing a comparison of MW and conventionally sintered WC–Co in which transmission electron microscopy (TEM) was used to show that the cobalt phase in the MW-processed product dissolves nearly no tungsten.<sup>153</sup> This is noteworthy given that conventionally up to 20 wt % tungsten can be dissolved into the Co binder phase. In addition, a more uniform distribution of the Co binder and finer WC grains were observed in the MW-produced composite, which resulted in a material 1–5 GPa harder than the conventionally synthesized product. It was also reported that the MW-synthesized sample is six times more resistant to

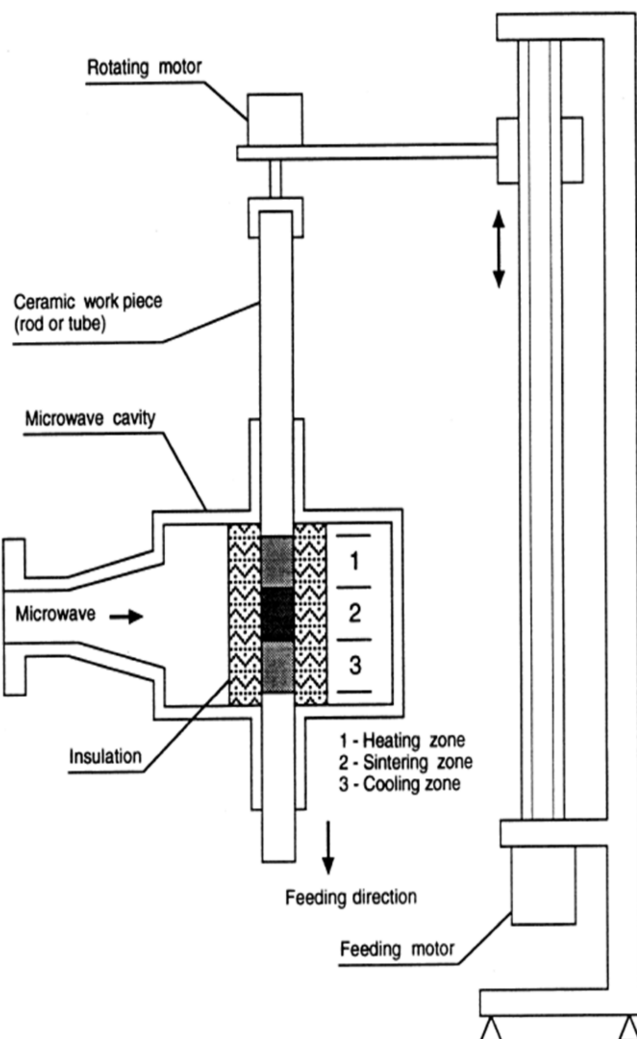


**Figure 13.** Apparatus for continuous MW sintering of ceramics up to 1 m long and 10 cm in diameter.<sup>154</sup> Reprinted with permission from ref 154. Copyright 1997 Springer Science and Business Media.

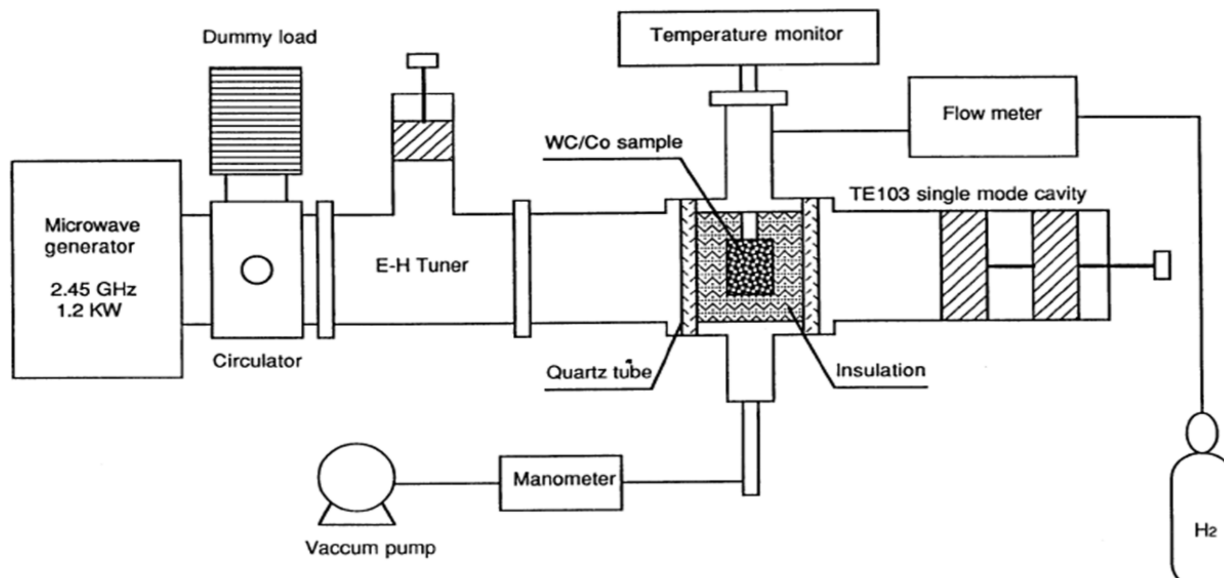


**Figure 12.** Schematic of the SMC used in the sintering of WC–Co.<sup>154</sup> Reprinted with permission from ref 154. Copyright 1997 Springer Science and Business Media.

Table 3. Penetration Depths of 2.45 GHz MWs in Different Materials<sup>144</sup>

metals		metallic conductors		insulators		powder-metallurgical green-parts		
Al	Co	WC	TiC	Al <sub>2</sub> O <sub>3</sub>	H <sub>2</sub> O	WC-6Co	Al <sub>2</sub> O <sub>3</sub> -10 Al	Al <sub>2</sub> O <sub>3</sub> -30 TiC
1.7 $\mu\text{m}$	2.5 $\mu\text{m}$	4.7 $\mu\text{m}$	8.2 $\mu\text{m}$	10 m	1.3 cm	7.5 cm	31 cm	36 cm

corrosion (measured via weight loss after immersion in 15% HNO<sub>3</sub> for 48 h) and twice as resistant to erosion (tested by a grit blasting method).

Given that there are numerous reports of rapid carbide syntheses by MWs, it is surprising to note that comparatively little work has been performed probing reaction mechanisms or to elucidate experimental observations. Rapid WC synthesis (W + C) published by Vallance et al. is one such article which begins to shed light on solid-state MW reactions, specifically of the transition metal carbides.<sup>147,151</sup> WC was synthesized in a single-mode cavity at 3 kW in 20 s. By monitoring reaction temperature using an optical pyrometer and measuring sample dielectric properties ex-situ it could be shown that reaction temperature, phase fraction, and dielectric properties were directly related, as illustrated in Figure 14. Ultimately this enabled a degree of control over the process as well as building on the understanding of how MWs interact with materials and as a result how these materials react. In addition, a temperature plateau was observed at high product purity manifesting in a self-terminating reaction. The authors attributed this behavior to the phenomenon of self-

limiting heating. This is where  $d\epsilon''/dT$  (change in dielectric loss) decreases rapidly above a certain temperature; in this reaction it coincides with formation of WC. This is in contrast with the rapid heating which initially occurs during reaction.

Vallance et al. also applied the same technique in the synthesis of Mo<sub>2</sub>C (achieved in 10 s from Mo + C), which revealed similar trends to those seen in the synthesis of WC.<sup>142</sup> Correlations between temperature and phase purity were also made in the synthesis of ZrC-SiC composites from oxide and carbon starting materials.<sup>133</sup> Das et al. examined the reaction kinetics by following the change in phase with temperature over a 30 min period.<sup>133</sup> This monitoring offered a detailed understanding of the phases present at specific temperatures and thus some indication of the reaction mechanism. It is also noted that a slow increase in the MW power up to 700 W was required initially to avoid pellet disintegration. This could well be due to the gas evolved from the pellet as the oxide starting materials are reduced.

In a systematic study, Carassiti et al. investigated the effects of several variables on the ultrarapid synthesis of high-purity SiC.<sup>129</sup> The variables investigated included the choice of Si and C source, use of a binder in pelletizing, and choice of MW source (MMC vs SMC). The effect of these variables on carbide purity and processing time were discussed. PXD of samples synthesized in an MMC revealed that reactions of silicon with activated carbon produce single-phase  $\beta$ -SiC after 5 min. When graphite was used, pellets always fractured during reaction in the MMC. Graphite and silicon reflections only disappeared after long irradiation times. In reactions of silica with activated carbon, violent pellet fracturing occurred and the course of the reaction appeared more complex. PXD showed  $\beta$ -SiC at short irradiation times, but as times increased graphite and SiO<sub>2</sub> reflections were apparent, and at extended times SiO<sub>2</sub> increased in phase fraction while SiC decreased. In the SMC phase-pure  $\beta$ -SiC was obtained from a dry pellet of Si and graphite in 20 s, as demonstrated in the PXD pattern in Figure 15a. Longer reactions started to produce the high-temperature polymorph, 6H-SiC. The type of cavity used and power applied also had a marked effect on the carbide morphology. MMC syntheses with Si and activated carbon produced SiC nanofibers, as shown in Figure 16, and a water binder appeared critical for their growth. SMC reactions produced denser materials, and larger crystallites were formed (Figure 15b). SMC reactions with activated carbon, however, produced the smallest carbide particle size, suggesting a degree of pseudomorphism in the reaction.

Synthesis of carbides from metal oxides is also possible. A susceptor is often required to drive reactions, e.g., in rapid synthesis of Mo<sub>2</sub>C from MoO<sub>3</sub>.<sup>142</sup> Hassine et al. used metal oxides in the synthesis of TiC (TiO<sub>2</sub> + C, <1550 °C) and TaC (Ta<sub>2</sub>O<sub>5</sub> + C, <1500 °C).<sup>136</sup> In both cases the power was slowly ramped from 500 W to 5 kW to avoid thermal shock of the reaction crucible, and both syntheses were completed in 1 h (cf. 6 h at 1750 °C required conventionally). Unfortunately, commercial-grade TiC could not be produced due to excessive grain growth as the temperature increased. Hassine et al. did, however, observe that the reaction proceeded via TiO<sub>7</sub> before reduction to Ti and that the more commonly observed

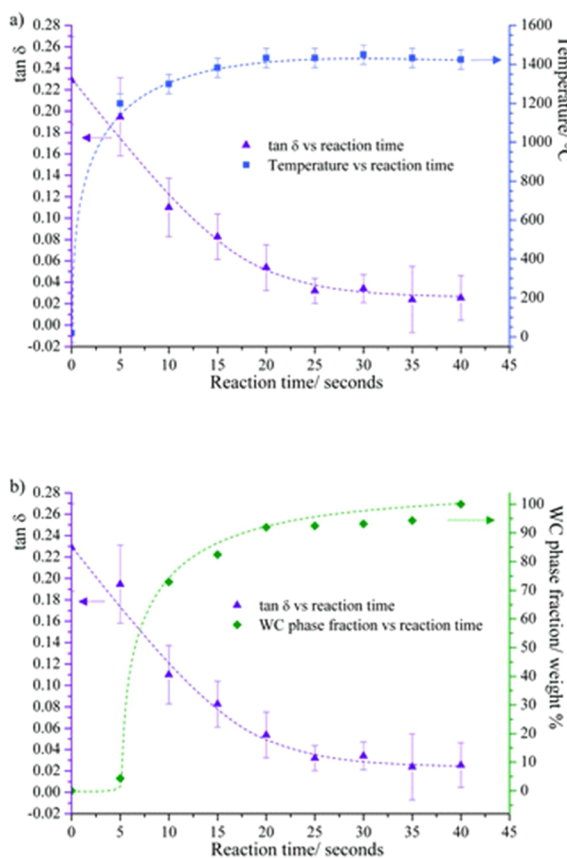
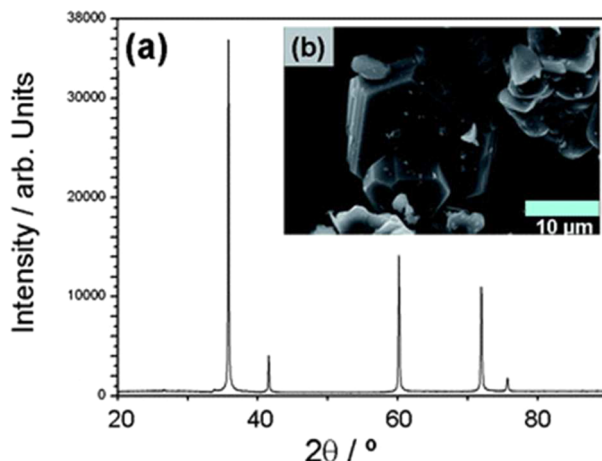
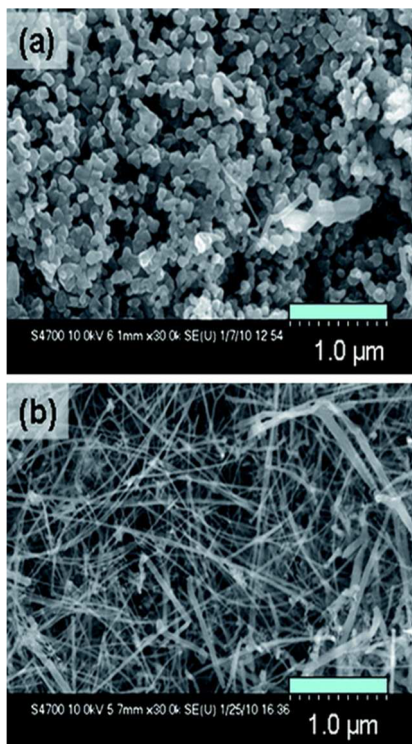


Figure 14. (a) Loss tangent and reaction temperature versus reaction time for reaction of W + C in the 3 kW SMC; (b) loss tangent and WC phase fraction versus reaction time for reaction of W + C in the 3 kW SMC (trend lines serve only as a guide to the eye).<sup>151</sup> Reprinted with permission from ref 151. Copyright 2012 The Royal Society of Chemistry.



**Figure 15.** (a) PXD pattern and (b) SEM micrograph of SiC synthesized in a SMC reactor by irradiation at 3 kW for 20 s.<sup>129</sup> Reprinted with permission from ref 129. Copyright 2011 The Royal Society of Chemistry.



**Figure 16.** SEM micrographs of SiC prepared from Si + C in a MMC: (a) nanoparticle clusters and (b) nanofibers.<sup>129</sup> Reprinted with permission from ref 129. Copyright 2011 The Royal Society of Chemistry.

intermediate  $Ti_2O_3$  was never present. This suggestion of an alternative reaction pathway may be due to the reduction in reaction temperature.

There are few examples of the MW synthesis of more complex carbides. In 2009, Valence et al. reported a MW heating route to binary and ternary niobium and tantalum carbides, which are used in the manufacture of cutting tools and wear-resistant parts.<sup>141</sup> The authors used a single-mode cavity reactor in the ultrarapid MW synthesis of ternary phases for the first time. Experiments were performed in a  $TE_{10n}$  single-mode cavity with

a power of 3 kW (at 2.45 GHz) and yielded a solid solution of single-phase carbides, each in a fraction of a minute.

### 6.5. Silicides

There are a number of silicide materials of significant interest for commercial applications.<sup>157</sup> Certain silicides with high thermal stability, corrosion resistance, and favorable mechanical properties have been recognized as potential materials for both high-temperature structural and electronic applications, e.g., jet engine components and field effect transistors, respectively.<sup>158</sup> This interest has made these compounds a key target for developing a simpler and faster synthetic route via application of MW technology. This has been achieved by a number of different groups with a variety of silicides (Table 4; Figure 17).

**Table 4. Examples of Some Silicides Successfully Synthesized by MW Methods Since 1999**

element	silicide
Li	$Li_{21}Si_5$ <sup>159</sup>
Mg	$Mg_2Si$ <sup>160</sup>
Ca	$CaAlSi$ and $CaAl_{1-x}Cu_xSi$ <sup>161</sup> (Figure 17)
Ti	$TiSi_2$ <sup>162</sup>
Co	$CoSi_2$ , <sup>158,162,163</sup> $CoSi$ <sup>158</sup>
Ni	$NiSi$ and $NiSi_2$ <sup>163</sup>
Mo	$MoSi_2$ , <sup>162</sup> $Mo_5Si_3$ <sup>164</sup>
W	$WSi_2$ <sup>162</sup>

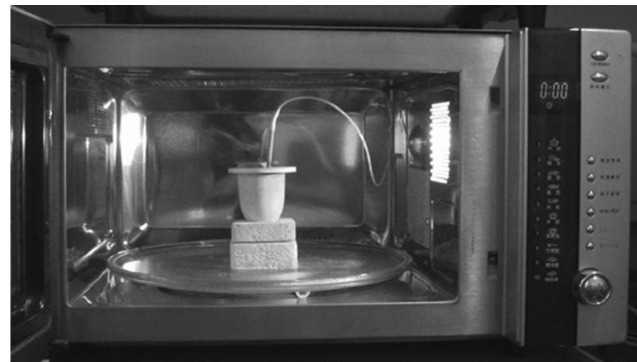


**Figure 17.** Reaction setup used by Yang et al. in the synthesis of pure and Cu-doped CaAlSi superconductors.<sup>161</sup> Reprinted with permission from ref 161. Copyright 2008 IOP Publishing.

Being brittle materials, the cobalt silicides, among others, pose a number of processing difficulties. Combustion synthesis is a technique often applied to the synthesis of bulk products. This technique uses an initiating “trigger” to begin a self-sustaining exothermic reaction. In the case of the cobalt silicides the reactions are not exothermic enough to be self-sustaining. In such cases combustion synthesis can lead to inhomogeneous products and thus nonuniform microstructure and properties. Many proposed routes of activation have been explored including thermal, mechanical, and electromagnetic energy.<sup>158</sup>

As a potential solution to these issues, Jokisaari et al. propose a route termed “MW activated combustion synthesis” (MACS), and since MW energy is absorbed volumetrically, relatively high homogeneity can be achieved.<sup>158</sup> Using the MACS setup shown in Figure 18, products were compared to those prepared via either thermally activated combustion synthesis (TACS) or conventional combustion synthesis (CS).

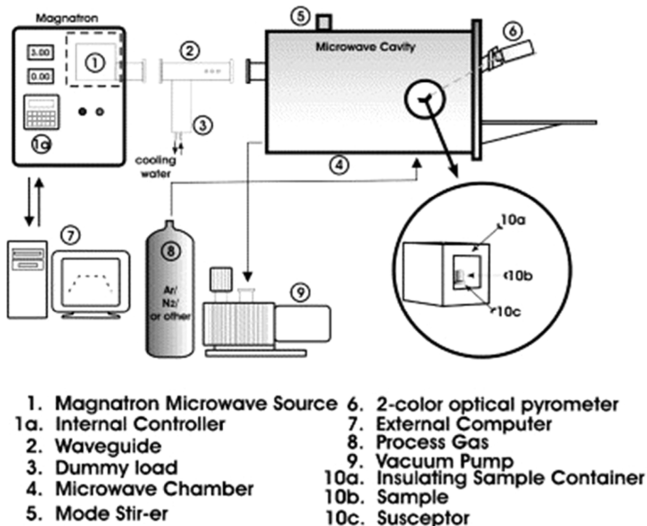


Figure 18. Schematic of the MACS system utilized by Jokisaari et al.<sup>158</sup> Reprinted from with permission from ref 158. Copyright 2005 Elsevier.

The reaction to produce CoSi behaved much the same way whether implemented by MACS, CS, or TACS methods; however, reaction to CoSi<sub>2</sub> behaves in a significantly different manner via MACS compared to CS. For the CS reactions, PXD showed residual silicon which was attributed to incomplete reaction. Samples had a banded microstructure with dense regions alternating with porous ones. In TACS, PXD confirmed that the product was a phase mixture of CoSi and CoSi<sub>2</sub>, with CoSi being the major phase. However, the product failed to densify. In MACS a uniformly porous product formed which was determined to be single-phase CoSi<sub>2</sub>. The product reached full density after an additional 20 min of processing. This also led to an increased grain size (>300 μm) and formation of a secondary Si-rich phase. The authors showed MACS to be a rapid and an effective means of synthesizing cobalt silicides with higher phase purity than more traditional methods.

This synthetic method was also employed by the same group in the synthesis of single-phase Mo<sub>5</sub>Si<sub>3</sub>.<sup>164</sup> Again, the MW reaction was compared to conventional CS and TACS. Via CS stable combustion could not be maintained. This gave an inhomogeneous product composed of Mo<sub>5</sub>Si<sub>3</sub>, MoSi<sub>2</sub>, Mo, and Si. Under TACS Mo<sub>5</sub>Si<sub>3</sub> was synthesized but was of low quality containing unreacted starting material and secondary phases. The MACS process successfully activated the reaction and drove the reaction to form nearly phase-pure products containing a small amount of Mo but with no other secondary phases present. The MACS sample also displayed a more uniform microstructure than the samples prepared by other methods.

#### 6.6. Nitrides and Pnictides

Nitride materials have been used in recent years in a wide range of applications.<sup>165–167</sup> Many binary nitrides possess very high thermal, mechanical, and chemical stability.<sup>168</sup> Conversely, other nitrides are characterized by low densities, which have technological interest in lightweight applications.<sup>169</sup> Usually, commercially important nitride powders are conventionally synthesized via carbothermal reaction of their oxides and subsequent nitridation or by direct nitridation of the metals.<sup>170,171</sup> In general, nitride formation from oxide precursors requires relatively long processing times, and this often results in incomplete nitridation, leading to oxygen (and carbon)

impurities. Moreover, in conventional processing, initial nitriding of the surface can limit nitrogen diffusion into the bulk metal.

MW synthesis has the potential to solve some of the problems encountered in traditional nitride syntheses. First, given that shorter reaction times and enhanced reaction kinetics are possible for appropriately designed MW syntheses, it becomes conceivable that the purity of nitride products might be improved. For instance, Liu et al. demonstrated that synthesis of TiN from rutile TiO<sub>2</sub> in a single-mode cavity at 1.5 kW was possible with reaction times reduced over conventional methods by a factor of 10.<sup>172</sup> Further, the reported reaction temperature was 1473 K as compared to 1573–1723 K required conventionally, and the purity of the final TiN product is increased vs the conventional carbothermal reduction.<sup>173</sup>

Second, the surface nitridation prevalent from conventional methods can be overcome by the inverse temperature gradient in MW synthesis, leading to complete nitridation of the metal. Titanium and chromium nitrides have been successfully synthesized in a multimode cavity by reaction of the appropriate metal powders in a fluidized bed with the reactive gas (N<sub>2</sub> and/or NH<sub>3</sub>) as the fluidizing medium.<sup>174</sup> Ultimately, the high reaction rates attributed to MW radiation can effectively influence the microstructure of the material synthesized; particle agglomeration and densification can be reduced, and in some cases a wide range of nanostructures have been produced unexpectedly. An example of this behavior has been reported by Vaidhyanathan and co-workers, who observed that AlN produced by MW-assisted combustion consisted mainly of fibers 100–200 nm thick and lengths varying from 20 to 40 μm.<sup>175</sup> These nanofibers were distributed throughout the surface, center, and bottom of the reaction pellet.<sup>175</sup> Single-crystalline whiskers of AlN with hexagonal morphology (>5 μm length) were also observed in some portions of the reaction compact, although in a minor proportion. Fabrication of TiN and VN by analogous routes, however, led to particles with average sizes estimated at 250 and 900 nm, respectively.<sup>175</sup>

Since the review by Rao et al. in 1999,<sup>6</sup> the majority of publications regarding MW synthesis of nitrides has involved the use of MMCs, e.g., rapid synthesis (25 s) of Ta<sub>2</sub>N in a 1.6 kW DMO.<sup>176</sup> There are, nevertheless, some limited examples where SMCs have been successfully employed, e.g., in the synthesis of Si<sub>3</sub>N<sub>4</sub><sup>177</sup> and AlN.<sup>178</sup> Table 5 summarizes binary and ternary

Table 5. Selected Nitrides Successfully Synthesized by MW Methods Since 1999

element	nitride
Li	LiSi <sub>2</sub> N <sub>3</sub> and Li <sub>2</sub> SiN <sub>2</sub> <sup>175</sup>
Al	AlN <sup>175,178,179</sup>
Si	LiSi <sub>2</sub> N <sub>3</sub> and Li <sub>2</sub> SiN <sub>2</sub> , <sup>175</sup> Si <sub>3</sub> N <sub>4</sub> <sup>177,180</sup>
Ti	TiN <sup>46,175,180</sup>
V	VN <sup>46,175,180,181</sup>
Mn	Mn <sub>4</sub> N and Mn <sub>3</sub> N <sub>2</sub> <sup>182</sup>
Ga	GaN <sup>46,175,183</sup>
Ta	Ta <sub>2</sub> N <sup>176</sup>

nitrides successfully produced using MW methods since the turn of the millennium. Some selected examples of various approaches to MW syntheses of nitrides are presented in more detail below.

Brooks et al. reported the synthesis of GaN, TiN, and VN in an MMC using an ammonia MIP.<sup>46</sup> The precursors for these syntheses were Ga<sub>2</sub>O<sub>3</sub>, TiO<sub>2</sub>, and V<sub>2</sub>O<sub>5</sub>, respectively. Initially,

these oxides were placed in an alumina boat within the cavity which was then slowly evacuated to  $10^{-2}$  mbar; subsequently, ammonia was introduced at a flow rate of  $113 \text{ cm}^3 \text{ min}^{-1}$  (20 mbar) to produce the nitrides. Reactions were completed at 2.5, 3.5, and 6 h respectively; intermediate grindings were necessary for full conversion. The authors estimated the plasma temperature to be 1043–1074 K at the power used (900 W) by exposing salts of known melting point (i.e., KCl and NaCl) to the plasma for 10 min. The melting process was thus useful as an indicator of the equilibrium temperature in the plasma. MIP reactions in an SMC have also been attempted for preparation of TiN from  $\text{TiO}_2$ , although interestingly longer reaction times were reported for these reactions than the MMC equivalents above.<sup>184</sup>

GaN has also been synthesized by plasma methods in a multimode MW via reaction of molten Ga metal previously heated conventionally to 883–973 K. Two stages of treatment were employed: (1) an  $\text{H}_2$  plasma and (2) an  $\text{N}_2$  plasma so as to eliminate oxide impurities and form the nitride, respectively.<sup>183</sup> Hydrogen and nitrogen plasmas operated at 420 W under pressures of 200 and 200–400 Pa respectively. It was reported that the yield of polycrystalline GaN increased at longer nitrogen plasma exposure times, reaching a yield of 96% of GaN after 3 h; images of the reaction products are shown in Figures 19 and 20.

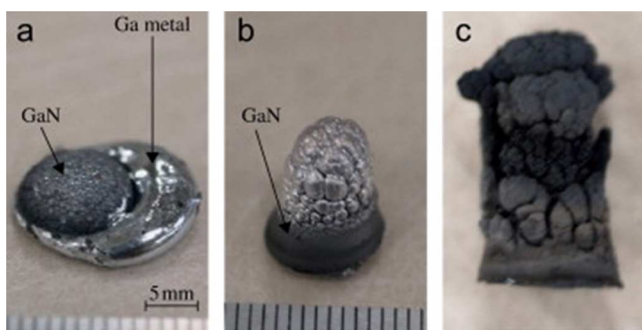


**Figure 19.** Typical GaN reaction products obtained at nitrogen plasma exposure times of (a) 10, (b) 60, and (c) 120 min.<sup>183</sup> Reprinted with permission from ref 183. Copyright 2008 Elsevier.

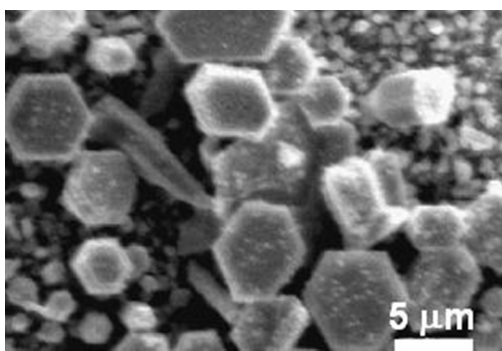


**Figure 20.** SEM image of the as-formed GaN material shown in Figure 19c.<sup>183</sup> Reprinted with permission from ref 183. Copyright 2008 Elsevier.

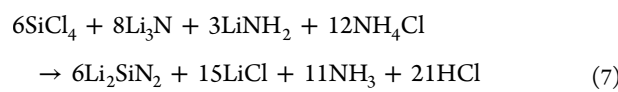
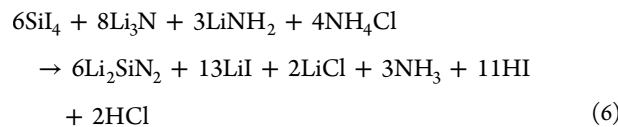
GaN grew from the bottom to the top of the BN crucible used. It was proposed that initial nitridation on the surface layer of the Ga melt forms Ga–N clusters, followed by displacement of the Ga–N clusters to the bottom of the melt by thermal convection.

In a variation on the plasma reactions described above, VN can be prepared via decomposition of gaseous vanadium oxytrichloride,  $\text{VOCl}_3$ , in an  $\text{N}_2/\text{Ar}/\text{H}_2$  MW plasma at atmospheric

pressure.<sup>181</sup> Kabouzi et al. estimated the temperature in a nitrogen discharge to be around 6000 K via studies on the rotational temperatures of  $\text{N}_2^+$  under a MW field.<sup>185</sup> Nanospheres (33–36 nm) of VN were produced by this method. Similarly, TiN,  $\text{Si}_3\text{N}_4$ , and VN can be prepared from the respective chloride precursors,  $\text{MCl}_4$ , using an analogous gas-phase method.<sup>180</sup>

Nitrides can be prepared by MW methods from solid metal-containing sources without invoking MIPs, however. Vaidyanathan et al. utilized MW combustion synthesis in the synthesis of TiN, VN, AlN, and GaN via reaction of the compacted porous metal powders (or  $\text{Ga}_2\text{O}_3$  for GaN) with  $\text{N}_2$  gas at 800 W in an MMC.<sup>175</sup> Metal powders were mixed thoroughly with  $\text{NH}_4\text{Cl}$  in a 1:1 weight ratio and compacted at a pressure of 75–300 MPa. The porosity in the metal powders is created by sublimation of  $\text{NH}_4\text{Cl}$  at temperatures below the ignition temperature.  $\text{N}_2$  gas was flowed throughout the sample ( $500 \text{ mL min}^{-1}$ ) in order to “occupy the voids” left by sublimation of  $\text{NH}_4\text{Cl}$ . A dual-wavelength optical pyrometer indicated that  $\text{NH}_4\text{Cl}$  sublimation starts at 673 K and lasts for less than 1 min. Ignition and combustion temperatures ( $T_{\text{ig}}$  and  $T_{\text{co}}$ ), which ranged from 848 to 1273 K, were found to be totally dependent on the metal used. It was found that  $T_{\text{ig}}$  and  $T_{\text{co}}$  increased in the order  $\text{AlN} > \text{VN} > \text{TiN}$ , which was attributed to (1) a higher reaction enthalpy for the formation of AlN ( $-418.4 \text{ kJ mol}^{-1}$ ) vs TiN ( $-336 \text{ kJ/mol}$ ) and (2) the higher thermal conductivity of Al (AlN), which facilitates dissipation of thermal energy; hence, greater temperatures for reaction completion are needed. The authors reported a high crystallinity and yield of ca. 100% for the nitrides described in this paper, which contrasts with the conventional combustion synthesis where a purification step is required.<sup>179</sup> Peng and Binner later reported the synthesis of AlN from reaction of an Al powder bed under  $\text{N}_2$ ; the higher reaction temperatures achieved here (1439–1553 K) might compensate for the absence of the aforementioned  $\text{NH}_4\text{Cl}$  additive.<sup>186</sup>

Solid-state metathesis (SSM) has also been used in MW synthesis of nitrides. Anderson et al. reported synthesis of the fast ionic conductor  $\text{Li}_2\text{SiN}_2$  via a metathesis reaction involving the silicon halides ( $\text{SiCl}_4$  or  $\text{SiI}_4$ ) and  $\text{Li}_3\text{N}$  as a nitrogen source.<sup>187</sup> Here, the heat is derived from the ability of the ionic conductor,  $\text{Li}_3\text{N}$ , to couple efficiently with MWs (without the need for a MW susceptor). This heat was sufficient to initiate the metathesis reaction. Reactions were initiated at 1100 W (100% power setting), and after approximately 1–3 min for  $\text{SiI}_4$  and 10–18 min for  $\text{SiCl}_4$  the applied field was stopped. Figure 21 shows a typical thermal image of an SSM reaction in progress showing multiple reaction zones.  $\text{NH}_4\text{Cl}$  and  $\text{LiNH}_2$  were added so as to regulate the reaction temperature and enhance the yield of  $\text{Li}_2\text{SiN}_2$  (vs  $\text{LiSi}_2\text{N}_3$ ), respectively. The reactions produced by this method are shown in eqs 6 and 7.  $\text{Li}_2\text{SiN}_2$  was isolated by washing with water-free solvents such as dimethyl formamide and dry methanol.



To the best of our knowledge, there is only one report in the literature of MW-synthesized pnictides other than nitrides.<sup>188</sup> In

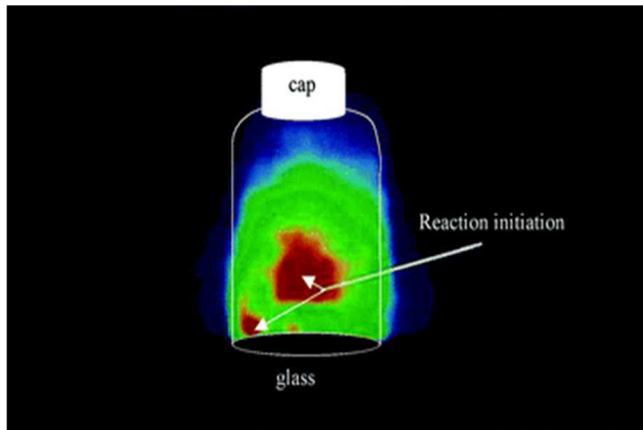


**Figure 21.** Thermal image taken through the door of the DMO during reaction 7. Reaction zones (orange-red light) are marked with arrows, and the outline of the reaction vial is added in white. Red, orange, and yellow areas correspond to the hottest areas in the reaction vessel, whereas green and blue regions represent cooler areas.<sup>187</sup> Reprinted with permission from ref 187. Copyright 2006 The Royal Society of Chemistry.

this study, the intermetallic lithium alloys  $\text{Li}_3\text{Bi}$  and  $\text{Li}_3\text{Sb}$  were successfully prepared from the elements in an evacuated carbon-coated quartz ampule. Syntheses were conducted using an MMC (900 W, 80% power, 2.45 GHz) for 2 and 1 min, respectively. The preparation method reported here contrasts to the conventional alloying and electrochemical deposition techniques used for this purpose, which often require high temperatures and complicated apparatus.<sup>189,190</sup> Despite the limited examples to date, we would anticipate that MW methods could address the main difficulties encountered in conventional pnictide syntheses, namely, long processing times, high reaction temperatures, and complicated synthetic routes.<sup>191</sup>

### 6.7. Carbonitrides and Oxynitrides

The focus of MW processing in formation of carbonitrides has very much been on chemical vapor deposition, which is beyond the scope of this review.<sup>192–196</sup> Solid-state MW synthesis of members of the  $\text{V}_{1-x}\text{Ti}_x(\text{C}, \text{N})$  system is reported by West et al.<sup>138</sup> The MW carbothermal reduction ammonolysis/carburiza-

tion (MW-CRAC) was carried out in a modified reactor, shown in Figure 22, which allowed reaction under anaerobic conditions. Anaerobic conditions were essential for prevention of oxide formation. This modified reactor also offered control over feed gas and gas flow rates. For the synthesis of the bimetallic nitrides,  $\text{V}_2\text{O}_5$  and  $\text{TiO}_2$  were ground in a 2:1 ratio with excess amorphous carbon (acting as reductant, carbon source, and susceptor) and reacted under a flowing  $\text{NH}_3$  gas stream. PXD revealed  $\text{NaCl}$  structures with a cell parameter,  $a$ , that increases with  $x$ . PXD and energy-dispersive X-ray analysis (EDX) both supported the conclusion that mixed metal carbonitrides were being formed in each of the experiments. Reaction times are an order of magnitude quicker than those for the respective monometallic carbides and nitrides prepared by conventional heating methods.<sup>197</sup>

MW heating has been used in the synthesis of aluminum oxynitride (ALON), which has promising mechanical and optical properties due to its unusual transparency.<sup>198</sup> Cheng and co-workers synthesized single-phase ALON ( $\text{Al}_{123}\text{O}_{27}\text{N}_5$ ) from a ball-milled mixture containing 67.5 mol %  $\text{Al}_2\text{O}_3$  and 33.5 mol % AlN. MW heating was performed in a single-mode cavity reactor for 60 min under flowing ultra-high-purity  $\text{N}_2$  gas at 1 atm. This synthesis yielded both a marked reduction in processing time and a high phase purity compared to conventional synthesis methods.<sup>199</sup>

A silicon aluminum oxynitride,  $\beta'$ -SiAlON, has also been synthesized using a similar MW-assisted carbothermal reduction/nitridation process using the mineral kaolinite ( $\text{Al}_2\text{Si}_2\text{O}_5(\text{OH})_4$ ) and carbon black as starting materials.<sup>200</sup> It was observed that the optimum conditions for synthesis of a single-phase oxynitride of formula  $\beta'$ - $\text{Si}_3\text{Al}_3\text{O}_3\text{N}_5$  involved MW heating at 600 W for a total of 60 min under flowing nitrogen. A combination of PXD and  $^{19}\text{Si}$  nuclear magnetic resonance (NMR) spectroscopy data collected from samples at different stages of reaction was used to gather information about the mechanism of the oxynitride formation, with SiC, mullite ( $\text{Al}_6\text{Si}_2\text{O}_{13}$ ), and  $\text{SiO}_2$  observed as intermediate phases in the synthesis.

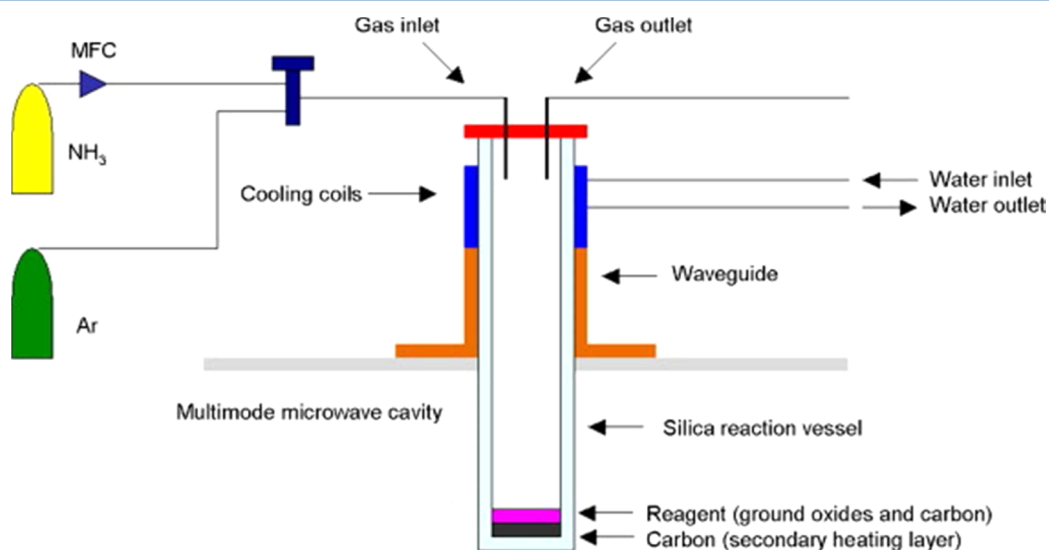


**Figure 22.** Schematic of the MW-CRAC reactor.<sup>138</sup> Reprinted with permission from ref 138. Copyright 2009 Elsevier.

## 7. IN-SITU APPROACHES TO THE STUDY OF MICROWAVE REACTIONS

### 7.1. Necessity of in-Situ Techniques

In the past decade, huge numbers of publications have demonstrated that MW techniques are a viable route to the synthesis of an extensive selection of solids from all areas of the periodic table. However, the reasons behind the advantages that MW methods undoubtedly bring to solid-state synthesis remain unclear. As discussed above, it has been consistently observed that MW reactions lead to significantly faster reaction times, lower reaction temperatures, alternative mechanistic pathways, and novel reaction products when compared to conventional solid-state synthesis methods. Unfortunately, there are also numerous issues with the use of MW heating in solid-state syntheses, which mainly arise from the lack of control and reproducibility of the reactions, the considerable difficulty in rationalizing the outcomes, and a fundamental lack of understanding of the interaction of MWs with solids. Analysis of the products of MW reactions allows characterization of the materials formed but gives little insight into the mechanisms of these reactions or how or why they occur.

Ultimately, in-situ reaction probes are needed to gain this additional information, but the challenge of developing such in-situ methods is considerable. First, the ultrafast nature of MW reactions requires at least an equally fast analysis technique. Second, it is necessary for the analytical procedure to be compatible with the requirements of MWs; the technique must not interact with the MW field and must be able to be applied to a sample that is contained within a MW applicator. Temperature measurement, for instance, is difficult to achieve in a MW system, as devices that would be used conventionally, such as thermocouples, are made of metals and so distort the MW field. In some reaction configurations, it is possible to use an optical pyrometer to determine temperature, but even then pyrometers are limited to a certain restricted temperature range and provide a measurement only of the surface temperature of a sample, which may be significantly different from the bulk. Studying the mechanism or the structural evolution of components in a MW reaction has additional complications because it is necessary to combine the requirements of both the analytical technique and the MW reactor. In consequence, in-situ structural investigations of these reactions are very few in number, but a handful of ground-breaking studies have been published.

### 7.2. In-Situ Studies Using X-rays

There have been several reports of the use of X-rays as an in-situ structural probe in MW reactions. Robb et al. used laboratory PXD to study the MW heating of silver iodide, which undergoes a phase transition from wurtzite-type  $\beta\text{-AgI}$  at room temperature to body-centered cubic  $\alpha\text{-AgI}$  at elevated temperatures.<sup>201</sup> Heating was performed using a prototype MW applicator, shown in Figure 23, and also by convection heating with a variable-temperature heat gun for comparison. Using conventional heating, the phase transition from  $\beta$ - to  $\alpha\text{-AgI}$  was found to occur at  $412 \pm 2$  K, while under MW irradiation, the transition temperature ( $T_c$ ) was  $380 \pm 10$  K, as illustrated in Figure 24. A hypothesis for this observation was offered in which the MW energy is able to interact with low-energy transverse optical (TO) modes in the  $\beta\text{-AgI}$  via a multiphonon process, as opposed to interaction with rotational or vibrational modes, as is the case in conventional heating. Redistribution of the energy from these

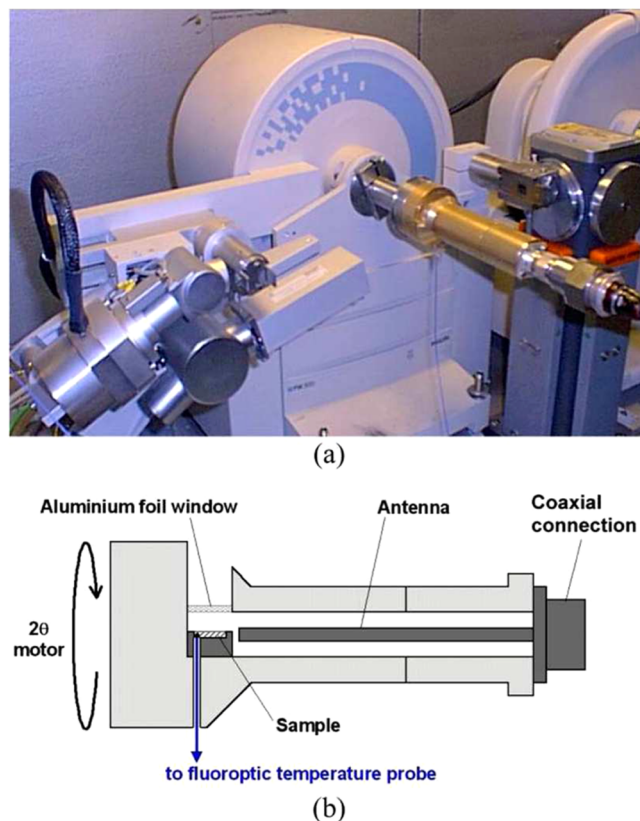


**Figure 23.** MW applicator for in-situ laboratory PXD: (a) applicator attached to the diffractometer and (b) schematic of applicator.<sup>201</sup> Reprinted with permission from ref 201. Copyright 2002 The Royal Society of Chemistry.

TO modes is slow compared to the input of energy from the MW field, which results in a nonclassical distribution of internal energies. The phase transition is initiated when there is enough energy in the relevant TO mode to either create sufficient silver ion defects or displace enough iodide ions to instigate structural change. At this point, the average energy in the structure is lower than that at the point of phase transition under conventional heating, so the transition temperature is consequently lower.

Using a laboratory X-ray source for in-situ studies is a technique of limited use on account of the relatively low beam penetration depth of X-rays, which severely restricts the design of the MW reactor used in an in-situ experiment. Furthermore, the low X-ray flux from lab sources results in comparatively long data collection times, which are incompatible with many fast MW reactions. In several cases, synchrotron X-rays have been used as an alternative in-situ structural probe, as the extremely high flux from synchrotron sources allows very rapid data collection. In 2006, Tompsett et al. used in-situ small-angle and wide-angle X-ray scattering (SAXS and WAXS) techniques to study the MW synthesis of zeolites.<sup>202</sup> Previous studies revealed that the rates of preparation of several zeolites were over an order of magnitude faster under MW irradiation than for conventional methods. The focus of the paper was on the zeolite silicalite, the conventional hydrothermal synthesis of which has been the subject of extensive investigation by both SAXS and WAXS.

In order to study the MW synthesis of silicalite, a MW reactor was developed that could be used with in-situ WAXS and SAXS and also Raman spectroscopy. The reactor was constructed using a SAIREM MW generator with a maximum power of 300 W and

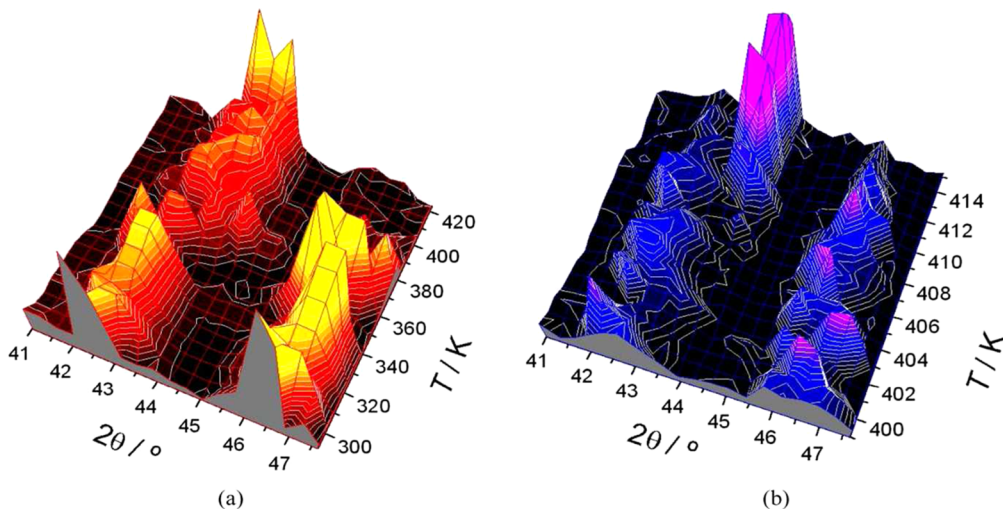


**Figure 24.** Diffraction peak evolution of AgI across the  $\beta$ - $\alpha$  phase transition with (a) MW heating,  $T_c = 380 \pm 10$  K, and (b) conventional heating,  $T_c = 412 \pm 2$  K.<sup>201</sup> Reprinted with permission from ref 201. Copyright 2002 The Royal Society of Chemistry.

WR-284 waveguide components with a sliding short circuit to adjust the positions of the maxima in the MW field. A hole in the waveguide allowed the synchrotron X-ray beam to enter, and a slot was provided for the scattered beam. Samples were contained within a variety of glass reaction vessels and the temperature monitored with a fiber optic probe. SAXS measurements collected at a reaction temperature of 403 K allowed the particle size to be calculated throughout the reaction. Corresponding WAXS measurements made it possible to establish the reaction induction time (the duration at the reaction temperature before nucleation commences) and monitor crystallization of silicalite from the precursor solution from the appearance of Bragg reflections from the emerging zeolite crystals. SAXS revealed that the particle size increased from the start of the reaction, reaching a plateau at 100 min, as shown in Figure 25. This was attributed to the crystallization of the particles, which was first seen to occur in the WAXS data after 100 min at 403 K. MW irradiation resulted in an enhanced crystallization rate compared to conventional synthesis. The reaction was also studied using Raman spectroscopy, but unfortunately this provided little insight. No conclusions were drawn regarding the mechanism of zeolite synthesis under MW heating in this experiment, but reaction mechanisms were discussed in a follow-up publication, which used the same in-situ setup to study formation of several other zeolites, specifically NaA, NaY, and beta zeolites.<sup>203</sup> The evolution of nanosized precursor particles during nucleation and crystallization of the zeolites was examined in great detail, providing considerable insight into the way in which these reactions proceed. Of particular interest was the observation that MW heating of a single zeolite precursor to form NaA, NaX, and sodalite resulted in a shift in the selectivity of the reaction toward NaA and NaY, where conventional heating forms almost pure sodalite.

Zeolite synthesis was also studied *in situ* when Wragg et al. used energy-dispersive X-ray diffraction (EDXRD) to investigate the reaction pathway and kinetics in the MW synthesis of aluminum phosphate frameworks.<sup>204</sup> In this case, the zeolites were synthesized using ionothermal conditions. Glass reaction tubes were positioned in the center of a bespoke MW cavity, which was adapted for *in-situ* measurements by addition of a small hole through which the incident X-ray beam could enter and a larger aperture covered with thin aluminum foil, through

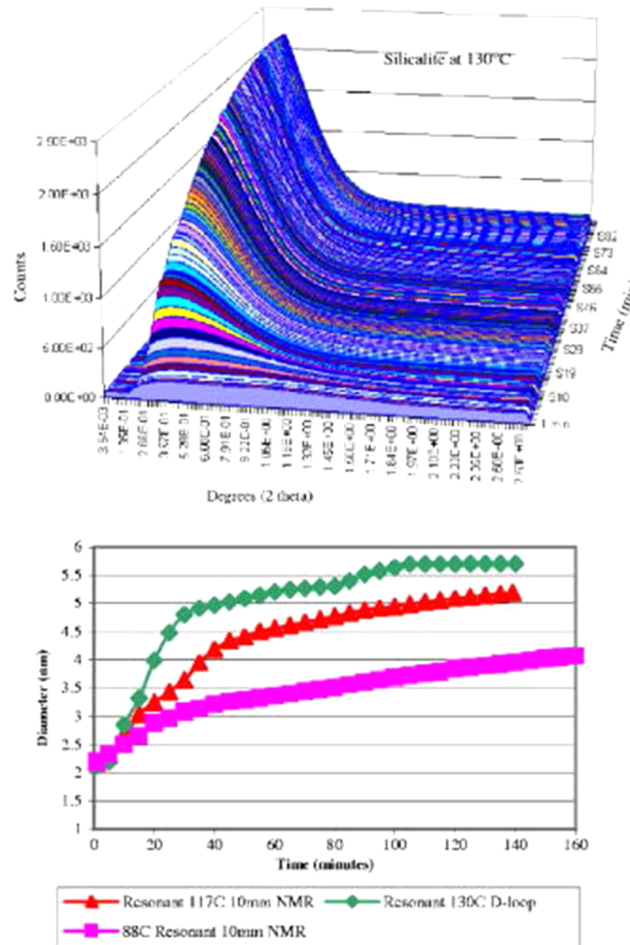


**Figure 25.** (a) SAXS patterns of silicalite formation at 130 °C for 90 min, and (b) plot of silicalite particle sizes with time for three reaction temperatures: 88, 117, and 130 °C.<sup>202</sup> Reprinted with permission from ref 202. Copyright 2006 AIP Publishing LLC.

which the diffracted beam could reach the detectors. Samples were heated using 2.45 GHz MW radiation, generated by a 20–1000 W Astex AX2110 source, and the cavity could be tuned remotely by moving a sliding short circuit, permitting control of

the efficiency of MW heating. Reaction temperature was monitored using a fiber-optic probe. EDXRD data were collected on Station 16.4 at the Daresbury Synchrotron Radiation Source. Analysis of the EDXRD data revealed that MW synthesis of zeolite SIZ-4 followed a significantly different reaction route than that seen for conventional synthesis of this material, with direct synthesis of the target zeolite being observed (Figure 26) and no

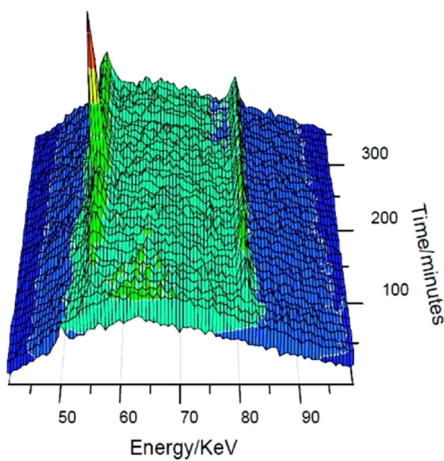


**Figure 26.** 3D plot of EDXRD data for MW synthesis of SIZ-4 showing direct formation of the final product with excellent crystallinity.<sup>204</sup> Reprinted with permission from ref 204. Copyright 2009 American Chemical Society.

evidence of the intermediate phases that had been reported previously for conventional heating pathways. It was suggested that this difference could be attributed to a more rapid onset of crystallization under MW heating. The speed and consistency that MW irradiation offers leads to a larger number of nucleation sites, which results in formation of very small crystals. This proposal was supported by scanning electron microscopy of the reaction products, which revealed small, spherical crystals in the MW-heated samples and larger plate-like crystals from conventionally synthesized samples.

In-situ synchrotron PXD was used in the study of MW heating conducted by Vaucher et al.<sup>205</sup> The experiment involved investigation of the mechanism of formation of quasi-crystalline aluminum–copper–iron alloys from ball-milled Al–Cu–Fe precursors.<sup>205</sup> Research efforts have focused on synthesis of these materials on a larger scale for industrial purposes, and MW heating was identified by the authors as a synthesis route with several advantages over conventional techniques. MW heating of the samples was achieved using a WR-340 waveguide terminated with a sliding short circuit, which could be adjusted to ensure that the sample was placed at a maximum in the MW field.

In-situ experiments were performed using synchrotron X-ray radiation at the powder diffraction station of the Materials Science X04SA beamline at the Swiss Light Source, Villigen, Switzerland. The ball-milled precursor contained a mixture of  $\beta$ -Al(Fe),  $\theta$ -Al<sub>2</sub>Cu, and pure Al. Upon MW heating, the material was found to undergo several phase transitions until ultimately forming the target product, quasi-crystalline  $\psi$ -(Al–Cu–Fe). The sequence of transformations, as shown by the PXD patterns in Figure 27, was identified as  $\beta$ -Al(Fe) +  $\theta$ -Al<sub>2</sub>Cu + Al  $\rightarrow$   $\omega$ -Al<sub>7</sub>Cu<sub>2</sub>Fe +  $\theta$ -Al<sub>2</sub>Cu  $\rightarrow$   $\omega$ -Al<sub>7</sub>Cu<sub>2</sub>Fe +  $\psi$ -(Al–Cu–Fe)  $\rightarrow$   $\psi$ -(Al–Cu–Fe). These findings did not contradict previous reports, but two phases (a body-centered cubic Al<sub>4</sub>Cu<sub>9</sub>-type  $\gamma$ -phase and Fe<sub>3</sub>Al) that had been previously reported as intermediates when

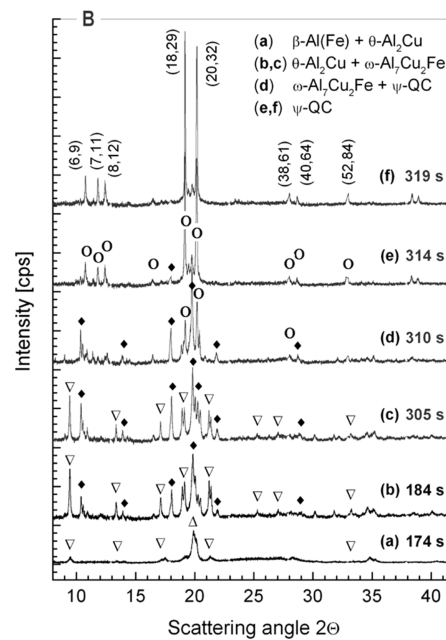


**Figure 27.** In-situ synchrotron PXD data showing the sequence of solid-state transitions leading to formation of single-phase  $\psi$ -(Al–Cu–Fe) quasicrystals [up triangles  $\beta$ -Fe(Al); down triangles  $\theta$ -Al<sub>2</sub>Cu; diamonds  $\omega$ -Al<sub>7</sub>Cu<sub>2</sub>Fe; open circles  $\psi$ -phase].<sup>205</sup> Reprinted with permission from ref 205. Copyright 2008 Materials Research Society

using conventional synthesis methods were not observed with MW heating. This suggests that either formation of these intermediates is suppressed under MW irradiation or they exist only as transient intermediates, which cannot be observed at the time resolution used. The striking difference in this report between MW and conventional heating is the rate of reaction. The authors refer to a previous in-situ study (using conventional heating) that indicated only 96% transformation from  $\omega$ -Al<sub>7</sub>Cu<sub>2</sub>Fe to the target  $\psi$ -(Al–Cu–Fe) after 40 min at 973 K. In contrast, the phase transition was complete in <10 s under MW irradiation, as illustrated in Figure 27d–f.

Vaucher et al. also used in-situ synchrotron X-ray diffraction (SXRD) to study the mechanism of MW synthesis of Ti–Al intermetallics.<sup>206</sup> Ti–Al phases are conventionally prepared using combustion synthesis, and previous studies predicted different synthesis mechanisms at slow and high heating rates. In the MW heating experiment, elemental Ti and Al precursors were heated in sapphire capillaries in the in-situ setup described above. PXD patterns were collected at 10 s intervals, and temperature was monitored using an optical pyrometer. The resulting time-resolved PXD data were used to establish a reaction mechanism, which was found to proceed via a molten aluminum stage, in contrast with expectations from previous publications. Data were also used to perform a quantitative evaluation of the kinetics of the synthesis. Perhaps the most important aspect of this publication is the fact that the in-situ techniques developed in Vaucher et al.’s earlier paper,<sup>205</sup> discussed above, have been successfully applied to study another material and type of reaction. It is clear that the study of a wide variety of MW reactions is essential in developing knowledge and improving understanding of how and why these reactions proceed, and the experimental technique described by Vaucher et al. should be applicable to a wide range of other MW reactions involving solid-state materials. Technical details of apparatus and

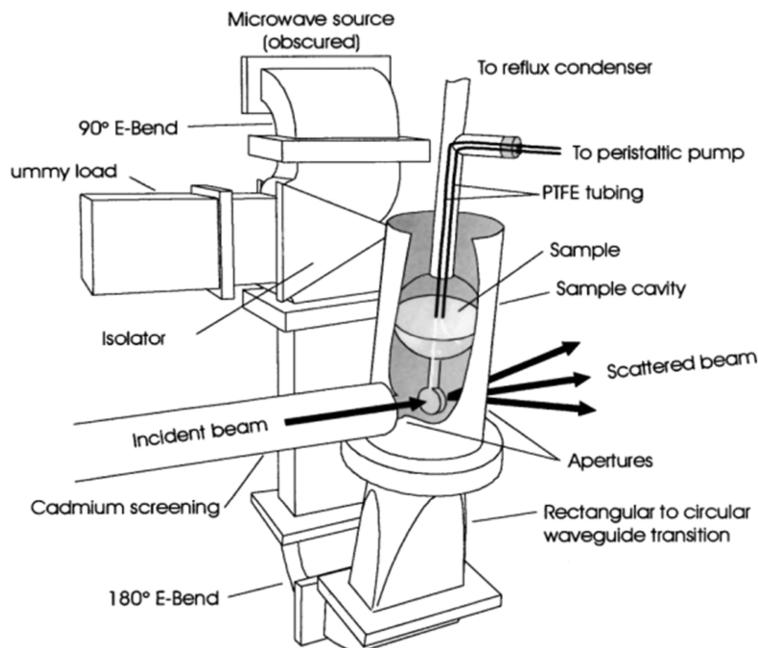
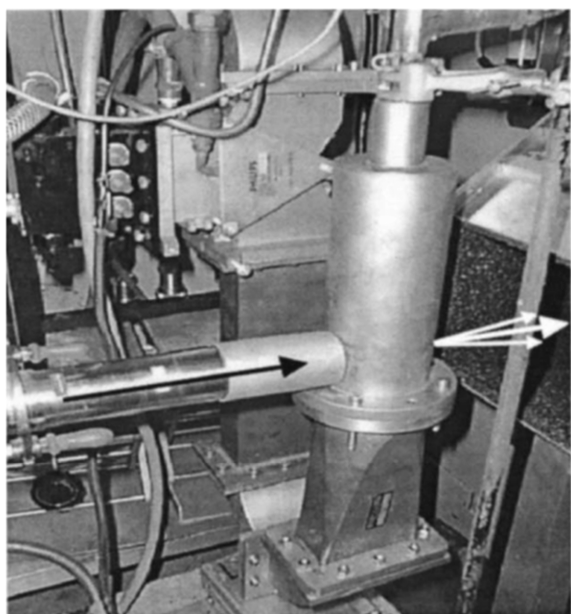


**Figure 28.** Photograph and schematic of the MW reactor used for in-situ SANS on the LOQ instrument at ISIS.<sup>207</sup> Reprinted with permission from ref 207. Copyright 2001 AIP Publishing LLC.

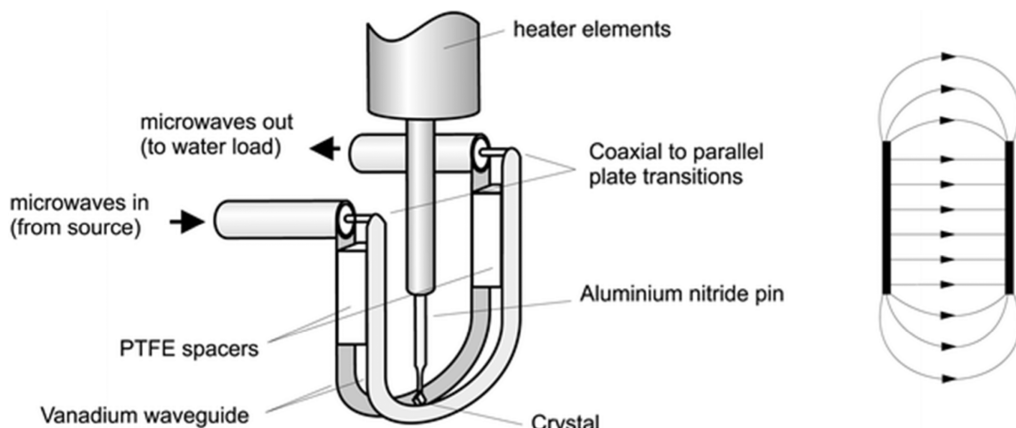


**Figure 29.** Schematic of the sample arrangement and MW applicator (left) and of the electric field between the vanadium plates at the sample (right) for in-situ single-crystal diffraction at the SXD neutron diffractometer at the ISIS Facility.<sup>208</sup> Reprinted with permission from ref 208. Copyright 2003 The Royal Society of Chemistry.

configurations will be vital to improve the design of next-generation reactors for in-situ SXRD experiments.

### 7.3. In-Situ Studies Using Neutrons

While SXRD offers considerable improvements over laboratory X-ray techniques and may seem an ideal choice for in-situ studies due to the very fast data collection times, they are limited by the issue of beam penetration. X-rays interact with the electrons of an atom, and this electromagnetic interaction is strong, resulting in significant attenuation of an X-ray beam by the majority of samples. As a result, the design of MW reactors suitable for in-situ X-ray analysis is extremely challenging, because the MW apparatus is generally made of materials that are opaque to X-rays. In addition, X-rays are normally capable of only probing close to the surface of a sample, and the reactivity in this region is not necessarily representative of the bulk. Importantly, also, the bulk is the very region of the solid sample where MWs interact most strongly. In contrast, neutrons interact with atomic nuclei,

so this interaction is very weak in comparison to X-rays. A neutron beam is therefore a highly penetrating form of radiation, so it can be used in a much wider variety of in-situ reaction configurations and probe bulk reactivity even in large samples. In addition, development of modern neutron detectors is enabling time-resolved study of reactions on very short time scales, so neutron scattering techniques perhaps provide the best opportunities for in-situ studies.

The first report of an in-situ neutron scattering study of a MW reaction came in 2001, when Whittaker et al. described apparatus designed to study the MW-driven growth of particles in solution by in-situ small-angle neutron scattering (SANS).<sup>207</sup> A MW reactor, shown in Figure 28, was designed for use on the LOQ instrument at the ISIS Facility, Rutherford Appleton Laboratory, and allowed investigation of the growth of particles of iron oxide and oxyhydroxide by the MW induced hydrolysis of iron-containing solutions. The experiments revealed that heating these solutions using MWs often results in different products to

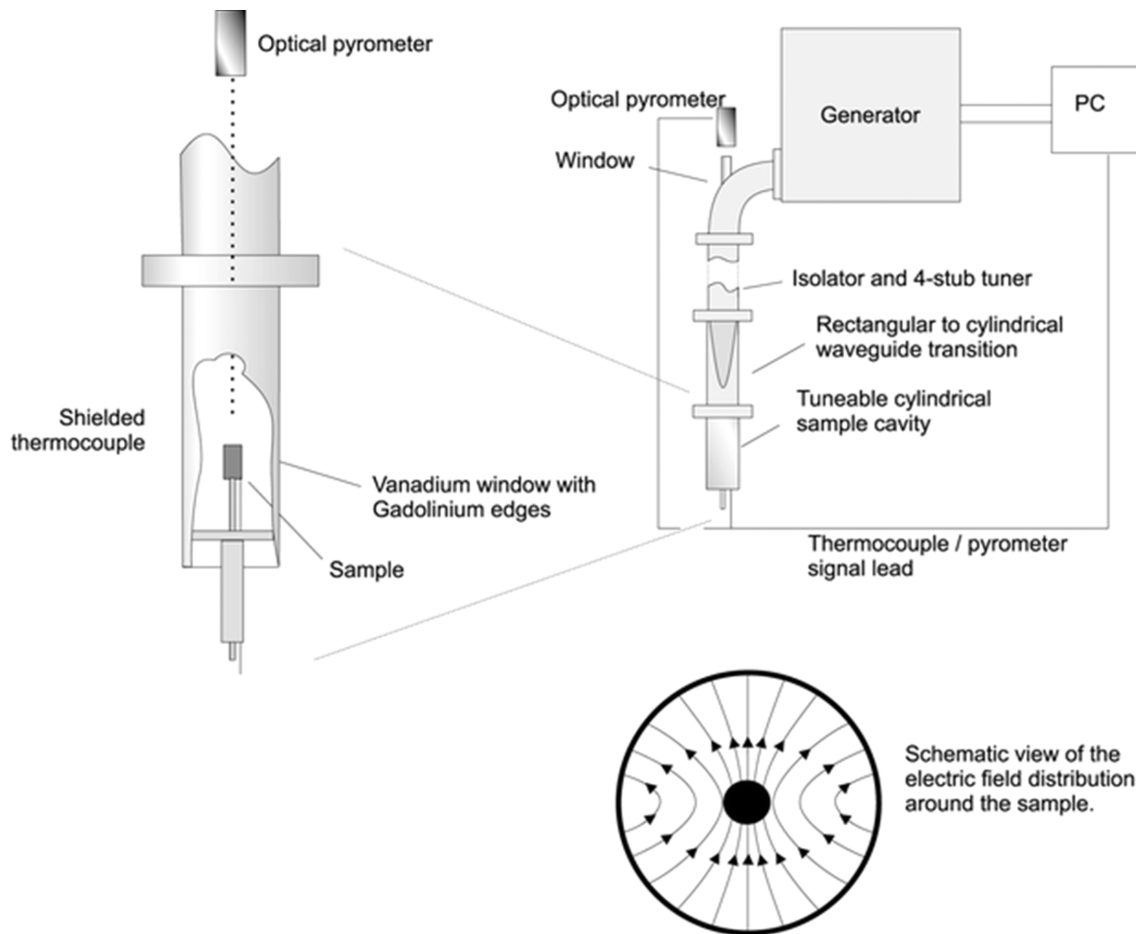


**Figure 30.** Schematic of the MW apparatus designed for in-situ powder neutron diffraction at HRPD at the ISIS Facility.<sup>208</sup> Sample and thermocouple are mounted in a resonant microwave cavity, connected to a microwave source whose output was controlled to maintain a set temperature. Reprinted with permission from ref 208. Copyright 2003 The Royal Society of Chemistry.

those observed with conventional heating. Of particular note was the experiment in which a mixture of ferrous and ferric ions was heated at  $\sim 80$  °C for several hours; the product of this reaction was acicular magnetite ( $\text{Fe}_3\text{O}_4$ ) rather than the expected hematite ( $\text{Fe}_2\text{O}_3$ ), which is obtained with conventional heating. In addition to the product being different from that expected, this was also the first synthesis of acicular magnetite directly from solution. The reactor was designed to be adaptable for study of other solution reactions, although no further work has been published. The experimental configuration is considerably different from that required for solid-state MW synthesis, but in principle, the design could be adapted to study such reactions.

In 2003, Harrison et al. performed the first in-situ neutron diffraction experiments on solid-state materials under MW heating. Single-crystal and powder neutron diffraction experiments were performed upon a crystal of aspirin and a sample of barium titanate powder, respectively.<sup>208</sup> Both experiments made use of bespoke MW reactors. For the single-crystal experiment, the aspirin crystal was mounted on a custom-made (MW transparent) aluminum nitride pin and the MWs were delivered to the sample by means of parallel plate vanadium waveguides, as shown in Figure 29. The temperature of the sample was set by cooling the sample pin with a cryostat, which in turn controlled the temperature of the crystal. Single-crystal neutron diffraction data were collected at 100, 200, and 300 K using the SXD diffractometer at the ISIS Facility, Rutherford Appleton

Laboratory, with the MW power output set at a constant 40 W. Barium titanate was selected for study by powder neutron diffraction (PND) on account of its susceptibility to MW heating and the fact that it passes through several well-defined phase transitions on heating, making it a suitable material for probing temperature through lattice parameters or atomic displacement parameters. The MW reactor was designed for use on the HRPD high-resolution powder neutron diffraction instrument at the ISIS Facility. The reactor setup is shown in Figure 30 and consisted of a MW generator which feeds MWs into a waveguide, where the field is tuned using a four-stub tuner. The MWs passed through a rectangular to cylindrical waveguide transition into the cylindrical sample cavity, in which the MWs could be further tuned using a sliding short circuit. The neutron beam entered the sample cavity through a vanadium window. Vanadium has a coherent neutron scattering cross section close to zero ( $\sigma_c = 0.0183$  barn),<sup>209</sup> so there was no significant Bragg diffraction from this window. The reaction temperature could be monitored using an optical pyrometer, and the output MW power was controlled using the output from the pyrometer via a PC.

Single-crystal and powder diffraction experiments gave contrasting results. Refinement of the single-crystal data showed a significant increase in the isotropic and anisotropic displacement parameters when the aspirin crystal was subjected to MW irradiation, as can be seen in Figure 31. However, the increase in the displacement parameters is approximately the same for all

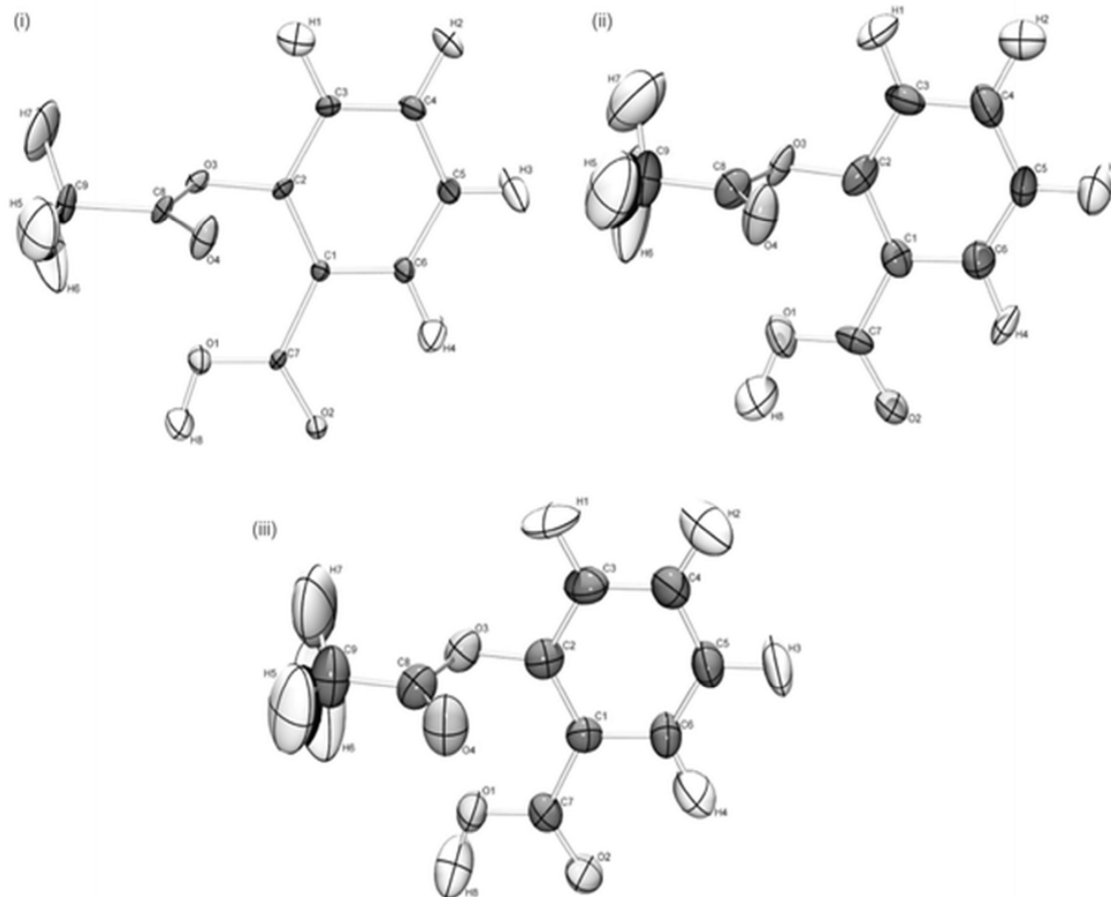


**Figure 31.** Structure of aspirin, showing ADPs at various temperatures and with different sources of heat: (i) 100 K with conventional heating, (ii) 100 K with MW heating, (iii) 300 K with conventional heating.<sup>208</sup> Reprinted with permission from ref 208. Copyright 2003 The Royal Society of Chemistry.

atoms, so there is no evidence for nonuniform equipartition of energy within the structure. The observations are explained by MW irradiation serving simply to heat the sample, with the energy distributed rapidly to all parts of the molecule, on the time scale of neutron diffraction. The authors acknowledge that in order to investigate the possibility that MW heating may have more localized energy effects on different parts of the molecule an alternative, more rapid technique would need to be used. In the case of barium titanate, systematic differences were observed between MW and conventional heating; the lattice parameters of the MW heated sample were considerably larger, while the anisotropic displacement parameters were smaller. The increased cell volume can be attributed to higher sample temperatures than are observed at the sample surface by the optical pyrometer. However, the smaller ADPs appear to contradict this. The authors rationalize the low ADP values with the suggestion that certain forms of ionic motion are damped by the MW field. The data also show a significant increase in the widths of diffraction reflections in the MW-heated sample, which is explained by the presence of thermal gradients or local hot spots within the sample, which leads to a distribution of cell parameters that manifests itself as peak broadening.

The most recent study involving in-situ neutron diffraction of a MW reaction was presented in 2005 by Günter et al.<sup>210</sup> Previous reports identified the apparent nonthermal effects of a MW field on mass transport properties of ionic solids. However, only ionic solids such as NaCl had been studied; Günter et al. investigated

whether this nonthermal effect extended to fast ion conducting materials and specifically the Sr/Mg-doped lanthanum gallate superionic conductor La<sub>0.9</sub>Sr<sub>0.1</sub>Ga<sub>0.8</sub>Mg<sub>0.2</sub>O<sub>2.85</sub>.<sup>210</sup> The experiment made use of apparatus that was able to subject the sample to both conventional and MW heating. The equipment involved a mirror furnace with two halogen lamps and two ellipsoid mirrors, into which a MW cavity could be inserted and connected via a waveguide to a MW generator. In-situ powder neutron diffraction data was collected at various temperatures using the D2B instrument at the Institut Laue-Langevin (ILL) in Grenoble. The setup of the apparatus for the D2B diffractometer is shown in Figure 32. The authors observed evidence which could be interpreted as nonthermal MW effect in their results, with MW heating leading to structural changes contrasting to those from the use of conventional heating. An alteration in the ionic diffusion pathway was also inferred in the MW-heated sample, which could not be attributed to the presence of an electric field alone.

Given the applications of in-situ PND described above in addressing the possible “non-thermal” effects of a MW field in solid-state synthesis, it is valuable in this section to consider briefly the nature of nonthermal MW effects in the solid state and the challenges associated with their validation experimentally. Anomalous reaction rates in liquid-phase microwave-induced reactions have been satisfactorily explained by effects such as superheating.<sup>211</sup> However, in the solid state it has been suggested that ion migration occurs due to a nonthermal mecha-

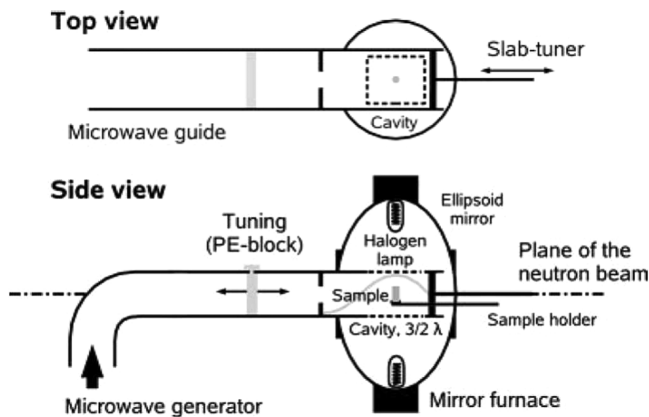


**Figure 32.** Schematic of the experimental setup for in-situ PND studies at the D2B instrument, ILL, using MW and alternative heating sources.<sup>210</sup> Reprinted with permission from ref 210. Copyright 2005 WILEY-VCH Verlag GmbH & Co. KGaA.

nism.<sup>212–214</sup> We can define MW nonthermal effects, in the present context, as those effects which result in the MW electric or magnetic field exerting a direct influence on ion motion, without the need for the microwave energy to first be repartitioned into thermodynamically equilibrated thermal energy modes.<sup>215</sup>

There is an expanding body of work on MW-processed ceramics which suggests both enhanced mass transport<sup>216</sup> and sintering rates which correspond to higher temperatures than those actually observed.<sup>217</sup> The validity of such analyses works on the assumption that the reported temperatures are accurate (as highlighted in sections 3 and 7.1). Given inverse heating profiles, a difference of several 100 K between the sample surface and core is possible. A thermocouple will only measure temperature in the zone close to its tip and must be shielded to protect against the systematic errors induced by MW field damage. Optical pyrometry is noninvasive but provides only the surface temperature, and since ceramics do not behave as black bodies, uncertainty in sample emissivity presents significant limitations.<sup>218</sup>

Attempts have previously been undertaken to separate the effects of the electric and magnetic components of the MW field on solids.<sup>219</sup> A large number of oxides containing 3d ions were reported to undergo a crystalline to amorphous phase transition in a 0.5 Oe magnetic field at 2.45 GHz in a few seconds at temperatures “far below the melting point”.<sup>219</sup> However, all temperatures were recorded using a single-wavelength infrared pyrometer using literature emissivity values, and it is not impossible to rule out a more conventional thermal explanation of these results despite the parallels drawn between the MW-induced amorphization in the above oxides and the effects observed by the bombardment of solid phases with high-energy neutrons or  $\alpha$ -particles.<sup>219</sup>

In other cases it is possible that results which were attributed to nonthermal effects may be interpreted as a conventional consequence of inhomogeneous heating. While conventional heating may be assumed to give rise to uniform temperatures throughout a small sample, microwave heating imparts energy directly to the sample and, particularly within large samples, inhomogeneous heating may occur, although it has been calculated that significant thermal gradients may not be maintained across particles at the micrometer scale under steady-state conditions.<sup>220</sup>

Undeniably, while inferences of nonthermal effects are relatively common, evidence-based explanations of these observations are somewhat limited. One interesting hypothesis in the understanding of nonthermal effects in MW-heated solids is that proposed by Booske et al.<sup>221</sup> Their premise is that high-frequency electromagnetic fields enhance solid-state ionic diffusion by exerting ponderomotive forces on mobile ions in solids. This effect is modeled as a consequence of gradients in the mobility of mobile charged species at or near grain boundaries or other physical interfaces.<sup>221</sup> This phenomenon can be considered as analogous to the ponderomotive forces observed in gas-phase plasmas, where charged species are driven away from high electric field gradients due to gradients in the radiation field intensity.<sup>221</sup> In an SMC however, at least on a macroscopic scale, this would result in ions diffusing away from the field strength maximum in the center of the waveguide, and with all ions moving in a similar direction, no extra mixing is likely. Thus, for this effect to play a relevant role, one would expect to have to consider an effect arising from microscale field strength variations occurring due to material inhomogeneities. Simulation work may yield some insight, but it would be difficult to measure the field strength variation directly because the microwave field would damage any semiconductor-based modulated-scatterer measurement.

Whether such effects are significant in microwave-heated ceramic systems remains an interesting point of debate but perhaps one that is less relevant than it might first seem. Studies of diffusion in microwave-heated ceramic systems show results that are consistent with the ponderomotive model, with diffusion enhancement in the early stages of sintering that is linked to the presence of small grains with proportionally large surface areas and intense intergrain field gradients.<sup>222</sup> However, such results do not represent unequivocal evidence of the significance of the ponderomotive effect at high temperatures. High temperatures under microwave heating are often associated with high microwave power densities and the presence of gas molecules that require less additional energy input for ionization. Under such conditions, it is possible that energy is imparted into plasma discharges between grains leading to highly localized heating in the presence of highly energetic gaseous species. As such unusual conditions are not well studied, it remains possible that plasma discharges may also be responsible for some of the nonclassical behavior that is observed in the solid state under a MW field.

Ultimately, the key question is to what extent nonthermal effects are actually important in influencing microwave synthesis. It is clear that more experimental evidence aimed at elucidating the nature of MW heating in solids is required before a conclusion can be drawn. Without an enhanced understanding of the nature of the interaction of solids with electromagnetic fields this is simply not feasible, and thus, in-situ analysis and monitoring is a vital step forward.

#### 7.4. In-Situ Studies Using Other Techniques

There are numerous examples of in-situ studies of organic MW reactions using spectroscopic techniques, including UV-vis,<sup>223</sup> infrared,<sup>224</sup> and Raman<sup>225,226</sup> spectroscopy. In solid-state chemistry, there are a rather limited number of examples of the use of spectroscopy. For instance, in their SAXS and WAXS study of zeolite synthesis discussed in section 7.2, Tompsett et al. also had the facility to perform in-situ Raman analysis.<sup>202</sup> Raman spectra obtained as the reaction progressed were used to monitor the progression from starting materials to the target silicalite, and data were found to support the reaction mechanism suggested by

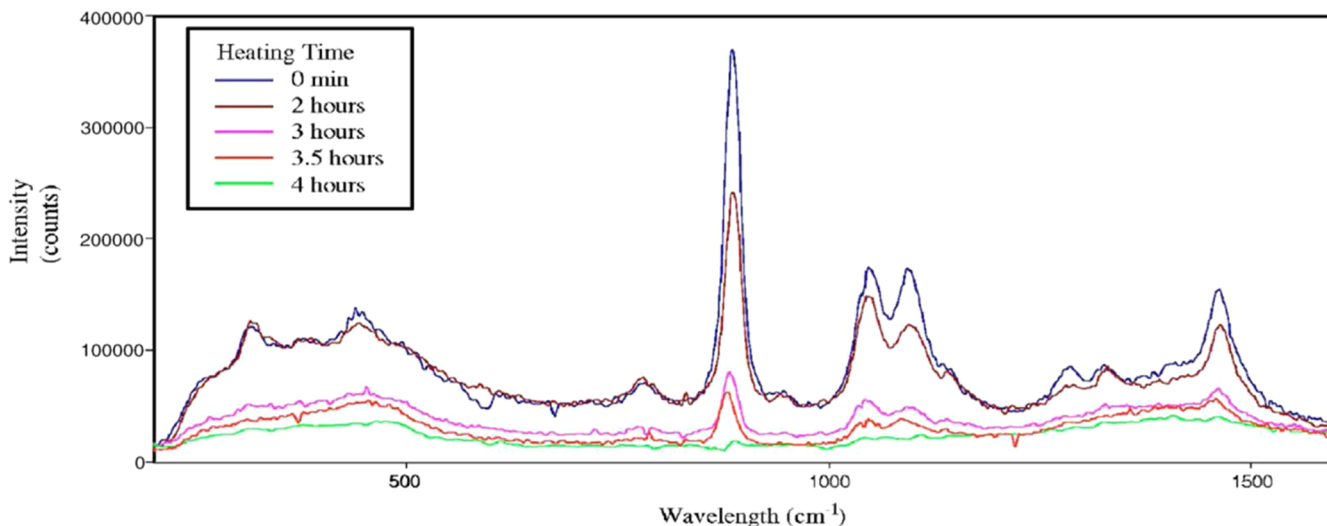


**Figure 33.** In-situ Raman spectra taken during MW synthesis of silicalite, in which the reaction temperature was maintained at 115 °C.<sup>202</sup> Reprinted with permission from ref 202. Copyright 2006 AIP Publishing LLC.

the X-ray scattering techniques (Figure 33). Infrared (IR) spectroscopy has also been used in the in-situ analysis of solid-state reactions, specifically in the study of heterogeneous catalyst activity. Silverwood et al. designed a cell that consisted of a parallel plate applicator surrounding a ceramic sample holder, with connections to allow the flow of reactant gases through the cell.<sup>227</sup> The experimental setup also allowed the exhaust gases from the reactions to be analyzed by mass spectrometry. The cell was used to study the oxidation of carbon monoxide over the EUROPT-1 Pt/SiO<sub>2</sub> catalyst, as shown in Figure 34.<sup>227,228</sup> While

the MW equipment could be used in the study of other systems. However, only in a few cases have there been further publications following from an original study. Isolated investigations into MW heating of specific compounds, while useful, only partially advance our understanding of MW reactions in general, so it is clear that a far more extensive study of a variety of reactions would be enormously beneficial. In addition, it is important to note that the two publications by Vaucher et al.<sup>205,206</sup> are the only examples of the structural study of MW *synthesis* of solid-state materials *in situ*; all other work has focused on either analysis of a sample during MW heating (as opposed to during reactions) or solution-based MW synthesis. Clearly there is a recognizable need for in-situ analysis of the synthetic chemistry in the solid state if we are to understand mechanisms, structure, bonding, and kinetics in these MW reactions to any significant extent.

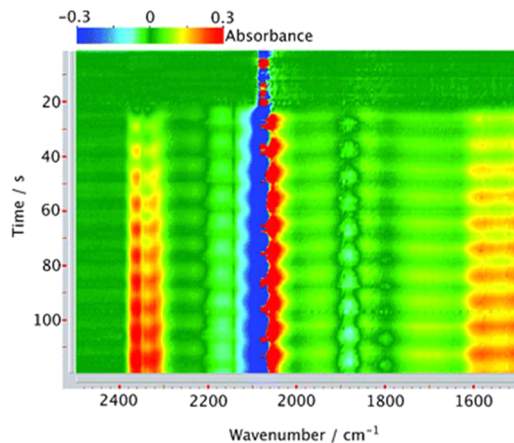


**Figure 34.** Time-resolved IR spectra of CO oxidation over the EUROPT-1 catalyst under MW heating.<sup>227</sup> Reprinted with permission from ref 227. Copyright 2006 The Royal Society of Chemistry.

no difference was seen between the rate of CO<sub>2</sub> production under MW heating and the rate seen conventionally in this case, the experimental configuration could equally well be used in the study of other catalytic systems where reports that catalytic activity is enhanced by MW irradiation exist.

### 7.5. Summary of in-Situ Techniques

In-situ studies (as discussed above) provide considerably improved insight into the reactions involved. Some of the authors of the papers discussed in sections 7.2–7.4 recognize that the methods could be applicable to a wide range of reactions and

## 8. CHEMISTRY–ENGINEERING INTERFACE

Development of continuous processing is an important consideration when discussing the commercial advancement of MW techniques for materials production. Despite being of paramount importance from an industrial perspective, relatively little work has been carried out on development of continuous-flow processes. Significant process development and scale up is difficult to consider without significant improvements in control and reproducibility, which is ultimately obtained from in-situ analysis and monitoring (section 7).

In terms of industrial processing, some of the potential advantages offered by MW methods include<sup>229,230</sup>

- rapid and uniform energy transfer,
- volumetric and selective heating,
- environmental compatibility,
- increased throughput,
- fast on and off switching,
- compact equipment—space savings,
- clean environment at the point of use-enhanced worker safety, and
- unique characteristics of the products.

The scale-up of MW processing is a complex process and will require a combination of computational simulation, expert system design, and comprehensive cost and benefits analysis.<sup>230</sup> It has already been established that a MW system can efficiently

deliver energy to a reaction vessel; however, there are several considerations which must be taken into account<sup>229</sup>

- ensuring a homogeneous electric field profile,
- optimum reactor design which takes into account penetration depths,
- control of temperature and pressure within the reactor,
- cost of the reactor and spare parts, and
- safety issues and MW leakage.

Reports of MW scale-up can be found in the literature but often refer to liquid-phase processes in organic chemistry. While not immediately transferable to processes in the solid state, many of the considerations and challenges are relevant. Leonelli et al. discuss some of the early successes of MWs in industry.<sup>229</sup> MWs have of course found application across the food sector. For example, the tempering of blocks of food from  $-20$  to  $-2$  °C can be done using a 60 kW system which occupies 1/6th of the space of conventional equipment.<sup>229</sup> Use of MW hybrid baking and cooking allows retention of distinctive flavor, color, and texture of oven baking with the increased throughput associated with MW. In the rubber industry MW heating of blocks of rubber of up to several hundred kilograms in weight has replaced conventional vulcanization.<sup>229</sup> Applications have also been found in various areas of waste processing: processing of automotive tires,<sup>231</sup> treatment of hospital and municipal wastes,<sup>232</sup> treatment of toxic substances (Figure 35),<sup>233</sup> and waste recovery of plastics.<sup>234</sup> In the case of hospital waste sterilization a 50% saving can be achieved in disposal costs.<sup>229</sup>

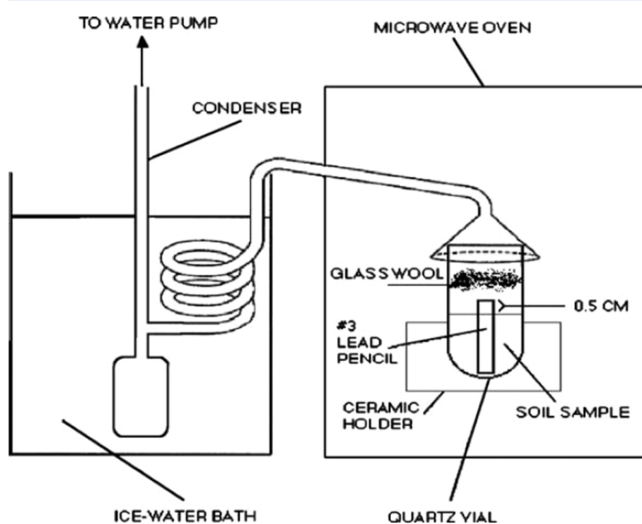


**Figure 35.** MW setup for treatment of soils contaminated with toxic metal ions employed by Abramovitch et al.<sup>233</sup> Reprinted with permission from ref 233. Copyright 2003 Elsevier.

Cherian discusses one strategy for scale up of MW processes, which exploits advanced reactors with control over time, temperature, sample movement rate, and microwave power input to manufacture battery electrode materials.<sup>235</sup> The quality of electrode materials used to form a battery has a significant influence upon performance.<sup>236</sup> Facile syntheses of the component ceramic phases are key to successful commercial production of efficient and cost-effective batteries, and MW synthesis has been demonstrated to be effective in synthesis of electrode materials (see section 6.1).<sup>61</sup> Cherian<sup>235</sup> considers the MW-enhanced synthesis of both  $\text{LiFePO}_4$ , a cathode material for lithium-ion batteries,<sup>237</sup> and  $\text{Li}_4\text{Ti}_5\text{O}_{12}$ , a promising anode

material.<sup>238</sup> Both materials had previously only been synthesized in lab-scale batches using MWs,<sup>239–242</sup> and so processing trials were performed using a programmable HAMiLab-V6 industrial microwave batch furnace. Three temperature monitoring points in the reactor provide feedback for output power regulation so that predetermined set temperatures can be programmed in these monitored regions. Simultaneously, times at set temperatures are controlled by setting the reaction vessel "push-through" rate to correspond to the holding time for the batch process. Importantly, these processing trials showed that both (i) phases of the appropriate purity could be obtained by a MW process and (ii) an optimum processing profile which could then be adapted to develop the continuous process.

Terigar et al. published the results of a scale-up from lab scale to pilot scale for extraction of oil from plant material, as shown in Figure 36.<sup>243</sup> Smaller scale experiments were used to determine optimal processing parameters which could then be directly transferred to the pilot scale. The authors briefly discuss some of the considerations required in scaling up MW processes. One consideration is the change in frequency of the system. It is noted that MWs at 915 MHz (used industrially in the United States) have much higher penetration depths as compared to those with a frequency of 2450 MHz commonly used in laboratory-sized equipment. Higher penetration depths allow for larger scale equipment to be used, e.g., larger diameter tubes, which allow for higher processing flow rates. Results indicated that oil yields obtained from both laboratory- and pilot-scale systems were better than the yields obtained by conventional extraction. The quality of the extracted oils was sufficient to meet biodiesel feedstock standard specifications, and a MW-based extraction method was considered a viable alternative to the current state of the art.

Bowman et al. discuss the technical design considerations for the scale-up of a variety of MW-promoted reactions and the strengths and weaknesses of a continuous-flow MW cell as opposed to batch processing (whether using one large vessel or parallel batch reactors).<sup>42</sup> It is noted that continuous-flow apparatus can be difficult to implement in processing solids and heterogeneous mixtures. They also note the likely time implications of development from small-scale to industrial-scale implementation. One advantage of batch processing is that, theoretically, reaction mixtures will be homogeneous. The penetration depth of MWs into the reactor is however a significant limiting factor.

The influence of reactor size on the leaching outcome of copper from chalcopyrite in  $\text{Fe}_2(\text{SO}_4)_3-\text{H}_2\text{SO}_4$  solution was reported by Al-Harahsheh et al. (Figure 37).<sup>244</sup> In this study it is reported that a single-mode MW reactor (diameter 50 mm) allowed copper recovery comparable to that obtained conventionally. However, in a smaller reactor (diameter 20 mm) enhanced recovery was observed. This was explained by the authors as an effect of selective heating in heterogeneous systems in MW reactors. Hydrometallurgical systems such as  $\text{Fe}_2(\text{SO}_4)_3-\text{H}_2\text{SO}_4$  solution are composed of both liquid and solid material, each of which has its own behavior in a MW field. This highlights the importance of knowing the properties of each component of a system for enhanced extraction efficiency. The reduced effectiveness of the larger reactor was attributed to the presence of a superheated layer at the wall of the reactor due to a low penetration depth. Such considerations might become relevant in solid-state synthesis and processing, particularly for low melting point systems.

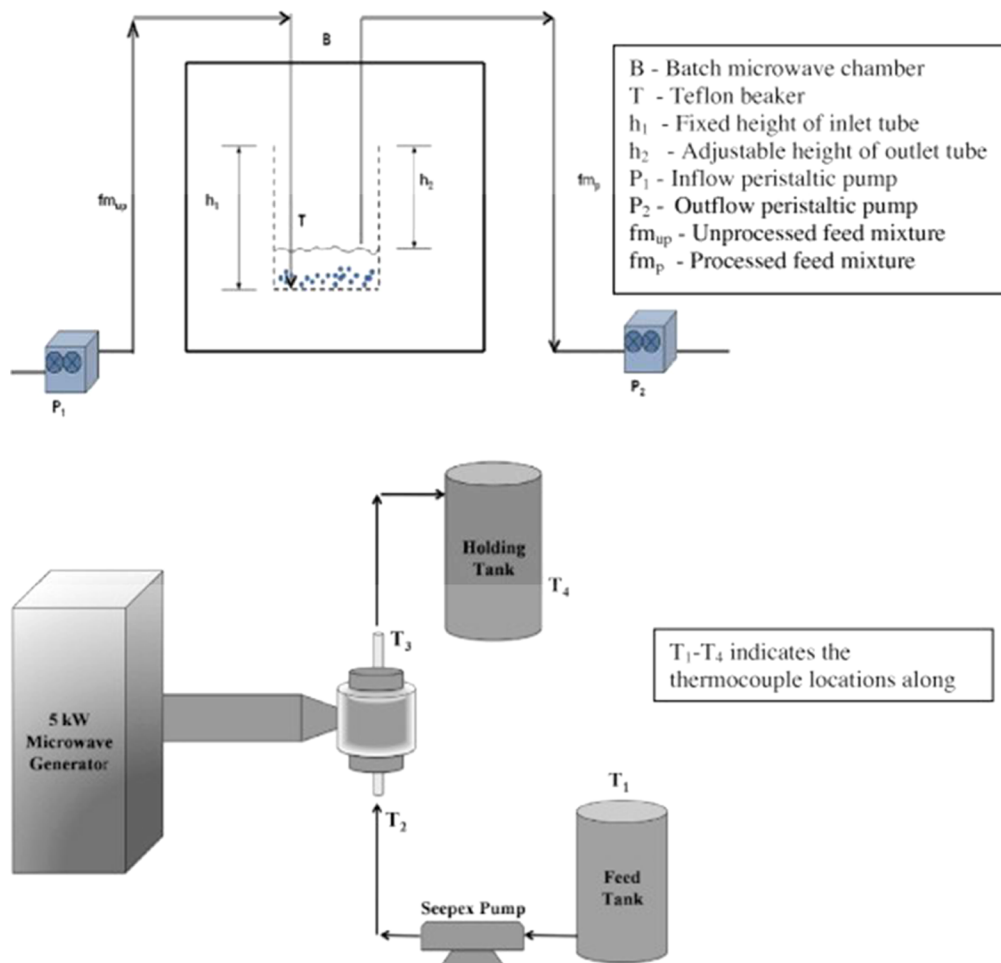


**Figure 36.** Schematic representation of the laboratory-scale (top) and pilot-scale (bottom) continuous MW-assisted extraction systems described by Terigar et al.<sup>243</sup> Reprinted with permission from ref 243. Copyright 2011 Elsevier.

Recently there has been a report of a continuous MW treatment system developed for treatment of oil-contaminated drill cuttings at a pilot scale.<sup>245</sup> Previous MW studies of drill cuttings had been carried out at small scale using both single- and multimode systems.<sup>246</sup> In moving from the lab scale to a continuous treatment it is imperative to maximize power density to allow conversion of water to steam without significant heat loss to the surroundings. Electromagnetic simulations, shown in Figure 38, were employed to optimize the MW applicator geometry for optimal power density distribution. An analogous approach is likely to be essential when designing scale-up processes for manufacture of solids.

The requirement for maximum power density almost certainly eliminates the use of multimode cavities at a pilot scale due to their low peak power density and high power density distribution. In single-mode cavities, very high peak power densities can be achieved but such cavities exhibit a very high power density distribution varying from zero at the edge of the cavity walls to a peak value in the center.<sup>247</sup> This would lead to uneven heating across the cavity. Robinson et al. discussed and implemented an alternate MW design which was employed to attain more uniform electric fields in the processing of the above-mentioned drill cuttings.<sup>245</sup> Process material was moved by a MW transparent conveyor belt, as shown in the schematic in Figure 39. MWs enter orthogonally from the top of a  $TE_{10}$  waveguide such that the polarization in the waveguide is

perpendicular to the direction of material movement. The orthogonal feed of the waveguide creates a uniform power density across the width of the applicator. Three hot spots are generated as a result of the cavity geometry. However, this geometry can be manipulated so that the hot spots overlap to give a high power density in the vertical direction. This specialized system design was capable of treating  $500 \text{ kg h}^{-1}$  of material. It was also shown that the treatment was successful in meeting the environmental targets required for disposal of the drill cuttings.

Kumar et al. report the scale-up of aseptic MW processing of vegetable purees from pilot to full industrial scale.<sup>248</sup> One of the major issues in implementing such a process is the nonuniform temperature distribution within the product. This is an issue which is also encountered in the large-scale MW processing of solids. This study utilized pilot-scale (Figure 40) and industrial-scale bespoke applicators to overcome issues associated with scale-up. Two vegetable purees were processed for a run time of 8 h (a typical duration of plant operation in industry) in the industrial-scale system based on the procedures developed. Temperature measurement revealed significant temperature nonuniformity in the pilot-scale 5 kW MW system, as shown in Figure 41. The temperature difference between the center and the wall of the applicator tube at the outlet became smaller with increasing reaction temperature. The authors propose that this could be due to the enhanced absorption of MWs at higher

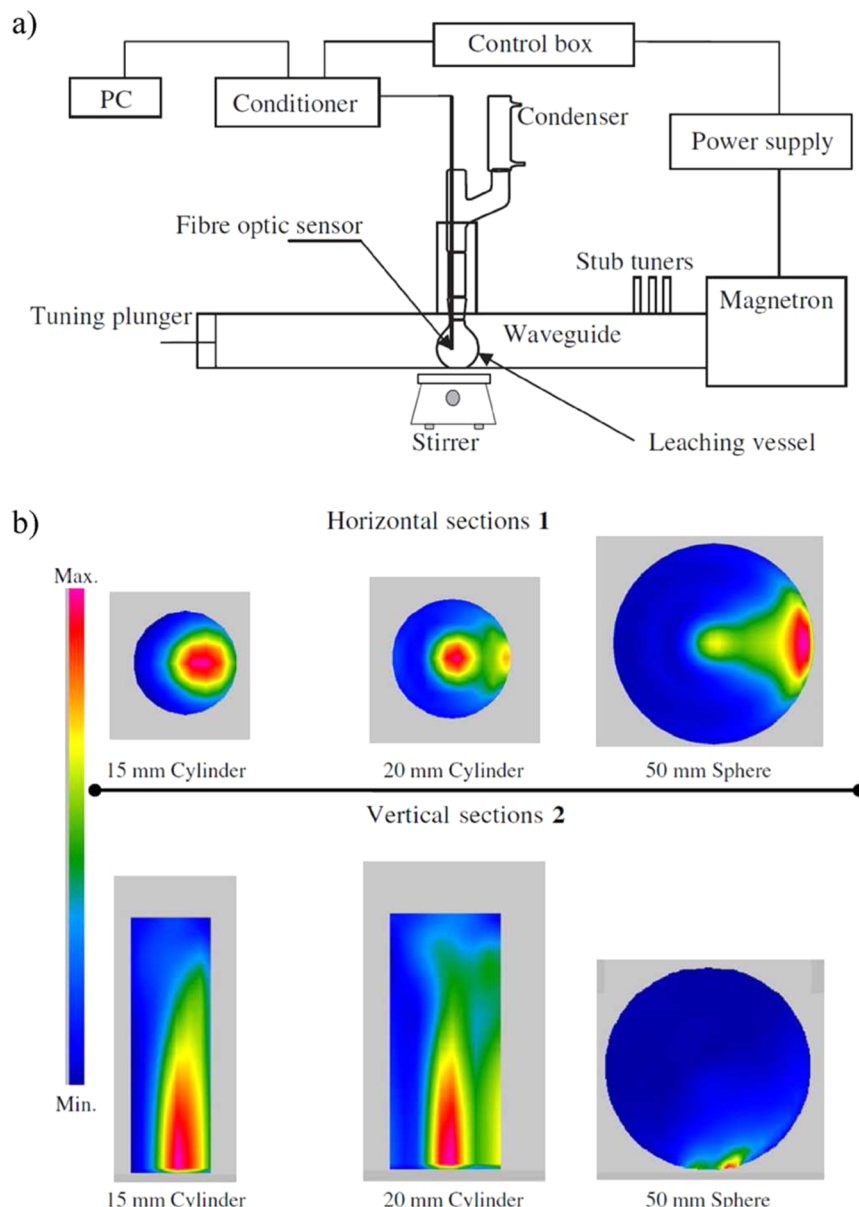


**Figure 37.** (a) Schematic of the instrumentation for SMC experiments as described by Al-Harahsheh et al. (b) Power density maps taken along the horizontal and vertical axis of the SMC.<sup>244</sup> Reprinted from with permission from ref 244. Copyright 2006 Elsevier.

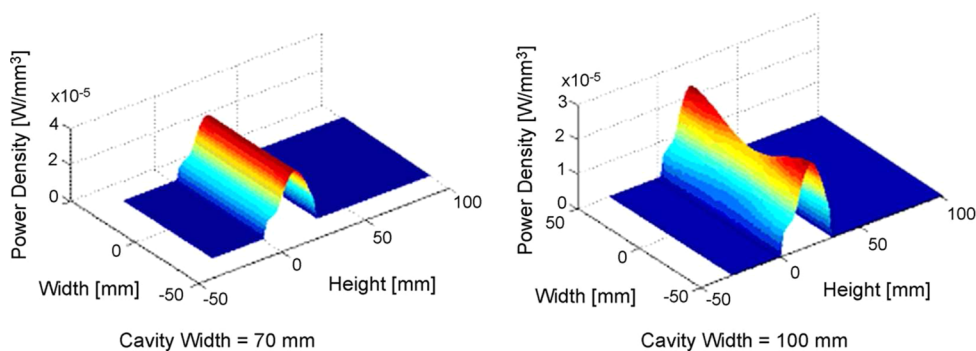


**Figure 38.** Electromagnetic simulations showing the effect of cavity width on power density distribution within the MW applicator.<sup>245</sup> Reprinted with permission from ref 245. Copyright 2010 Elsevier.

temperatures or the reduced viscosity of the purees at higher temperatures facilitating faster thermal dissipation. Temperature nonuniformity was to be overcome by the use of static mixers

installed at the exit of each microwave applicator, in which the purees were channeled through a geometric arrangement of mixing elements.

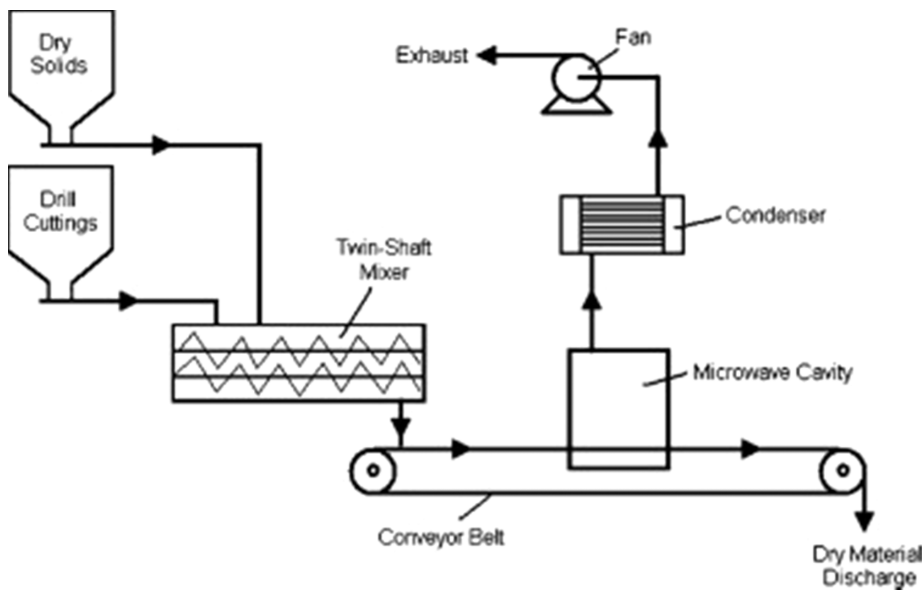


**Figure 39.** Schematic of the pilot-scale apparatus for continuous treatment of contaminated drill cuttings.<sup>245</sup> Reprinted with permission from ref 245. Copyright 2010 Elsevier.

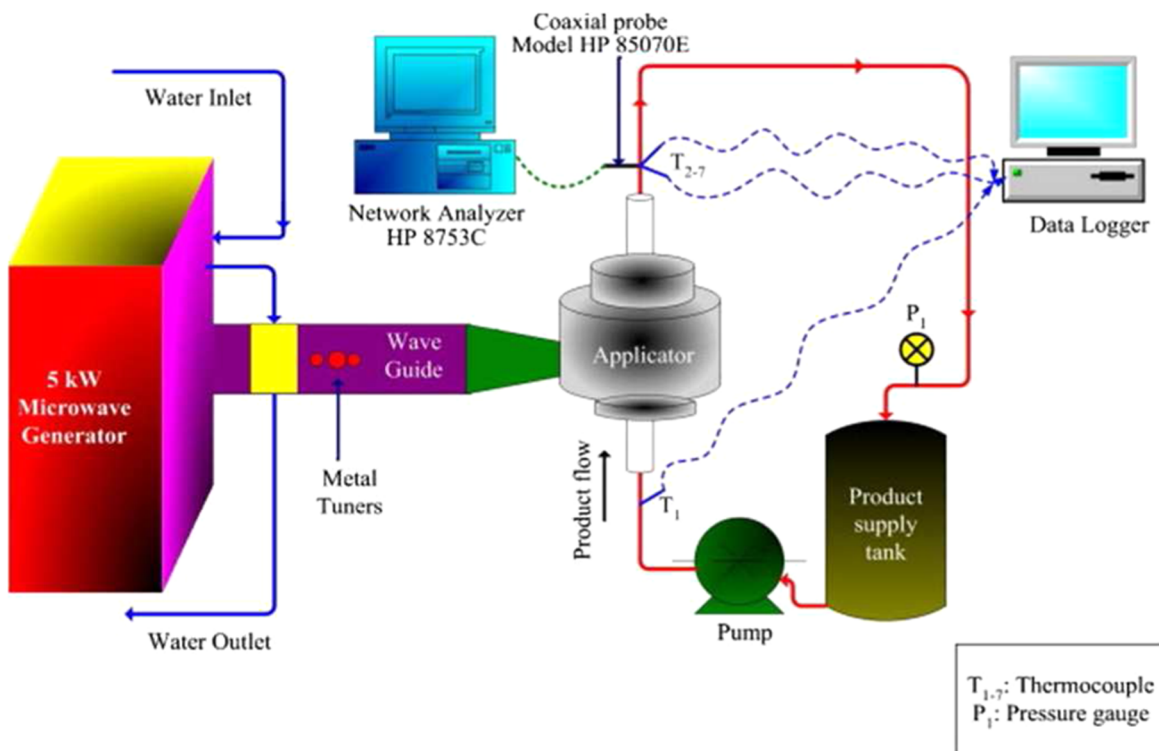


**Figure 40.** Schematic representation of the pilot-scale 5 kW MW aseptic food-processing system.<sup>248</sup> Reprinted with permission from ref 248. Copyright 2008 Elsevier.

For further scale-up the purees were processed in a 60 kW MW system (Figure 42) with the objective of successful operation for at least 8 h. The mixers employed successfully decreased the temperature difference (Tables 6 and 7). Processing was performed for 8 h in the 60 kW MW system with an output power of 30–40 kW and a flow rate of  $3.78 \text{ L min}^{-1}$ .

These results illustrate the effectiveness of mixers to reduce temperature differences during reaction. One of the key challenges in solid-state MW synthesis, particularly during scale up, is temperature nonuniformity. Successful use of the static

mixers to decrease temperature differences in the above example is a strong indication that with careful engineering control these effects can be minimized.

The importance of simulation in the development and optimization of MW systems has only been briefly discussed in some of the examples above.<sup>244,245</sup> Whereas the role of theoretical and empirical models in describing the microwave sintering process is considered in some depth by Rybakov et al.,<sup>222</sup> it is worth considering at this point how modeling might be applied to solid-state microwave synthesis processes in more

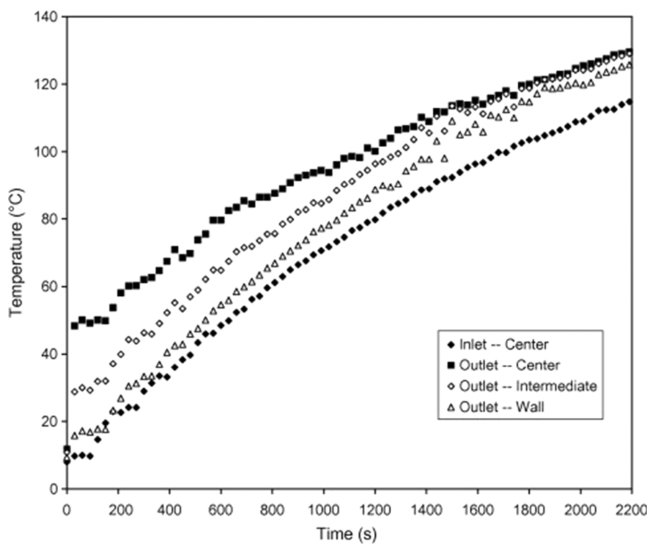


**Figure 41.** Temperature profile across different regions of the applicator during processing of carrot puree in a 5 kW MW system.<sup>248</sup> Reprinted with permission from ref 248. Copyright 2008 Elsevier.

detail. Although it is beyond the scope of this contribution to consider the specifics of the mathematical models, the understanding garnered by such approaches is likely to be profound in the design of scaled up processes.

Simulation of a microwave heating process requires at least an electromagnetic solver tool. The finite-difference time-domain method is one of the most popular, because it is accurate and

**Table 6. Average Cross-Sectional Temperature Differences in the 5 kW System**

reaction temperature/K	vegetable used	temperature difference <sup>a</sup> /K
323.15	green peas	8.6
403.15	green peas	5
323.15	carrot	32.9
403.15	carrot	3.6

<sup>a</sup>Taken between the center and the wall of the applicator tube at the outlet.

**Table 7. Average Cross-Sectional Temperature Differences in the 60 kW System**

vegetable used	temperature difference <sup>a</sup> /K	
	without mixers	with mixers
green peas	17.2	5.2
carrot	54.5	11.6

<sup>a</sup>Taken between the center and the wall of the applicator tube at the outlet.

robust and avoids the problem-size limitations associated with frequency-domain techniques.<sup>249</sup> In the simplest approach, the electric field strength is calculated for a given load and then the temperature rise is inferred in postprocessing by considering the specific heat capacity of the material.<sup>250</sup> Where the materials' electrical properties are temperature dependent, the heat transport equations should also be solved. This results in a nonlinear mathematical system that yields complex behavior such as hot spots and waiting time.<sup>251</sup> The fundamental time

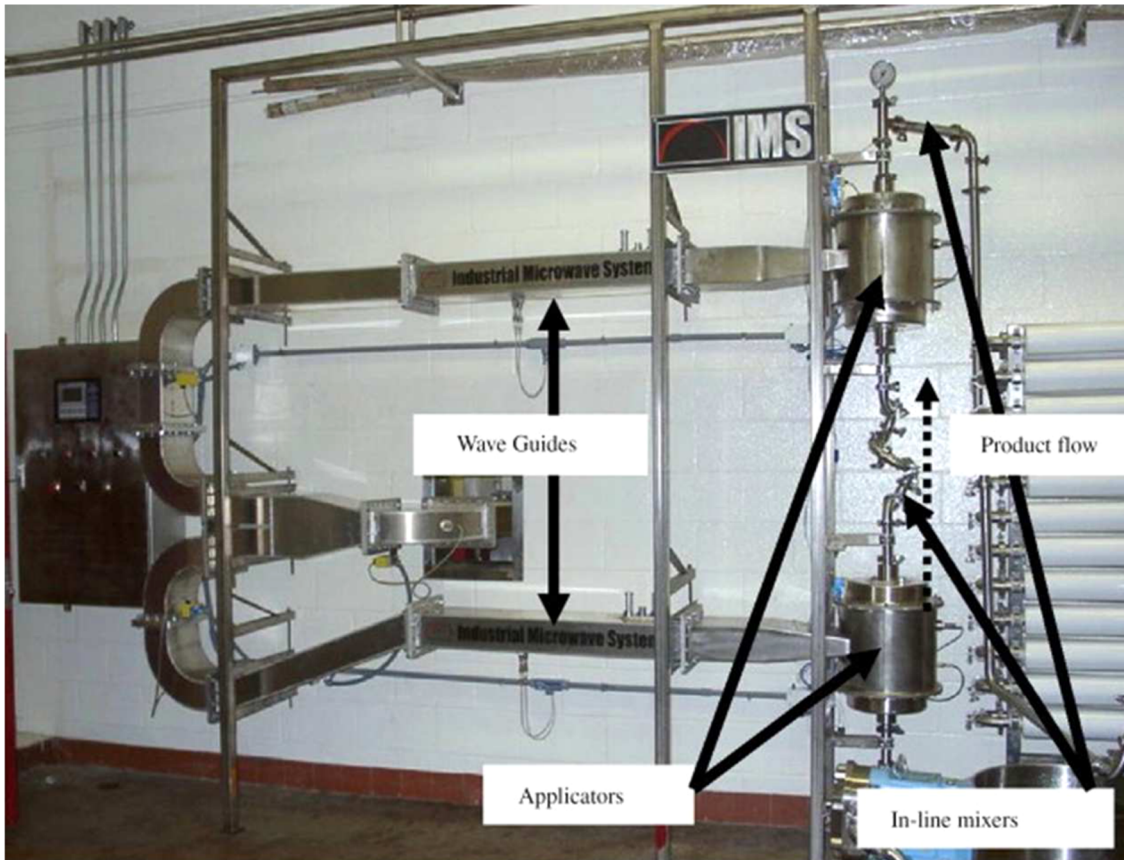


**Figure 42.** MW (60 kW) continuous-flow system used by Kumar et al.<sup>248</sup> Reprinted with permission from ref 248. Copyright 2008 Elsevier.

scale of the electrodynamics is far shorter than that of the thermodynamics, so an iterative approach is typically taken when both aspects are solved numerically.<sup>252</sup> Such a methodology is well known in the food industry.<sup>253</sup> The methodology is similar for application to heating of chemical reactions, except that chemical change is expected to significantly affect the field distribution.

Coupling of electromagnetic and thermal solvers to chemical reaction solvers is currently problematic due to a lack of spatially resolved chemical modeling algorithms that can handle complex dynamics such as phase changes (e.g., melting of solids and evaporation of liquids). For example, numerical analysis of a saponification reaction in dilute solution coupled a finite-difference time-domain solver to a thermal transport solver and a chemical solver based on the rate equation, but the results were restricted to a small temperature change of less than 10 °C, starting from room temperature.<sup>254</sup> To the best of our knowledge, there has been little further progress on coupling to numerical chemical solvers, with attention instead focusing on coupling via Navier–Stokes equations to fluid flow in liquids.<sup>255,256</sup>

A further challenge lies in validating the simulation (see section 7). For a MW heating application, it is difficult to validate the electric field distribution directly, because it is usually inside an enclosed cavity. Further, electric field probes are conductive and typically disturb the measurement. Modulated scattering methods<sup>257</sup> reduce the disturbance, but only mechanically driven schemes are viable for use in high-field strengths, and this would limit their use to outside of the load, unless it was liquid. The temperature profile can be more readily measured without disturbing MW fields. A number of approaches are available, but typically they offer only a surface temperature map (infrared imaging) or are invasive and offer only poor spatial resolution (thermocouples, fiber optic thermometers).<sup>258</sup> An innovative approach is to use magnetic resonance imaging, which can infer a rise in temperature from the drop in precession frequency of the water proton.<sup>259</sup> This approach is presently impractical for solid-state synthesis reactions due to the lack of water in the system, but neutron diffraction offers an average temperature reading.

## 9. CONCLUDING REMARKS

It is often assumed that MWs do not offer a cheap form of energy when compared to conventional heating sources, although detailed costs for MW processes are notoriously difficult to uncover. Some data were reported in a paper in 1988 based on MW applications in the ceramics industry.<sup>260</sup> The typical cost of MW generators was reported, at that time, to be somewhere between US \$1000 and \$5000/kW, with the generator typically accounting for less than 50% of the system expense and the applicator representing more than 50% of the expense. In order to justify the significantly inflated capital cost when compared to conventional heating, it could be argued that other process advantages are required to justify the expenditure in the value proposition. Unless driven by environmental legislation, one view is that MWs will only see commercial implementation if they are able to deliver a benefit that no other technology can. The examples in the previous sections show that MW heating almost always provides considerably reduced reaction times with commensurate savings likely to be made in terms of processing. This feature alone may not be sufficient to prompt a switch to MW heating in industrial processes. The driving factors may prove to be more closely related to volumetric or selective

heating or to very significant improvements in the properties of the target materials.

On analysis of the position of MW synthesis and processing in inorganic materials chemistry since the turn of the 21st century, three key areas are identifiable: (1) applicability and utility of MW methods across a wide range of materials systems; (2) increasing importance of in-situ methodologies in determining the origins of MW interactions with solids and understanding the mechanisms of MW-driven reactions; (3) advantages, but conversely challenges, associated with the process and electrical engineering in the scaling up of MW approaches toward materials manufacturing.

Not only has proliferation of MW-based materials chemistry become more widespread over the past decade but also so has the area begun to mature and become more sophisticated. Development of experiment design has allowed greater emphasis to be attached to reproducibility and repeatability, greater control to be exerted over materials homogeneity and temperature measurement and management and greater understanding to be applied to use of input power, frequency, and susceptors. These advances have been made in part through growth of in-situ, time-resolved, characterization, and measurement techniques. Accurate measurement of temperature within the bulk of MW-heated materials—during chemical reactions—remains a challenge, but contactless methods that avoid perturbation of the MW field are central to this development. Further, just as in other (extreme) reaction environments, to the solid-state chemist, the ability to monitor and elucidate phase composition and structure with time is a crucial step toward rationalizing the reaction mechanism. Even under conventional heating conditions, compared to the molecular case, the reaction mechanism in the solid state is elusive; for MWs the challenge is compounded further given processes that are complete over second time scales. Advances in instrumentation (both hardware and software) however are able to put such ambitions within reach for the first time.

Beyond the fundamental objectives above, the remaining requirements that have the potential to propel MW methods from the laboratory to the marketplace depend on the efficiency of processes and economic cost. Optimizing the synthesis environment especially via modeling of electromagnetic field distributions and cavity design is at the core of the former. Manipulating MW penetration depth will be vital to develop the flow processes that underpin manufacturing and mass production. Finally, full life cycle analysis is a priority not only in terms of deriving definitive economic parameters but also in assessing the sustainability and green credentials of future processes. Given the tremendous advances that have already taken place since the turn of the millennium, then there is every reason to be optimistic that such goals can be achieved to transform materials manufacturing within a generation.

## AUTHOR INFORMATION

### Corresponding Author

\*E-mail: Duncan.Gregory@Glasgow.ac.uk.

### Notes

The authors declare no competing financial interest.

**Biographies**

Helen Kitchen received her M.Chem. degree from Hertford College, University of Oxford, in 2009. She is currently undertaking a Ph.D. at the University of Glasgow, under the supervision of Professor Duncan H. Gregory. Her current research is focused on development of in-situ powder neutron diffraction techniques for time-resolved study of solid-state microwave synthesis, particularly synthesis of transition metal carbides.

University of Glasgow, where she is currently studying for an interdisciplinary Ph.D. degree between Electrical Engineering and Chemistry under the supervision of Dr. Timothy D. Drysdale and Professor Duncan H. Gregory. Her research interests center on developing energy-efficient microwave syntheses of refractory ceramics and establishing structure–property relationships.



Nuria Tapia-Ruiz graduated from the University of Barcelona with her B.Sc. degree (Hons) in Inorganic Chemistry in 2009. She then moved to the University of Glasgow, where she is currently studying for her Ph.D. degree in Materials Chemistry under the supervision of Professor Duncan H. Gregory. Her research interests center on developing new routes for synthesis of nitrides with applications as energy storage and conversion materials. This work includes preparation of nitrides using microwave techniques.



Simon Vallance graduated in 2007 with his Ph.D. degree at the University of Nottingham under Professor Duncan Gregory and Professor Sam Kingman. His research was focused on microwave synthesis of transition metal carbides. This involved development of microwave reactors and novel experimental design in addition to mechanistic study of reactions and characterization and mechanical testing of carbide materials. Since graduating he has worked as a fire and explosions investigator at Hawkins & Associates.



Lucia Carassiti graduated from the Sapienza University of Rome with her M.Sc. degree in the Chemistry of Materials in 2007. She then moved to the University of Glasgow, where she graduated with her Ph.D. degree in 2012 under the supervision of Professor Duncan H. Gregory. Her research involved microwave synthesis of silicon carbide and its characterization. Since graduating she has worked for Jaguar Land Rover as a Chassis Engineer.



Jennifer Kennedy graduated from the University of Glasgow with her M.Sc. degree (Hons) in Chemistry in 2011. She remained at the



Timothy D. Drysdale graduated with his Ph.D. degree (2003) in Electronics and Electrical Engineering from the University of Canterbury, New Zealand. He was awarded a Royal Society of Edinburgh & Scottish Executive Personal Research Fellowship in 2004, which he took at the University of Glasgow, and was appointed as a lecturer in 2006. He has published in the fields of electromagnetic modeling, terahertz technology, and digital imaging and holds a patent in microwave processing. He exhibited at the Royal Society Summer Science Exhibition 2006 and gave the Isambard Kingdom Brunel Award Lecture at the British Science Festival 2012.



Sam Kingman obtained his Ph.D. degree in Chemical Engineering at the University of Birmingham in 1999. In 2000 he moved to the University of Nottingham to take up a lectureship. He was awarded a personal chair at Nottingham in 2006, which at the time made him one of the youngest professors in the United Kingdom. He is Director of the National Centre for Industrial Microwave Processing (NCIMP), which is one of the largest activities of its type in the world. The center is focused upon development of a fundamental understanding of the interaction of microwave energy with materials and use of this understanding to underpin process scale up.



Gavin Whittaker studied at the University of Oxford, completing his Ph.D. degree in 1994 under Professor Mike Mingos. He was a Postdoctoral researcher and then Lecturer in Physical Chemistry at the University of Edinburgh until 2006. Thereafter, he set up Tan Delta Microwaves as a microwave consultancy and equipment sales company and Miramodus producing chemical structure models. His interests covered fundamental microwave interactions with solid-state materials and now include industrial applications of microwave heating.



Duncan H. Gregory studied at the University of Southampton, completing his Ph.D. degree in 1993 under Professor Mark Weller. He was an EPSRC Advanced Fellow, Lecturer, and Reader in Materials Chemistry at the University of Nottingham until 2006. He then took up the WestCHEM Chair in Inorganic Materials at the University of Glasgow and is Head of Inorganic Chemistry. His research interests encompass functional, structural, and energy materials with a focus on sustainable synthesis and processing of inorganic solids.



#### ACKNOWLEDGMENTS

D.H.G. thanks the STFC for a studentship for H.J.K, ScotCHEM for a studentship for N.T.R and the University of Glasgow/GRPE for a studentship for LC. D.H.G. and S.W.K. thank the

University of Nottingham for a studentship for S.R.V. D.H.G. and T.D.D. thank the University of Glasgow for a studentship for J.L.K.

## REFERENCES

- (1) Adam, D. *Nature* **2003**, *421* (6923), 571.
- (2) Mingos, D. M. P.; Baghurst, D. R. *Chem. Soc. Rev.* **1991**, *20* (1), 1.
- (3) Majetich, G.; Hicks, R. *J. Microwave Power Electromag. Energy* **1995**, *30* (1), 27.
- (4) Galema, S. A. *Chem. Soc. Rev.* **1997**, *26* (3), 233.
- (5) de la Hoz, A.; Diaz-Ortiz, A.; Moreno, A. *Chem. Soc. Rev.* **2005**, *34* (2), 164.
- (6) Rao, K. J.; Vaidyanathan, B.; Ganguli, M.; Ramakrishnan, P. A. *Chem. Mater.* **1999**, *11* (4), 882.
- (7) Liu, S. W.; Wightman, J. P. *J. Appl. Chem. Biotechnol.* **1971**, *21* (6), 168.
- (8) Gedye, R.; Smith, F.; Westaway, K.; Ali, H.; Baldisera, L.; Laberge, L.; Rousell, J. *Tetrahedron Lett.* **1986**, *27* (3), 279.
- (9) Bykov, Y. V.; Rybakov, K. I.; Semenov, V. E. *J. Phys. D: Appl. Phys.* **2001**, *34* (13), R55.
- (10) Whittaker, A. G.; Mingos, D. M. P. *J. Microwave Power Electromag. Energy* **1994**, *29* (4), 195.
- (11) Lidstrom, P.; Tierney, J.; Wathey, B.; Westman, J. *Tetrahedron* **2001**, *57* (45), 9225.
- (12) Rao, K. J.; Ramesh, P. D. B. *Mater. Sci.* **1995**, *18* (4), 447.
- (13) Giguere, R. J.; Bray, T. L.; Duncan, S. M.; Majetich, G. *Tetrahedron Lett.* **1986**, *27* (41), 4945.
- (14) Stuerga, D. A. C.; Gaillard, P. *J. Microwave Power Electromag. Energy* **1996**, *31* (2), 87.
- (15) Stuerga, D. A. C.; Gaillard, P. *J. Microwave Power Electromag. Energy* **1996**, *31* (2), 101.
- (16) Sutton, W. H. *Am. Ceram. Soc. Bull.* **1989**, *68* (2), 376.
- (17) Katz, J. D. *Annu. Rev. Mater. Sci.* **1992**, *22*, 153.
- (18) Agrawal, D. K. *Curr. Opin. Solid State Mater. Sci.* **1998**, *3* (5), 480.
- (19) Clark, D. E.; Sutton, W. H. *Annu. Rev. Mater. Sci.* **1996**, *26*, 299.
- (20) Mingos, D. M. P.; Baghurst, D. R. *Br. Ceram. Trans. J.* **1992**, *91* (4), 124.
- (21) Whittaker, A. G.; Mingos, D. M. P. *J. Chem. Soc., Dalton Trans.* **1995**, *12*, 2073.
- (22) Dudnik, E. V.; Zaitseva, Z. A.; Shevchenko, A. V.; Lopato, L. M. *Powder Metall. Met. Ceram.* **1995**, *34* (5–6), 263.
- (23) Binner, J. G. P.; Vaidyanathan, B. *Euro Ceramic VII, Pts 1–3: Key Engineering Materials*; 2004; Vols. 264–268, p 725.
- (24) Schanche, J.-S. *Mol. Diversity* **2003**, *7* (2–4), 293.
- (25) Metaxas, A. C.; Meredith, R. J. *Industrial Microwave Heating*; The Institution of Engineering and Technology, London: 1983.
- (26) Zhang, X. L.; Hayward, D. O.; Mingos, D. M. P. *Catal. Lett.* **2003**, *88* (1–2), 33.
- (27) Whittaker, A. G.; Mingos, D. M. P. *J. Chem. Soc., Dalton Trans.* **1992**, *18*, 2751.
- (28) Kraus, J. D. *Electromagnetics*, 3rd ed.; McGraw Hill: New York, 1984.
- (29) Bossavit, A. *Computational Electromagnetism*; Academic Press: Boston, 1998.
- (30) Kenkre, V. M.; Skala, L.; Weiser, M. W.; Katz, J. D. *J. Mater. Sci.* **1991**, *26* (9), 2483.
- (31) Kriegsmann, G. A. *J. Appl. Phys.* **1992**, *71* (4), 1960.
- (32) Peng, J. H.; Binner, J.; Bradshaw, S. *Mater. Sci. Technol.* **2002**, *18* (12), 1419.
- (33) Lee, H. K.; Cao, H.; Rana, T. M. *J. Comb. Chem.* **2005**, *7* (2), 279.
- (34) Ding, D. R.; Li, X.; Wang, X.; Du, Y. L.; Shen, J. K. *Tetrahedron Lett.* **2006**, *47* (39), 6997.
- (35) Biswas, A.; Shogren, R. L.; Selling, G.; Salch, J.; Willett, J. L.; Buchanan, C. M. *Carbohydr. Polym.* **2008**, *74* (1), 137.
- (36) Leadbeater, N. E.; Barnard, T. M.; Stencel, L. M. *Energy Fuels* **2008**, *22* (3), 2005.
- (37) Leadbeater, N. E.; Smith, R. J. *Org. Lett.* **2006**, *8* (20), 4588.
- (38) Ferguson, J. D. *Mol. Diversity* **2003**, *7* (2–4), 281.
- (39) Frecentese, F.; Fiorino, F.; Perissutti, E.; Severino, B.; Magli, E.; Esposito, A.; De Angelis, F.; Massarelli, P.; Nencini, C.; Viti, B.; Santagada, V.; Caliendo, G. *Eur. J. Med. Chem.* **2010**, *45* (2), 752.
- (40) Schmink, J. R.; Kormos, C. M.; Devine, W. G.; Leadbeater, N. E. *Org. Process Res. Dev.* **2010**, *14* (1), 205.
- (41) Paulus, R. M.; Erdmenger, T.; Becer, C. R.; Hoogenboom, R.; Schubert, U. S. *Macromol. Rapid Commun.* **2007**, *28* (4), 484.
- (42) Bowman, M. D.; Holcomb, J. L.; Kormos, C. M.; Leadbeater, N. E.; Williams, V. A. *Org. Process Res. Dev.* **2008**, *12* (1), 41.
- (43) Asmussen, J.; Lin, H. H.; Manring, B.; Fritz, R. *Rev. Sci. Instrum.* **1987**, *58* (8), 1477.
- (44) Cherradi, A.; Marinelli, S.; Lakhdari, Z.; Desgardin, G.; Provost, J.; Raveau, B. *Microwave J.* **1998**, *41* (2), 84.
- (45) Douthwaite, R. E. *Dalton Trans.* **2007**, No. 10, 1002.
- (46) Brooks, D. J.; Douthwaite, R. E. *Rev. Sci. Instrum.* **2004**, *75* (12), S277.
- (47) Iwasaki, M.; Takizawa, H.; Uheda, K.; Endo, T.; Shimada, M. J. *Mater. Chem.* **1998**, *8* (12), 2765.
- (48) Selvam, M. P.; Rao, K. J. *Adv. Mater.* **2000**, *12* (21), 1621.
- (49) Bhat, M. H.; Miura, A.; Vinatier, P.; Levasseur, A.; Rao, K. J. *Solid State Commun.* **2003**, *125* (10), 557.
- (50) Liu, Y. F.; Liu, X. Q.; Meng, G. Y. *Mater. Lett.* **2001**, *48* (3–4), 176.
- (51) Rao, K. J.; Ramakrishnan, P. A.; Gadagkar, R. *J. Solid State Chem.* **1999**, *148* (1), 100.
- (52) Guo, J.; Dong, C.; Yang, L. H.; Fu, G. C. *J. Solid State Chem.* **2005**, *178* (1), 58.
- (53) Vanetsev, A. S.; Ivanov, V. K.; Tret'yakov, Y. D. *Dokl. Chem.* **2002**, *387* (4–6), 332.
- (54) Saremi-Yarahmadi, S.; Vaidyanathan, B.; Wijayantha, K. G. U. *Int. J. Hydrogen Energy* **2010**, *35* (19), 10155.
- (55) Vaidyanathan, B.; Saremi-Yarahmadi, S.; Wijayantha, K. G. U. In *Fabrication of Nanostructured alpha-Fe<sub>2</sub>O<sub>3</sub> Films for Solar-driven Hydrogen Generation using Hybrid Heating. 5th International Symposium on Nanostructured Materials and Nanotechnology, 35th International Conference and Exposition on Advanced Ceramics and Composites (ICACC)*, Daytona Beach, FL, Jan 23–28, 2011; Daytona Beach, FL, 2011; p 11.
- (56) Binner, J.; Vaidyanathan, B.; Paul, A.; Annaporani, K.; Raghupathy, B. *Int. J. Appl. Ceram. Technol.* **2011**, *8* (4), 766.
- (57) Reguera, E.; Diaz-Aguila, C.; Yee-Madeira, H. *J. Mater. Sci.* **2005**, *40* (19), 5331.
- (58) Vaidyanathan, B.; Singh, A. P.; Agrawal, D. K.; Shrout, T. R.; Roy, R.; Ganguly, S. *J. Am. Ceram. Soc.* **2001**, *84* (6), 1197.
- (59) Vaidyanathan, B.; Agrawal, D. K.; Roy, R. *J. Am. Ceram. Soc.* **2004**, *87* (5), 834.
- (60) Gibbons, K. E.; Jones, M. O.; Blundell, S. J.; Mihut, A. I.; Gameson, I.; Edwards, P. P.; Miyazaki, Y.; Hyatt, N. C.; Porch, A. *Chem. Commun.* **2000**, No. 2, 159.
- (61) Yang, G.; Wang, G.; Hou, W. H. *J. Phys. Chem. B* **2005**, *109* (22), 11186.
- (62) Panneerselvam, M.; Rao, K. J. *J. Mater. Chem.* **2003**, *13* (3), 596.
- (63) Agostino, A.; Benzi, P.; Castiglioni, M.; Rizzi, N.; Volpe, P. *Supercond. Sci. Technol.* **2004**, *17* (4), 685.
- (64) Peelamedu, R. D.; Roy, R.; Agrawal, D. K. *Mater. Lett.* **2002**, *55* (4), 234.
- (65) Panneerselvam, M.; Subanna, G. N.; Rao, K. J. *J. Mater. Res.* **2001**, *16* (10), 2773.
- (66) Nakayama, M.; Watanabe, K.; Ikuta, H.; Uchimoto, Y.; Wakihara, M. *Solid State Ionics* **2003**, *164* (1–2), 35.
- (67) Grossin, D.; Marinelli, S.; Noudem, J. G. *Mater. Res. Innovations* **2005**, *9* (3), 71.
- (68) Brooks, D. J.; Brydson, R.; Douthwaite, R. E. *Adv. Mater.* **2005**, *17* (20), 2474.
- (69) Brooks, D. J.; Douthwaite, R. E.; Gillie, L. *J. Chem. Commun.* **2005**, No. 38, 4857.
- (70) Chou, Y. H.; Morgan, A. J.; Hondow, N. S.; Brydson, R.; Douthwaite, R. E. *DT&R* **2010**, *39* (26), 6062.
- (71) Dwivedi, R.; Maurya, A.; Verma, A.; Prasad, R.; Bartwal, K. S. J. *Alloys Compd.* **2011**, *509* (24), 6848.

- (72) Kumar, S.; Marinel, S.; Miclau, M.; Martin, C. *Mater. Lett.* **2012**, *70*, 40.
- (73) Thomas, P.; Sathapathy, L. N.; Dwarakanath, K.; Varma, K. B. R. *Bull. Mater. Sci.* **2007**, *30* (6), 567.
- (74) Yu, H. T.; Liu, H. X.; Luo, D. B.; Cao, M. H. *J. Mater. Process. Technol.* **2008**, *208* (1–3), 145.
- (75) Jung, K. Y.; Kang, Y. C. *Phys. B* **2010**, *405* (6), 1615.
- (76) Wang, J.; Binner, J.; Vaidhyanathan, B.; Joomun, N.; Kilner, J.; Dimitrakis, G.; Cross, T. E. *J. Am. Ceram. Soc.* **2006**, *89* (6), 1977.
- (77) Grossin, D.; Marinel, S.; Noudem, J. G. *Ceram. Int.* **2006**, *32* (8), 911.
- (78) Prado-Gonjal, J.; Arevalo-Lopez, A. M.; Moran, E. *Mater. Res. Bull.* **2011**, *46* (2), 222.
- (79) Yakovleva, I. S.; Nadeev, A. N.; Gerasimov, E. Y.; Ivanov, D. V.; Dovlitova, L. S.; Sutormina, E. F.; Saputina, N. F.; Litvak, G. S.; Isupova, L. A. *Kinet. Catal.* **2013**, *54* (1), 119.
- (80) Kaddouri, A.; Ifrah, S. *Catal. Commun.* **2006**, *7* (2), 109.
- (81) Vileno, E.; Zhou, H.; Zhang, Q. H.; Suib, S. L.; Corbin, D. R.; Koch, T. A. *J. Catal.* **1999**, *187* (2), 285.
- (82) Zhao, Y.; Hong, J. M.; Zhu, J. J. *J. Cryst. Growth* **2004**, *270* (3–4), 438.
- (83) Liao, X. H.; Chen, N. Y.; Xu, S.; Yang, S. B.; Zhu, J. J. *J. Cryst. Growth* **2003**, *252* (4), 593.
- (84) Palchik, O.; Kerner, R.; Zhu, Z.; Gedanken, A. *J. Solid State Chem.* **2000**, *154* (2), 530.
- (85) Grisaru, H.; Pol, V. G.; Gedanken, A.; Nowik, I. *Eur. J. Inorg. Chem.* **2004**, No. 9, 1859.
- (86) Harpness, R.; Gedanken, A. *New J. Chem.* **2003**, *27* (8), 1191.
- (87) Zhou, B.; Zhao, Y.; Pu, L.; Zhu, J. J. *Mater. Chem. Phys.* **2006**, *96* (2–3), 192.
- (88) Grisaru, H.; Palchik, O.; Gedanken, A.; Palchik, V.; Slifkin, M. A.; Weiss, A. M. *J. Mater. Chem.* **2002**, *12* (2), 339.
- (89) Zhang, W. X.; Yang, Z. H.; Liu, J. W.; Qian, Y. T.; Yu, W. C.; Jia, Y. B.; Liu, X. M.; Zhou, G.; Zhu, J. S. *J. Solid State Chem.* **2001**, *161* (2), 184.
- (90) Liao, X. H.; Zhu, J. J.; Chen, H. Y. *Mater. Sci. Eng., B* **2001**, *85* (1), 85.
- (91) Liu, X. Y.; Tian, B. Z.; Yu, C. Z.; Tu, B.; Zhao, D. Y. *Chem. Lett.* **2004**, *33* (5), 522.
- (92) Panigrahi, P. K.; Pathak, A. *Mater. Res. Bull.* **2011**, *46* (12), 2240.
- (93) Cao, X. B.; Zhao, C.; Lan, X. M.; Yao, D.; Shen, W. *J. J. Alloys Compd.* **2009**, *474* (1–2), 61.
- (94) Susaki, M. *Jpn. J. Appl. Phys.* **2005**, *44* (24–27), L866.
- (95) Yoshino, K.; Ikari, T.; Shirakata, S.; Miyake, H.; Hiramatsu, K. *Appl. Phys. Lett.* **2001**, *78* (6), 742.
- (96) Palchik, O.; Gedanken, A.; Palchik, V.; Slifkin, M. A.; Weiss, A. M. *J. Solid State Chem.* **2002**, *165* (1), 125.
- (97) Zhou, G. T.; Pol, V. G.; Palchik, O.; Kerner, R.; Sominski, E.; Koltypin, Y.; Gedanken, A. *J. Solid State Chem.* **2004**, *177* (1), 361.
- (98) Manoharan, S. S.; Prasanna, S. J.; Kiwitz, D. E.; Schneider, C. M. *Phys. Rev. B* **2001**, *63* (21), 4.
- (99) Ouerfelli, J.; Srivastava, S. K.; Bernede, J. C.; Belgacem, S. *Vacuum* **2008**, *83* (2), 308.
- (100) Obut, A. *Miner. Eng.* **2007**, *20* (14), 1320.
- (101) Suriwong, T.; Thongtem, S.; Thongtem, T. *Mater. Lett.* **2009**, *63* (24–25), 2103.
- (102) Suriwong, T.; Thongtem, T.; Thongtem, S. *Micro Nano Lett.* **2011**, *6* (3), 170.
- (103) Lekse, J. W.; Pischera, A. M.; Aitken, J. A. *J. Mater. Res. Bull.* **2007**, *42* (3), 395.
- (104) Mastrovito, C.; Lekse, J. W.; Aitken, J. A. *J. Solid State Chem.* **2007**, *180* (11), 3262.
- (105) Nagamatsu, J.; Nakagawa, N.; Muranaka, T.; Zenitani, Y.; Akimitsu, J. *Nature* **2001**, *410* (6824), 63.
- (106) Agostino, A.; Volpe, P.; Castiglioni, M.; Truccato, M. *Mater. Res. Innovations* **2004**, *8* (2), 75.
- (107) Agostino, A.; Bonometti, E.; Volpe, P.; Truccato, M.; Manfredotti, C.; Olivero, P.; Paolini, C.; Rinaudo, G.; Gozzelino, L. *Int. J. Mod. Phys. B* **2003**, *17* (4–6), 773.
- (108) Dong, C.; Guo, J.; Fu, G. C.; Yang, L. H.; Chen, H. *Supercond. Sci. Technol.* **2004**, *17* (12), L55.
- (109) Xia, Q. L.; Yi, J. H.; Peng, Y. D.; Luo, S. D.; Li, L. Y. *Mater. Lett.* **2008**, *62* (24), 4006.
- (110) Zeng, R.; Zhou, S.; Lu, L.; Li, W. X.; Dou, S. X. *Phys. C* **2010**, *470*, S669.
- (111) Chauhan, S. R.; Chaudhary, S. *IEEE Trans. Appl. Supercond.* **2010**, *20* (1), 26.
- (112) Pan, X. F.; Cheng, C. H.; Zhou, J. D.; Zhao, Y. *Supercond. Sci. Technol.* **2009**, *22* (4).
- (113) Kang, W. N.; Kim, H. J.; Choi, E. M.; Jung, C. U.; Lee, S. L. *Science* **2001**, *292* (5521), 1521.
- (114) Jung, C. U.; Park, M. S.; Kang, W. N.; Kim, M. S.; Lee, S. Y.; Lee, S. I. *Phys. C* **2001**, *353* (3–4), 162.
- (115) Bud'ko, S. L.; Lapertot, G.; Petrovic, C.; Cunningham, C. E.; Anderson, N.; Canfield, P. C. *Phys. Rev. Lett.* **2001**, *86* (9), 1877.
- (116) Zhiyong, H.; Lin, L.; Xiaoyan, P. *China's Refractories* **2005**, *14*, 26.
- (117) Setoudeh, N.; Welham, N. *J. J. Alloys Compd.* **2006**, *420* (1–2), 225.
- (118) Guo, S.; Nishimura, T.; Kagawa, Y. *Scr. Mater.* **2011**, *65* (11), 1018.
- (119) Zhang, X.-B.; Hu, P.; Han, J.-C.; Xu, L.; Meng, S.-H. *Scr. Mater.* **2007**, *57* (11), 1036.
- (120) Baldridge, T.; Gupta, M. C. *Nanotechnology* **2008**, *19* (27).
- (121) He, J.-H.; Wan, Y.-Q.; Xu, L. *Chaos, Solitons Fractals* **2007**, *33* (1), 26.
- (122) Kosolapova, T. Y. *Carbides: Properties, Production and Applications*; Plenum Press: New York, 1971.
- (123) Alexander, A. M.; Hargreaves, J. S. *J. Chem. Soc. Rev.* **2010**, *39* (11), 4388.
- (124) Casady, J. B.; Johnson, R. W. *Solid-State Electron.* **1996**, *39* (10), 1409.
- (125) Palmour, J. W.; Edmond, J. A.; Kong, H. S.; Carter, C. H. *Phys. B* **1993**, *185* (1–4), 461.
- (126) Storms, E. K. *The Refractory Carbides*. Academic Press: New York, London, 1967.
- (127) Ahlers, R.; Ruschewitz, U. Z. *Anorg. Allg. Chem.* **2005**, *631* (6–7), 1241.
- (128) Xia, Q. L.; Yi, J. H.; Huang, J. W.; Ye, T. M.; Peng, Y. D.; Li, L. Y. *Supercond. Sci. Technol.* **2006**, *19* (12), 1282.
- (129) Carassiti, L.; Jones, A.; Harrison, P.; Dobson, P. S.; Kingman, S.; MacLaren, I.; Gregory, D. H. *Energy Environ. Sci.* **2011**, *4* (4), 1503.
- (130) Ebadzadeh, T.; Marzban-Rad, E. *Mater. Charact.* **2009**, *60* (1), 69.
- (131) Satapathy, L. N.; Ramesh, P. D.; Agrawala, D.; Roy, R. *Mater. Res. Bull.* **2005**, *40* (10), 1871.
- (132) Panneerselvam, M.; Agrawal, A.; Rao, K. J. *Mater. Sci. Eng., A* **2003**, *356* (1–2), 267.
- (133) Das, B. P.; Panneerselvam, M.; Rao, K. J. *J. Solid State Chem.* **2003**, *173* (1), 196.
- (134) Wei, G. D.; Qin, W. P.; Han, W.; Yang, W. Y.; Gao, F. M.; Jing, G. Z.; Kim, R. J.; Zhang, D. S.; Zheng, K. Z.; Wang, L. L.; Liu, L. *J. Phys. Chem. C* **2009**, *113* (45), 19432.
- (135) Deksnys, T. P.; Menezes, R. R.; Fagury-Neto, E.; Kiminami, R. *Ceram. Int.* **2007**, *33* (1), 67.
- (136) Hassine, N. A.; Binner, J. G. P.; Cross, T. E. *Int. J. Refract. Met. Hard Mater.* **1995**, *13* (6), 353.
- (137) Liu, P.; Zeng, L.; Wang, H.; Cheng, X.; Shui, A.; Zhang, H.; Duan, B.; Deng, W. Method of continuous microwave synthesizing nano-class titanium carbide. Chinese Patent 1834009, Sept 20 2006.
- (138) West, C. P.; Harrison, I.; Cussen, E. J.; Gregory, D. H. *J. Eur. Ceram. Soc.* **2009**, *29* (11), 2355.
- (139) Kitwan, M.; Atong, D. *JSME Int. J., Ser. A* **2006**, *49* (1), 85.
- (140) Roy, R.; Agrawal, D.; Chen, J. P.; Gedevanishvili, S. *Nature* **1999**, *399* (6737), 668.
- (141) Vallance, S. R.; Round, D. M.; Ritter, C.; Cussen, E. J.; Kingman, S.; Gregory, D. H. *Adv. Mater.* **2009**, *21* (44), 4502.

- (142) Vallance, S. R.; Kingman, S.; Gregory, D. H. *Chem. Commun.* **2007**, No. 7, 742.
- (143) Pang, M.; Li, C.; Ding, L.; Zhang, J.; Su, D. S.; Li, W. Z.; Liang, C. H. *Ind. Eng. Chem. Res.* **2010**, *49* (9), 4169.
- (144) Rodiger, K.; Dreyer, K.; Gerdes, T.; Willert-Porada, M. *Int. J. Refract. Met. Hard Mater.* **1998**, *16* (4–6), 409.
- (145) Lindholm, M.; Waldenstroem, M.; Ahlgren, M. Method of making cemented carbide. International Patent WO 00/03049, Jan 20 2000.
- (146) Lackner, A.; Ferstl, W.; Knuenz, G.; Dinesh, A.; Jiping, C. Method for the production of metal carbide powders in a microwave oven. International Patent WO 01/42135, June 14 2001.
- (147) Vallance, S. R.; Kingman, S.; Gregory, D. H. *Adv. Mater.* **2007**, *19* (1), 138.
- (148) Essaki, K.; Rees, E. J.; Burstein, G. T. *Mater. Lett.* **2009**, *63* (26), 2185.
- (149) Rees, E. J.; Essaki, K.; Brady, C. D. A.; Burstein, G. T. *J. Power Sources* **2009**, *188* (1), 75.
- (150) Shen, P. K.; Yin, S. B.; Li, Z. H.; Chen, C. *Electrochim. Acta* **2010**, *55* (27), 7969.
- (151) Vallance, S. R.; Kitchen, H. J.; Ritter, C.; Kingman, S.; Dimitrakis, G.; Gregory, D. H. *Green Chem.* **2012**, DOI: 10.1039/c2gc35272a.
- (152) Sunil, B. R.; Sivaprahasam, D.; Subasri, R. *Int. J. Refract. Met. Hard Mater.* **2010**, *28* (2), 180.
- (153) Breval, E.; Cheng, J. P.; Agrawal, D. K.; Gigl, P.; Dennis, A.; Roy, R.; Papworth, A. J. *Mater. Sci. Eng., A* **2005**, *391* (1–2), 285.
- (154) Cheng, J. P.; Agrawal, D. K.; Komarneni, S.; Mathis, M.; Roy, R. *Mater. Res. Innovations* **1997**, *1* (1), 44.
- (155) Lu, J. L. L.; Jiang, Z. H.; Shen, S. P.; Li, P. K.; Lin. *J. Power Sources* **2012**, *202*, 56.
- (156) Hu, F. P.; Cui, G. F.; Wei, Z. D.; Shen, P. K. *Electrochim. Commun.* **2008**, *10* (9), 1303.
- (157) Petrovic, J. J.; Vasudevan, A. K. *Mater. Sci. Eng., A* **1999**, *261* (1–2), 1.
- (158) Jokisaari, J. R.; Bhaduri, S.; Bhaduri, S. B. *J. Alloys Compd.* **2005**, *394* (1–2), 160.
- (159) Zhou, G. T.; Palchik, O.; Nowik, I.; Herber, R.; Koltypin, Y.; Gedanken, A. *J. Solid State Chem.* **2004**, *177* (9), 3014.
- (160) Zhou, S.-C.; Bai, C.-G. *Trans. Nonferrous Met. Soc. China* **2011**, *21* (8), 1785.
- (161) Yang, L.; Dong, C.; Liu, H.; He, B.; Chen, H. *Supercond. Sci. Technol.* **2008**, *21* (1), 015010.
- (162) Vaidhyanathan, B.; Rao, K. J. *J. Mater. Res.* **1997**, *12* (12), 3225.
- (163) Thompson, D. C.; Kim, H. C.; Alford, T. L.; Mayer, J. W. *Appl. Phys. Lett.* **2003**, *83* (19), 3918.
- (164) Jokisaari, J. R.; Bhaduri, S.; Bhaduri, S. B. *Mater. Sci. Eng., A* **2002**, *323* (1–2), 478.
- (165) Matsumura, Y.; Chujo, T.; Uchida, H.; Uchida, H. H. *Surf. Coat. Technol.* **1993**, *60* (1–3), 489.
- (166) Giebler, M.; Ramsteiner, M.; Brandt, O.; Yang, H.; Ploog, K. H. *Appl. Phys. Lett.* **1995**, *67* (6), 733.
- (167) Oyama, S. T. *Catal. Today* **1992**, *15* (2), 179.
- (168) Niewa, R.; DiSalvo, F. J. *J. Chem. Mater.* **1998**, *10* (10), 2733.
- (169) Gregory, D. H. *Chem. Rec.* **2008**, *8* (4), 229.
- (170) Matthew, D. V. *Am. Ceram. Soc. Bull.* **1999**, *78* (6), 69.
- (171) Raghavan, N. S.; Poste, S. D.; Pattemore, D. *Mater. Sci. Eng., B* **1993**, *19* (3), 240.
- (172) Liu, B. H.; Zhang, Y.; Ouyang, S. X.; Gu, H. C. *Acta Metall. Sin.* **1998**, *11* (4), 291.
- (173) White, G. V.; Mackenzie, K. J. D.; Johnston, J. H. *J. Mater. Sci.* **1992**, *27* (16), 4287.
- (174) Whittaker, A. G.; Mingos, D. M. P. *J. Chem. Soc., Dalton Trans.* **1993**, No. 16, 2541.
- (175) Vaidhyanathan, B.; Agrawal, D. K.; Roy, R. *J. Mater. Res.* **2000**, *15* (4), 974.
- (176) Jain, A.; Brezinsky, K. *J. Am. Ceram. Soc.* **2003**, *86* (2), 222.
- (177) Craciun, S.; Craciun, E. *Rev. Rom. Mater.* **2005**, *35*, 97.
- (178) Hsieh, C. Y.; Lin, C. N.; Chung, S. L.; Cheng, J.; Agrawal, D. K. *J. Eur. Ceram. Soc.* **2007**, *27* (1), 343.
- (179) Chung, S. L.; Yu, W. L.; Lin, C. N. *J. Mater. Res.* **1999**, *14* (5), 1928.
- (180) Bang, C. U.; Hong, Y. C.; Uhm, H. S. *Surf. Coat. Technol.* **2007**, *201* (9–11), 5007.
- (181) Hong, Y. C.; Shin, D. H.; Uhm, H. S. *Mater. Chem. Phys.* **2007**, *101* (1), 35.
- (182) Huang, J. W.; Li, J.; Peng, H. *Powder Metall.* **2007**, *50* (2), 137.
- (183) Ozawa, T.; Dohi, M.; Matsuura, T.; Hayakawa, Y. *J. Cryst. Growth* **2008**, *310* (7–9), 1785.
- (184) Houmes, J. D.; zurLoye, H. C. *Chem. Mater.* **1996**, *8* (11), 2551.
- (185) Kabouzi, Y.; Calzada, M. D.; Moisan, M.; Tran, K. C.; Trassy, C. *J. Appl. Phys.* **2002**, *91* (3), 1008.
- (186) Peng, J. H.; Binner, J. *J. Mater. Sci. Lett.* **2002**, *21* (3), 247.
- (187) Anderson, A. J.; Blair, R. G.; Hick, S. M.; Kaner, R. B. *J. Mater. Chem.* **2006**, *16* (14), 1318.
- (188) Zhou, G. T.; Palchik, O.; Pol, V. G.; Sominski, E.; Koltypin, Y.; Gedanken, A. *J. Mater. Chem.* **2003**, *13* (10), 2607.
- (189) Weppner, W.; Huggins, R. A. *J. Solid State Chem.* **1977**, *22* (3), 297.
- (190) Huggins, R. A. *Power Sources* **1999**, *81*, 13.
- (191) Hector, A. L.; Parkin, I. P. Z. *Naturforsch., B: J. Chem. Sci.* **1994**, *49* (4), 477.
- (192) Blaszczyk-Lezak, I.; Wrobel, A. M.; Kivitorma, M. P. M.; Vayrynen, U.; Tracz, A. *Appl. Surf. Sci.* **2007**, *253* (17), 7211.
- (193) Qin, L.; Yu, J.; Kuang, S. Y.; Xiao, C.; Bai, X. D. *Nanoscale* **2012**, *4* (1), 120.
- (194) Bulou, S.; Le Brizoual, L.; Miska, P.; de Pouques, L.; Hugon, R.; Belmahi, M.; Bougdira, J. *Thin Solid Films* **2011**, *520* (1), 245.
- (195) Wrobel, A. M.; Blaszczyk-Lezak, I.; Uznanski, P.; Glebocki, B. *Chem. Vap. Deposition* **2010**, *16* (7–9), 211.
- (196) Zhang, H. A.; Yi, J. Y.; Gu, S. Y. *Int. J. Refract. Met. Hard Mater.* **2011**, *29* (2), 158.
- (197) Choi, J. G.; Ha, J.; Hong, J. W. *Appl. Catal., A* **1998**, *168* (1), 47.
- (198) McCauley, J. W.; Corbin, N. D. *J. Am. Ceram. Soc.* **1979**, *62* (9–10), 476.
- (199) Cheng, J. P.; Agrawal, D.; Roy, R. *J. Mater. Sci. Lett.* **1999**, *18* (24), 1989.
- (200) Panneerselvam, M.; Rao, K. J. *Mater. Res. Bull.* **2003**, *38* (4), 663.
- (201) Robb, G. R.; Harrison, A.; Whittaker, A. G. *PhysChemComm* **2002**, *5*, 135.
- (202) Tompsett, G. A.; Panzarella, B.; Conner, W. C.; Yngvesson, K. S.; Lu, F.; Suib, S. L.; Jones, K. W.; Bennett, S. *Rev. Sci. Instrum.* **2006**, *77* (12), 124101.
- (203) Panzarella, B.; Tompsett, G.; Conner, W. C.; Jones, K. *ChemPhysChem* **2007**, *8* (3), 357.
- (204) Wragg, D. S.; Byrne, P. J.; Giriat, G.; Le Ouay, B.; Gyepes, R.; Harrison, A.; Whittaker, A. G.; Morris, R. E. *J. Phys. Chem. C* **2009**, *113* (48), 20553.
- (205) Vaucher, S.; Nicula, R.; Catala-Civera, J. M.; Schmitt, B.; Patterson, B. *J. Mater. Res.* **2008**, *23* (1), 170.
- (206) Vaucher, S.; Stir, M.; Ishizaki, K.; Catala-Civera, J. M.; Nicula, R. *Thermochim. Acta* **2011**, *522* (1–2), 151.
- (207) Whittaker, A. G.; Harrison, A.; Oakley, G. S.; Youngson, I. D.; Heenan, R. K.; King, S. M. *Rev. Sci. Instrum.* **2001**, *72* (1), 173.
- (208) Harrison, A.; Ibberson, R.; Robb, G.; Whittaker, G.; Wilson, C.; Youngson, D. *Faraday Discuss.* **2003**, *122*, 363.
- (209) Sears, V. F. *Neutron News* **1992**, *3* (3), 26.
- (210) Gunter, M. M.; Korte, C.; Brunauer, G.; Boysen, H.; Lerch, M.; Suard, E. Z. *Anorg. Allg. Chem.* **2005**, *631* (6–7), 1277.
- (211) Baghurst, D. R.; Mingos, D. M. P. *J. Chem. Soc., Chem. Commun.* **1992**, No. 9, 674.
- (212) Rybakov, K. I.; Semenov, V. E.; Freeman, S. A.; Booske, J. H.; Cooper, R. F. *PhRvB* **1997**, *55* (6), 3559.
- (213) Freeman, S. A.; Booske, J. H.; Cooper, R. F. *Phys. Rev. Lett.* **1995**, *74* (11), 2042.
- (214) Willert-Porada, M. *Microwaves: Theory and Application in Materials Processing IV*; American Ceramic Society: 1997; Vol. 80, p 11.
- (215) Whittaker, A. G. *Chem. Mater.* **2005**, *17* (13), 3426.

- (216) Demirskyi, D.; Agrawal, D.; Ragulya, A. *Mater. Sci. Eng., A* **2010**, *527* (7–8), 2142.
- (217) Rowley, A. T.; Wroe, R.; VazquezNavarro, D.; Lo, W.; Cardwell, D. A. *JMatS* **1997**, *32* (17), 4541.
- (218) Boch, P.; Lequeux, N. *Solid State Ionics* **1997**, *101*, 1229.
- (219) Roy, R.; Peelamedu, R.; Hurt, L.; Cheng, J. P.; Agrawal, D. *Mater. Res. Innovations* **2002**, *6* (3), 128.
- (220) Johnson, D. L. *J. Am. Ceram. Soc.* **1991**, *74* (4), 849.
- (221) Booske, J. H.; Cooper, R. F.; Freeman, S. A.; Rybakov, K. I.; Semenov, V. E. *PhPl* **1998**, *5* (5), 1664.
- (222) Rybakov, K. I.; Olevsky, E. A.; Krikun, E. V. *J. Am. Ceram. Soc.* **2013**, *96* (4), 1003.
- (223) Heller, E.; Klockner, J.; Lautenschlager, W.; Holzgrabe, U. *Eur. J. Org. Chem.* **2010**, No. 19, 3569.
- (224) Leadbeater, N. E. *Chem. Commun.* **2010**, *46* (36), 6693.
- (225) Leadbeater, N. E.; Schmink, J. R. *Nat. Protoc.* **2008**, *3* (1), 1.
- (226) Pivonka, D. E.; Empfield, J. R. *Appl. Spectrosc.* **2004**, *58* (1), 41.
- (227) Silverwood, I. P.; McDougall, G. S.; Whittaker, A. G. *Phys. Chem. Chem. Phys.* **2006**, *8* (46), 5412.
- (228) Silverwood, I.; McDougall, G.; Whittaker, G. *J. Mol. Catal. A: Chem.* **2007**, *269* (1–2), 1.
- (229) Leonelli, C.; Mason, T. J. *Chem. Eng. Process.* **2010**, *49* (9), 885.
- (230) Ku, H. S.; Siories, E.; Taube, A.; Ball, J. A. R. *Comput. Ind. Eng.* **2002**, *42* (2–4), 281.
- (231) Appleton, T. J.; Colder, R. I.; Kingman, S. W.; Lowndes, I. S.; Read, A. G. *Appl. Energy* **2005**, *81* (1), 85.
- (232) Lee, B. K.; Ellenbecker, M. J.; Moure-Ersaso, R. *Waste Manage.* **2004**, *24* (2), 143.
- (233) Abramovitch, R. A.; Lu, C.; Hicks, E.; Sinard, J. *Chemosphere* **2003**, *53* (9), 1077.
- (234) Ludlow-Palafox, C.; Chase, H. A. *Ind. Eng. Chem. Res.* **2001**, *40* (22), 4749.
- (235) Cherian, K. *Adv. Mater. Processes* **2011**, *169* (1), 23.
- (236) Arico, A. S.; Bruce, P.; Scrosati, B.; Tarascon, J. M.; Van Schalkwijk, W. *Nat. Mater.* **2005**, *4* (5), 366.
- (237) Wongittharom, N.; Lee, T.-C.; Hsu, C.-H.; Fey, G. T.-K.; Huang, K.-P.; Chang, J.-K. *J. Power Sources* **2013**, *240*, 676.
- (238) Yi, T.-F.; Jiang, L.-J.; Shu, J.; Yue, C.-B.; Zhu, R.-S.; Qiao, H.-B. *J. Phys. Chem. Solids* **2010**, *71* (9), 1236.
- (239) Higuchi, M.; Katayama, K.; Azuma, Y.; Yukawa, M.; Suhara, M. *J. Power Sources* **2003**, *119*, 258.
- (240) Park, K. S.; Son, J. T.; Chung, H. T.; Kim, S. J.; Lee, C. H.; Kim, H. G. *Electrochem. Commun.* **2003**, *5* (10), 839.
- (241) Li, J.; Jin, Y.-L.; Zhang, X.-G.; Yang, H. *Solid State Ionics* **2007**, *178* (29–30), 1590.
- (242) Liu, J.; Li, X.; Yang, J.; Geng, D.; Li, Y.; Wang, D.; Li, R.; Sun, X.; Cai, M.; Verbrugge, M. W. *Electrochim. Acta* **2012**, *63*, 100.
- (243) Terigar, B. G.; Balasubramanian, S.; Sabliov, C. M.; Lima, M.; Boldor, D. *J. Food Eng.* **2011**, *104* (2), 208.
- (244) Al-Harahsheh, M.; Kingman, S.; Bradshaw, S. *Int. J. Miner. Process.* **2006**, *80* (2–4), 198.
- (245) Robinson, J. P.; Kingman, S. W.; Snape, C. E.; Bradshaw, S. M.; Bradley, M. S. A.; Shang, H.; Barranco, R. *Chem. Eng. Res. Des.* **2010**, *88* (2A), 146.
- (246) Robinson, J. P.; Kingman, S. W.; Onobrakpeya, O. *J. Environ. Manage.* **2008**, *88* (2), 211.
- (247) Robinson, J. P.; Kingman, S. W.; Snape, C. E.; Barranco, R.; Shang, H.; Bradley, M. S. A.; Bradshaw, S. M. *Chem. Eng. J.* **2009**, *152* (2–3), 458.
- (248) Kumar, P.; Coronel, P.; Truong, V. D.; Simunovic, J.; Swartzel, K. R.; Sandeep, K. P.; Cartwright, G. *Food Res. Int.* **2008**, *41* (5), 454.
- (249) A. Tafove, S. C. H., *Computational Electrodynamics*, 3rd ed.; Artech House: MA, 2005.
- (250) Saremi-Yarahmadi, S.; Whittow, W.; Vaidhyanathan, B. *Appl. Surf. Sci.* **2013**, *275*, 65.
- (251) Hill, J. M.; Marchant, T. R. *Appl. Math. Modell.* **1996**, *20* (1), 3.
- (252) Zhao, X.; Yan, L.; Huang, K. Review of Numerical Simulation of Microwave Heating Process. In *Advances in Induction and Microwave Heating of Mineral and Organic Materials*; Grundas, S., Ed.; InTech: 2011.
- (253) Pitchai, K.; Birla, S. L.; Subbiah, J.; Jones, D.; Thippareddi, H. *J. Food Eng.* **2012**, *112* (1–2), 100.
- (254) Huang, K. M.; Lin, Z.; Yang, X. Q. *Electromagnetic Waves Pier 49: Progress in Electromagnetics Research*; 2004; Vol. 49, p 273.
- (255) Lollchund, M. R.; Dookhitram, K.; Sunhaloo, M. S.; Boojhawon, R. Numerical Simulations of Microwave Heating of Liquids: Enhancements using Krylov Subspace Methods. *International Conference on Radio and Antenna Days of the Indian Ocean (RADIO)*, Flic en Flac, MAURITIUS, Sep 24–27, 2013; Flic en Flac, MAURITIUS, 2012.
- (256) Muley, P. D.; Boldor, D. *J. Microwave Power Electromagnetic Energy* **2012**, *46* (3), 139.
- (257) Balomey, J. C.; Gardiol, F. E. *Engineering Applications of the Modulated Scattering Technique*; Artech House: MA, 2001.
- (258) Datta, A. K.; Anantheswaran, R. C. *Handbook of Microwave Technology for Food Applications*; Marcell Dekker, Inc.: New York, 2001.
- (259) Knoerzer, K.; Regier, M.; Schubert, H. *Chem. Eng. Technol.* **2006**, *29* (7), 796.
- (260) Sheppard, L. M. *Am. Ceram. Soc. Bull.* **1988**, *67* (10), 1656.